

*Accelerator Physics and Technology Seminar, FNAL, Batavia,
IL, Feb. 7, 2008*

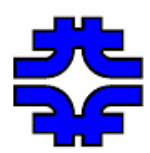
Superconducting Strand and Cable R&D for Future Accelerators

E. Barzi with the SC R&D and SC Magnets Groups, FNAL

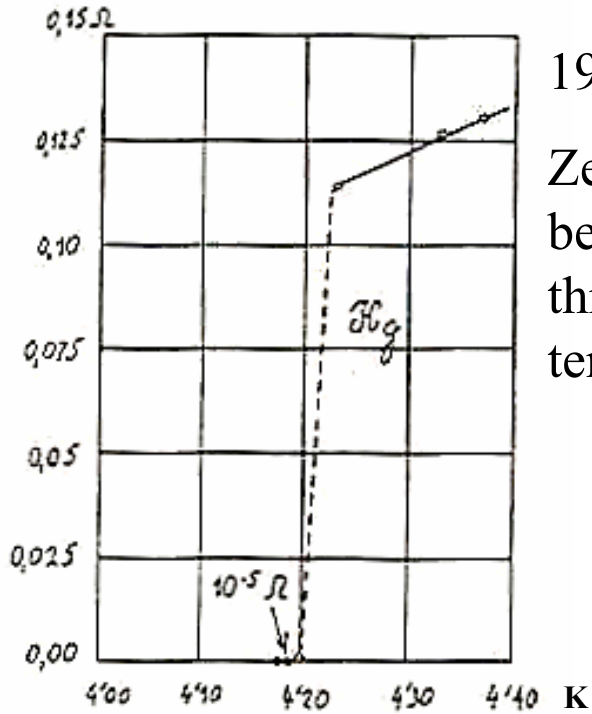


Outline

- **A few basics concepts.**
- **Available LTS and HTS conductors.**
- **Our applications and main results for LTS.**
- **Our applications and main results for HTS.**
- **Conclusions.**

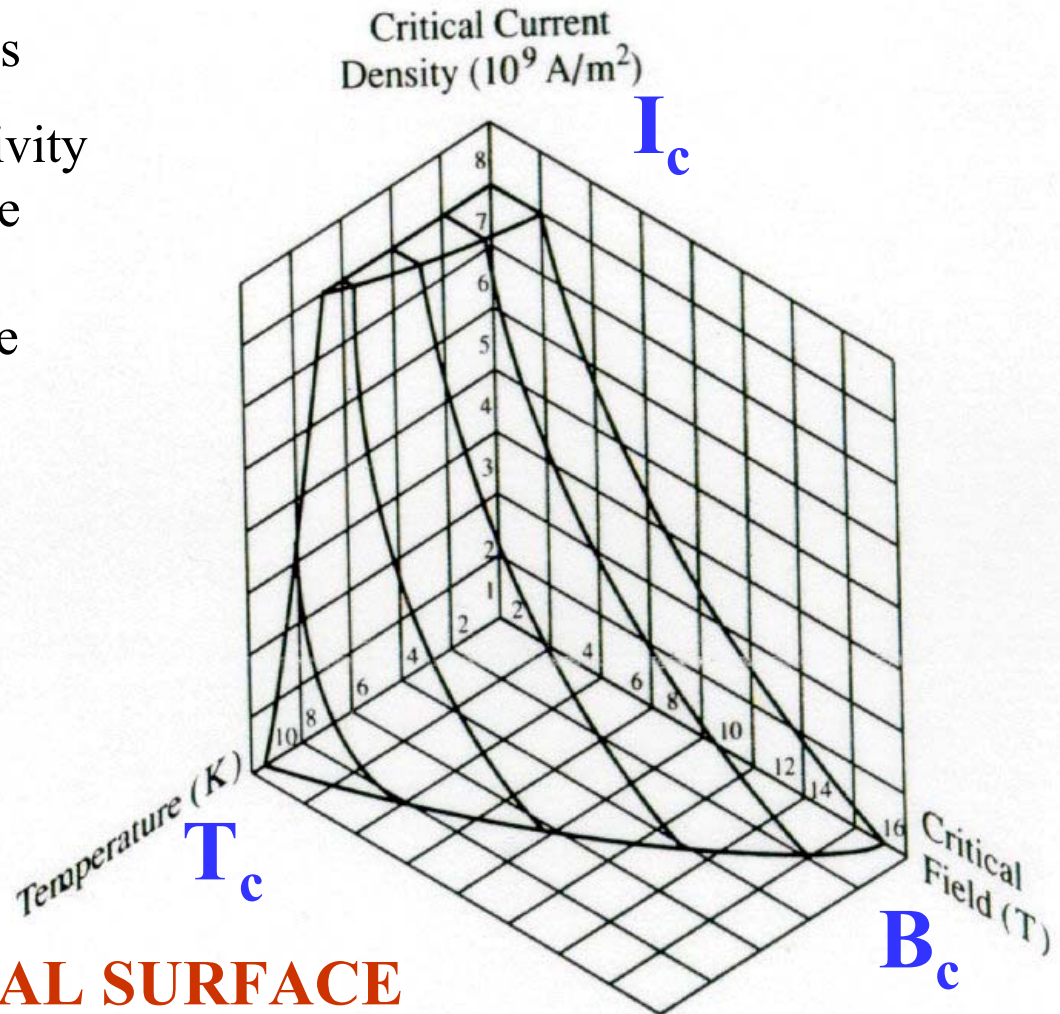


Superconductivity, first discoveries

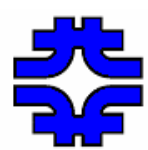


1913 Onnes

Zero resistivity
below some
threshold
temperature

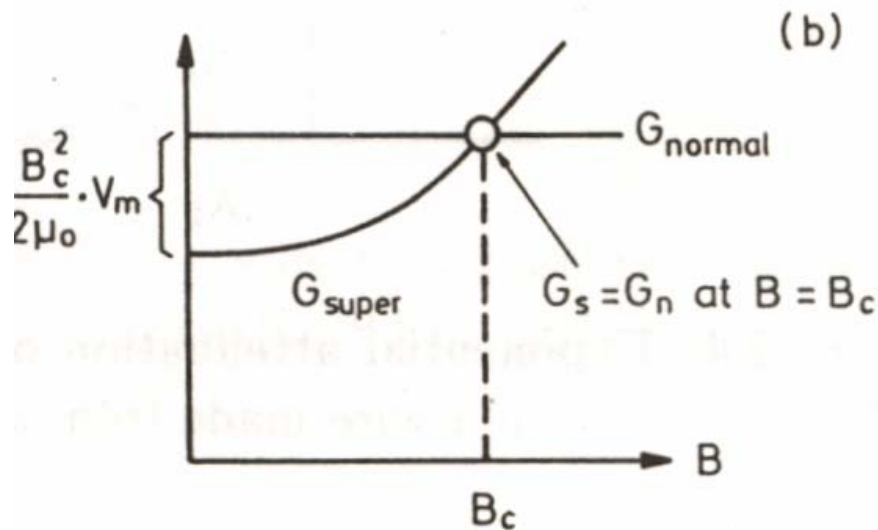
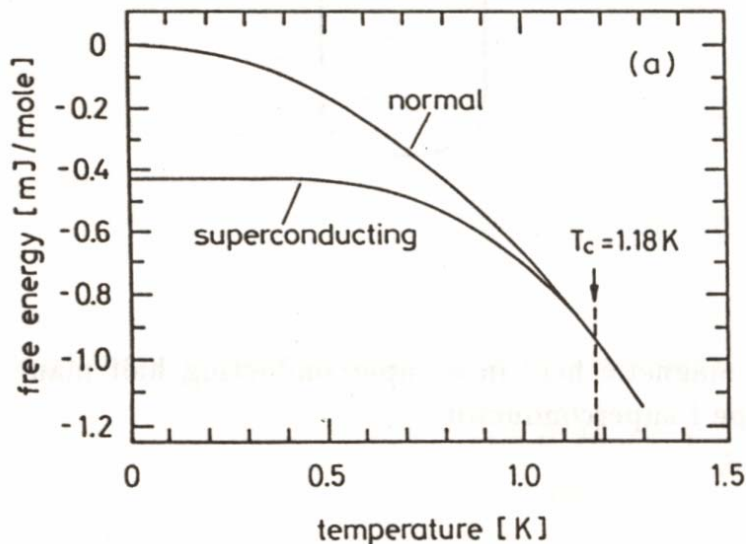


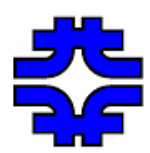
CRITICAL SURFACE



Why does Superconductivity occur ?

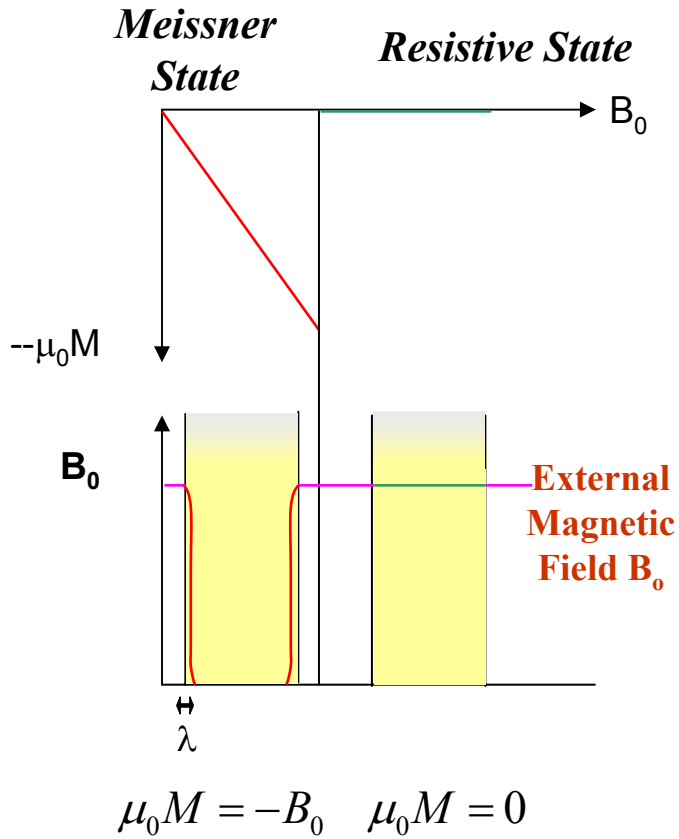
Below T_c , B_c , and I_c , the superconducting phase transition takes place because energetically favored.



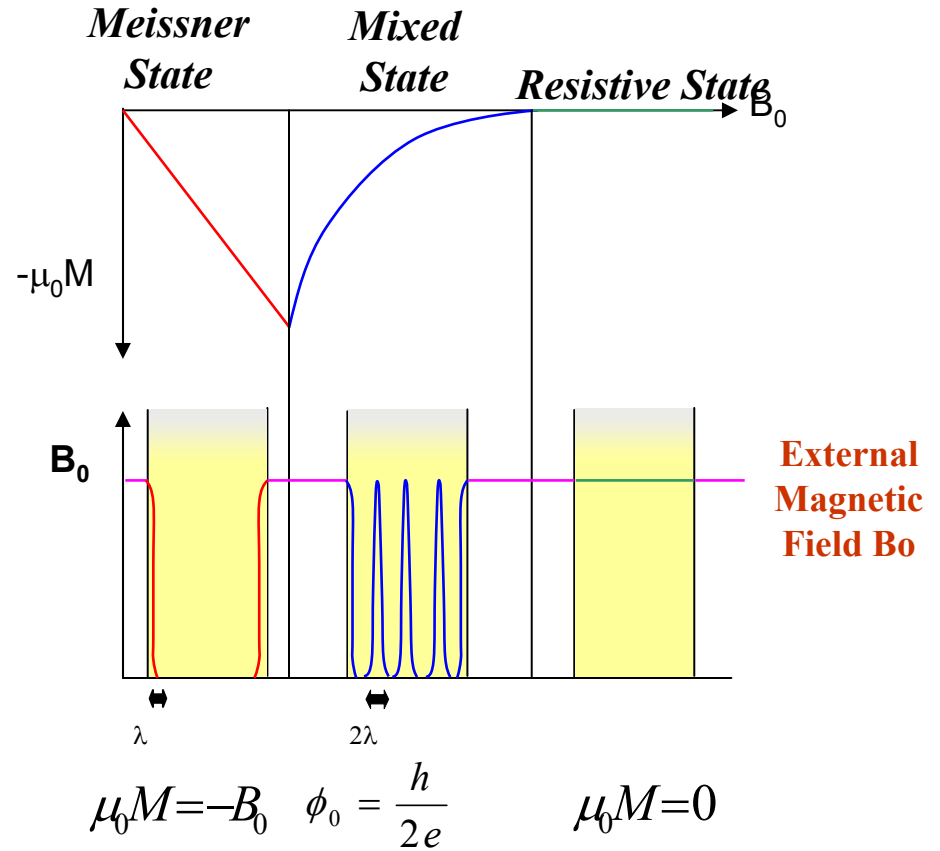


Types of Superconductors

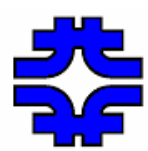
TYPE I



TYPE II

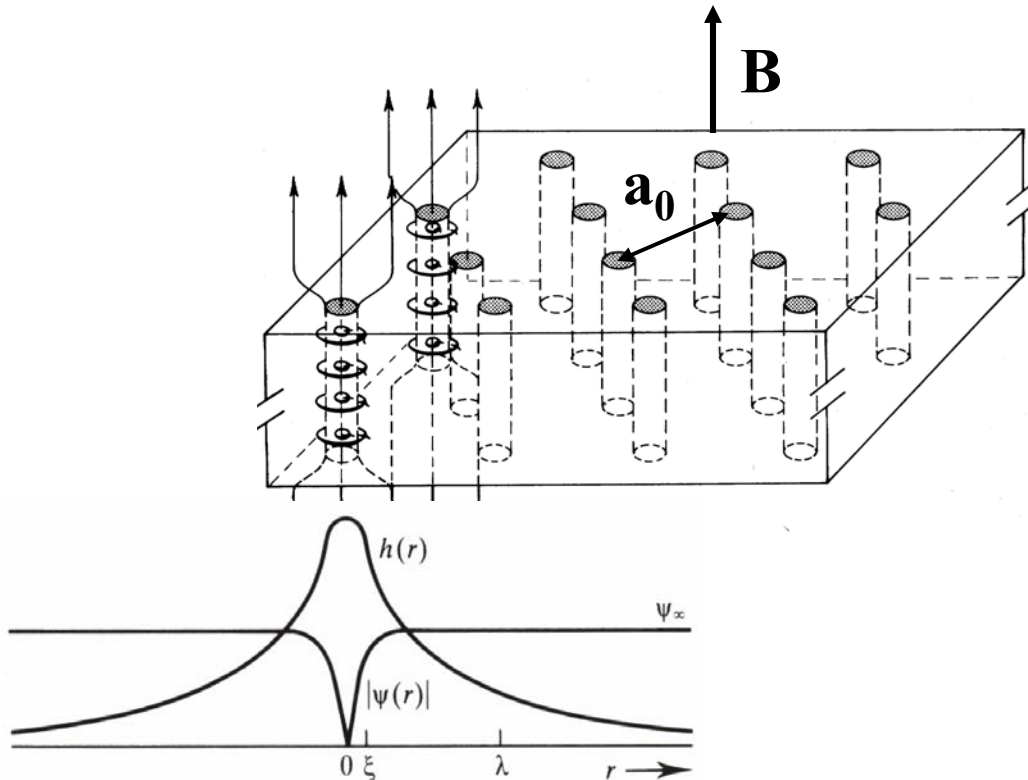


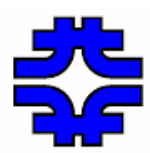
$$B_0 = \mu_0 (H - M)$$



Flux Pinning Mechanism in Type II's

In an external B , a type II SC is penetrated by quantized flux vortices (Φ_0). The flux will form a triangular lattice of uniform spacing $a_0 \propto B^{-1/2}$. The passage of a current imposes on the lattice a $F_L = J \times B$ per unit volume. The flux lattice is pinned in place by interacting with microstructural features like defects or discontinuities in the material.

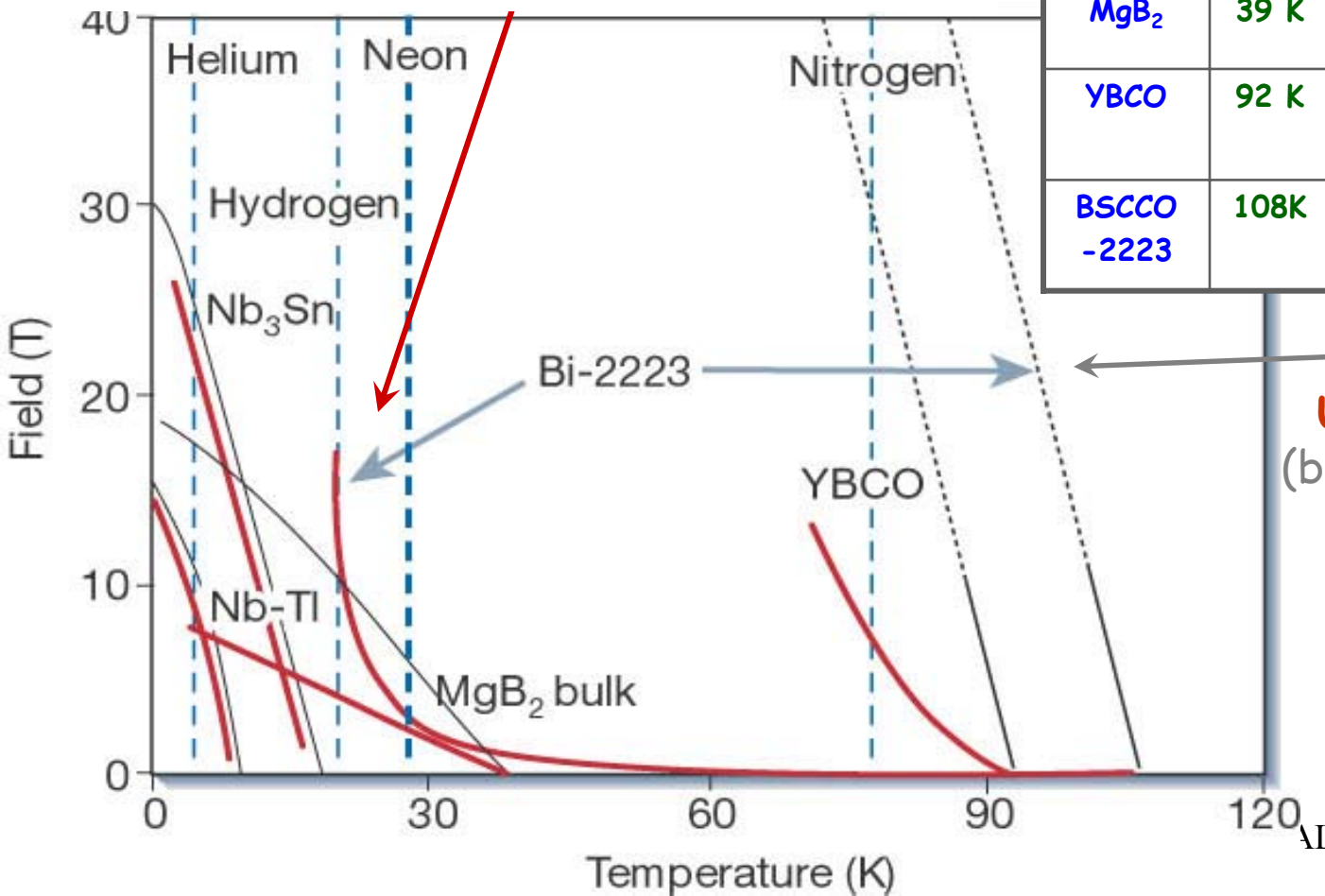




H-T diagram

H^* - Irreversibility Field

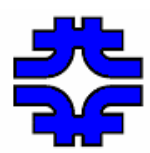
(the critical current density goes to zero, due to a dissipative fluxons-flow state driven by the Lorentz force)



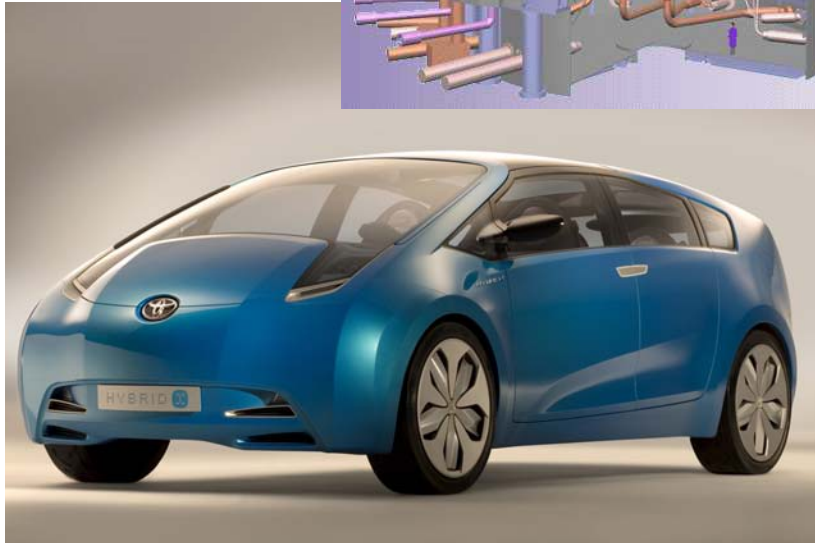
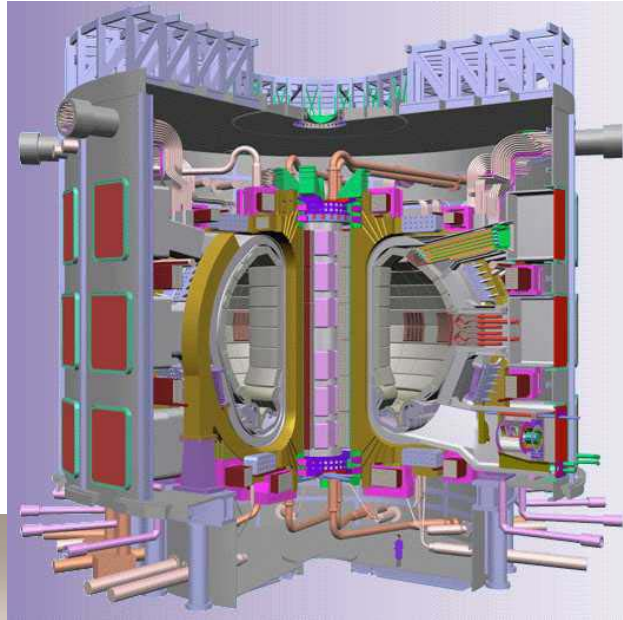
	T_c	H_{c2}	H^*
NbTi	9 K	12 T (4 K)	10.5 T (4 K)
Nb ₃ Sn	18 K	27 T (4 K)	24 T (4 K)
MgB ₂	39 K	15 T (4 K)	8 T (4 K)
YBCO	92 K	>100 T (4K)	5-7 T (77K)
BSCCO -2223	108K	>100 T (4K)	~0.2T (77K)

H_{c2}

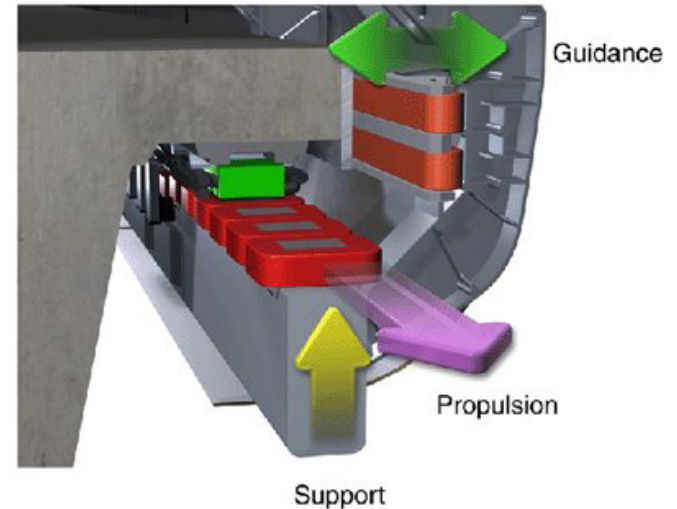
Upper critical field
(bulk superconductivity is destroyed)



Examples of Applications of Superconductivity

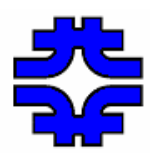


Electromagnetic Levitation



February 7, 2008

E. Barzi, SC Strand and Cable R&D for Future Accelerators, FNAL

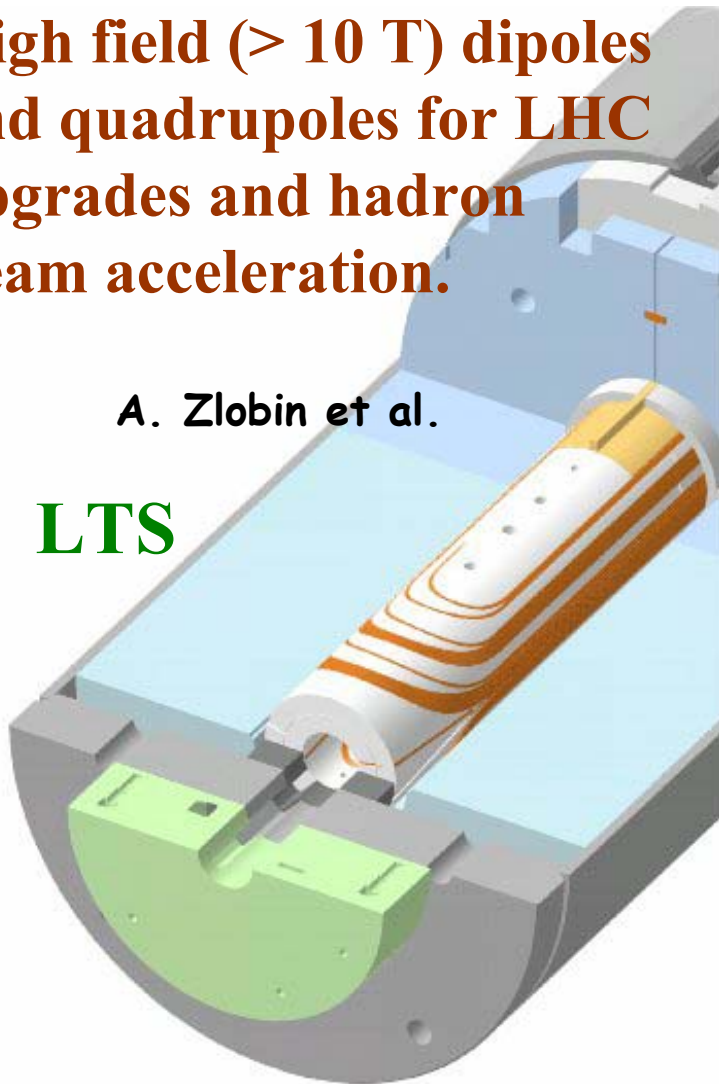


Magnets for Future Accelerators

High field (> 10 T) dipoles and quadrupoles for LHC upgrades and hadron beam acceleration.

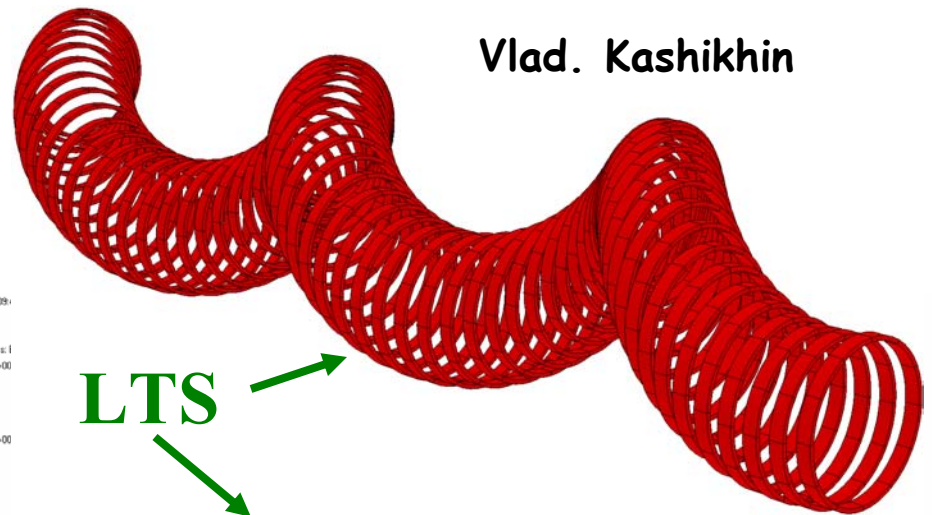
A. Zlobin et al.

LTS

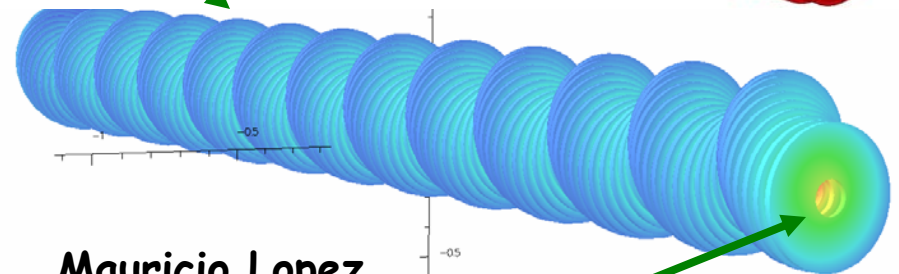
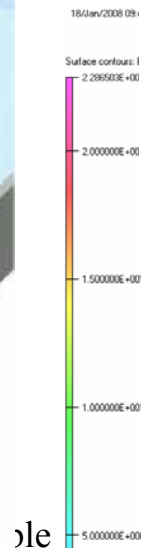


Prototype of muon cooling channel and high field (> 25 T) solenoids for muon beam acceleration.

Vlad. Kashikhin

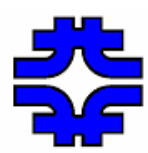


LTS

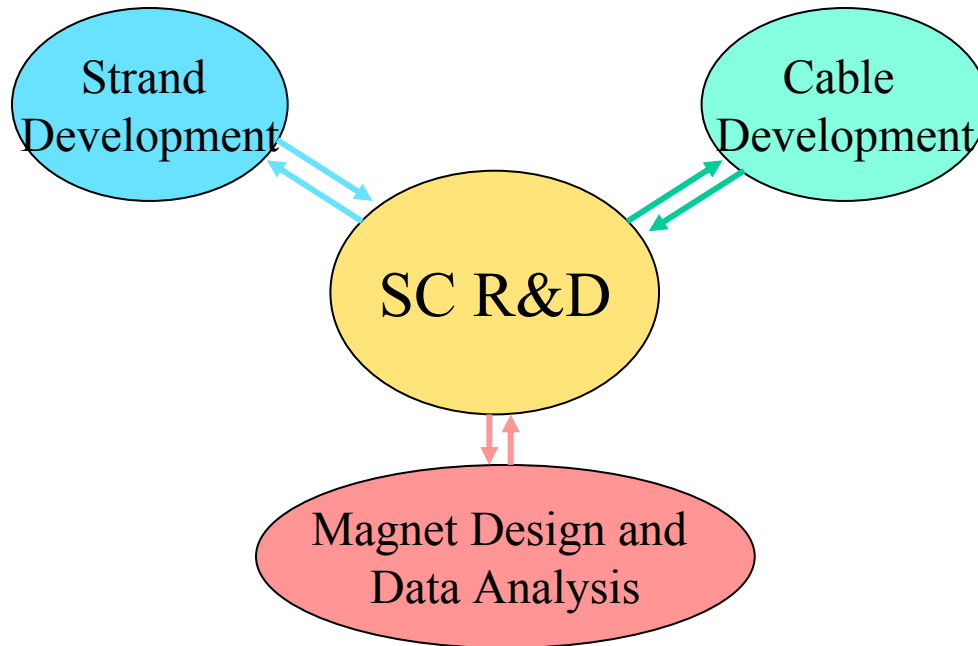


Mauricio Lopez

HTS

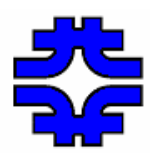


Superconductor R&D Program



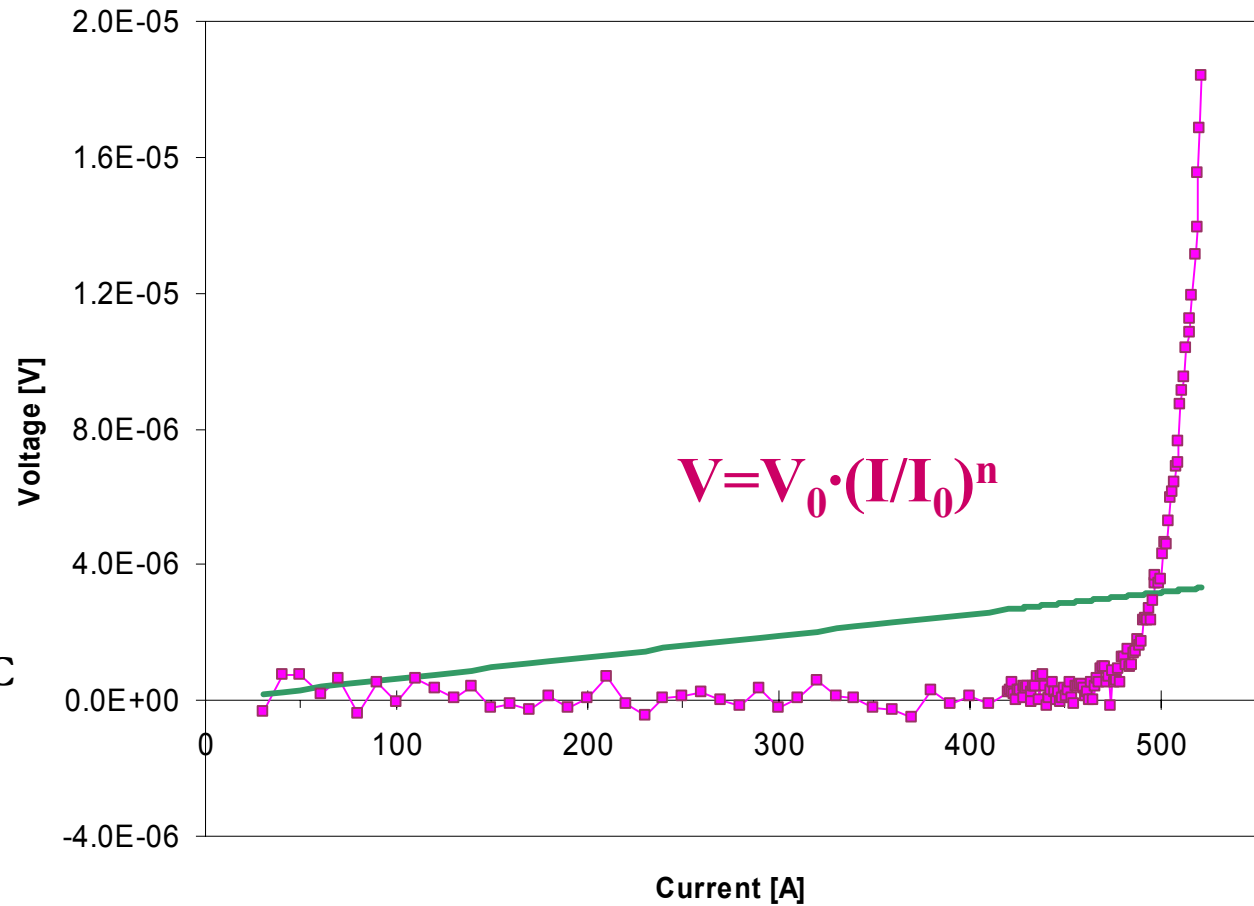
MISSION

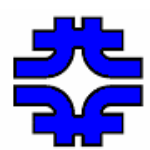
- **Serve as an interface between magnets and conductors beyond NbTi.**
- **Be a leading center for conductor technology: Focus research and scientific studies on the process of cable development.**
- **Help Industry and small companies produce the best possible strand for High Field accelerator quality magnets.**



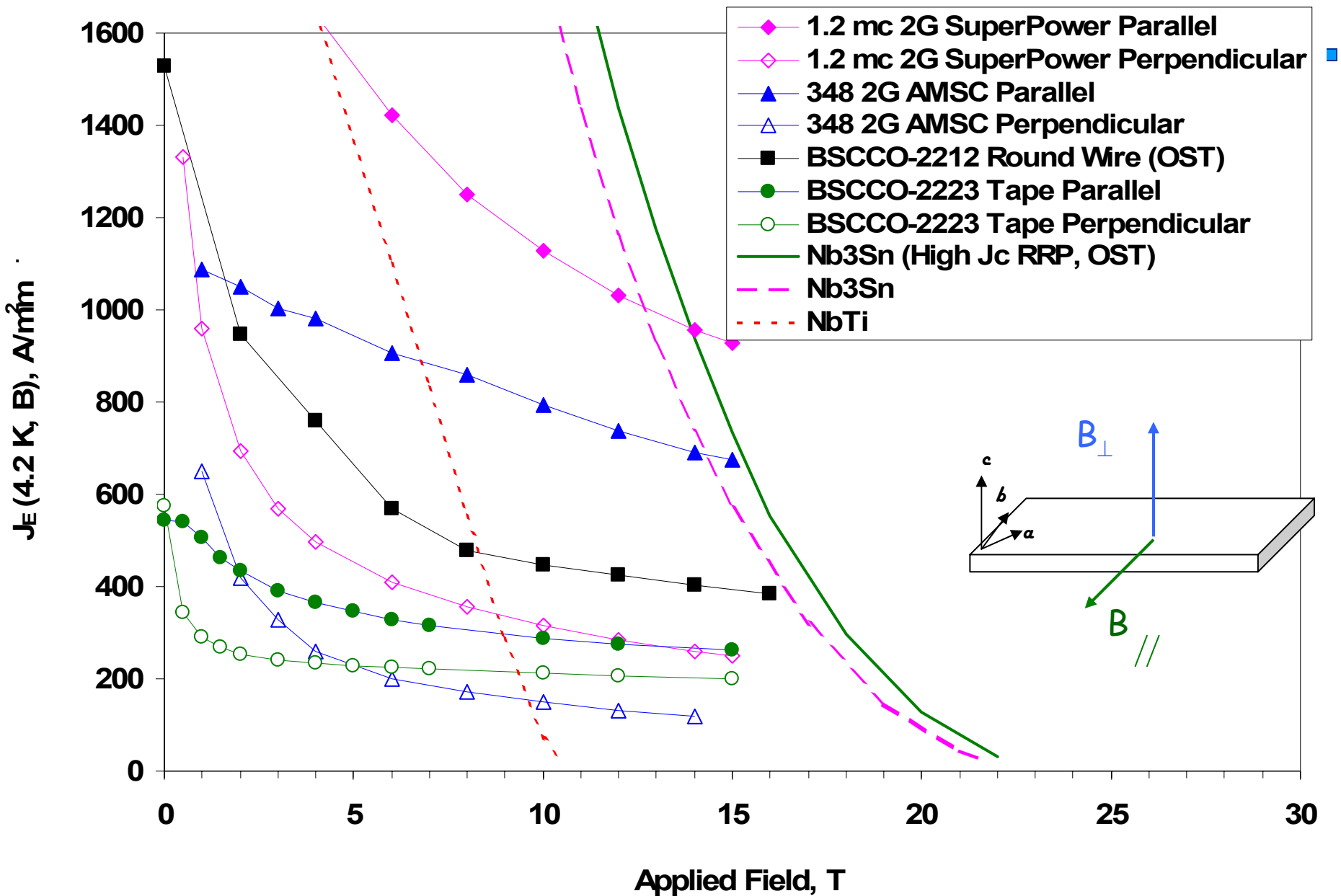
Voltage-Current (VI) Characteristics

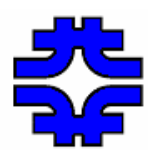
- $B = 2 - 15 \text{ T}$
- $T = 4.2 \text{ K}$
- $I_c @ 10^{-14} \Omega \cdot \text{m}$
- $n @ V = (1-10) \cdot V_C$





HTS and LTS Performance at 4.2 K

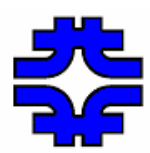




Target Specifications for HEP Conductor

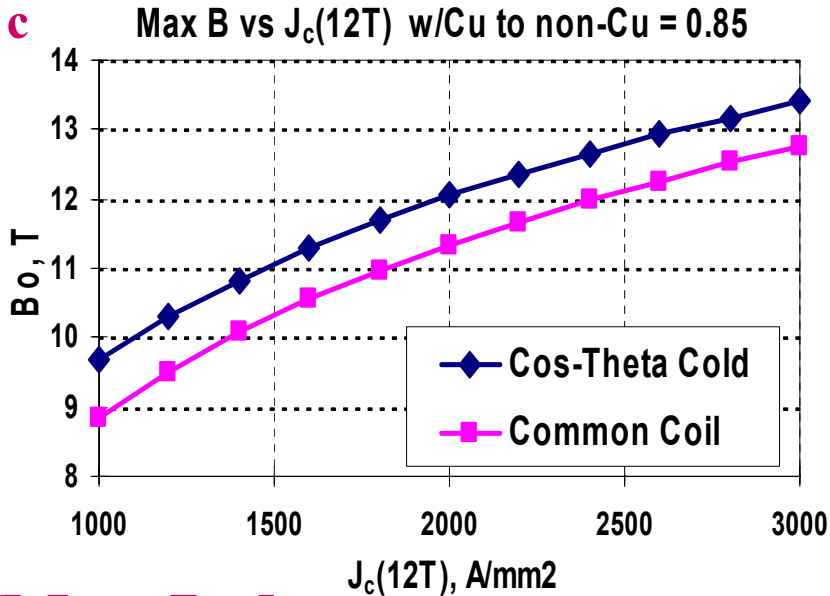
Parameter	Value
Strand diameter, mm	1.000 / 0.700
$J_c(4.2K, 12T)$, A/mm²	> 3000
d_{eff}, μm	< 40 / 30
Cu, %	50-60
RRR	> 100
Piece length, km	> 10
Cabling degradation	< 10 %
Cost, \$/kA-m (12T, 4.2K)	< 1.5

Plus stress requirements ≥ 150 MPa



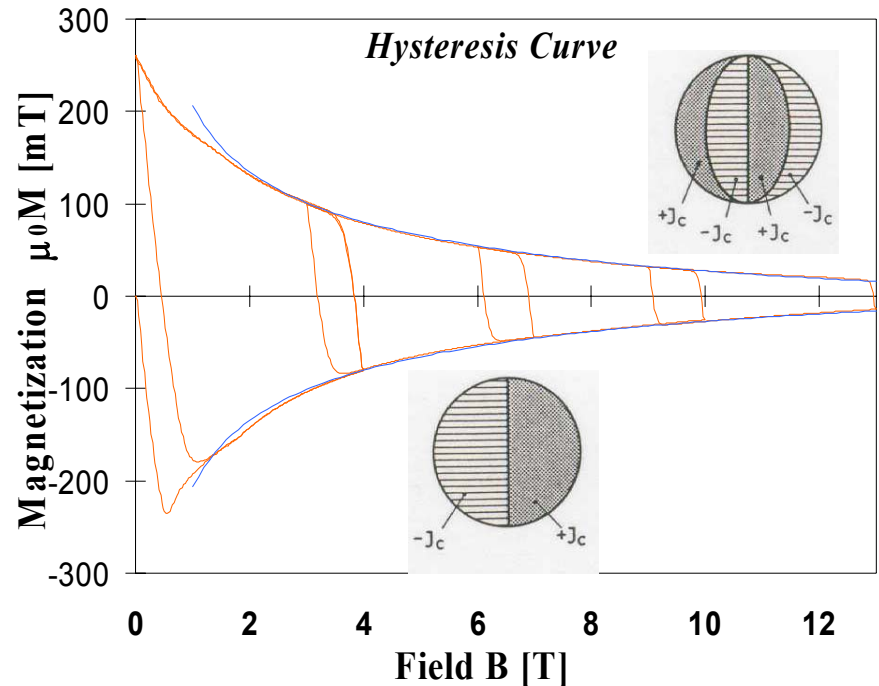
Why such requirements?

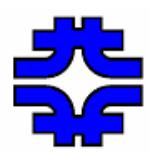
• J_c



• $\Delta M \propto J_c \cdot d_{eff}$

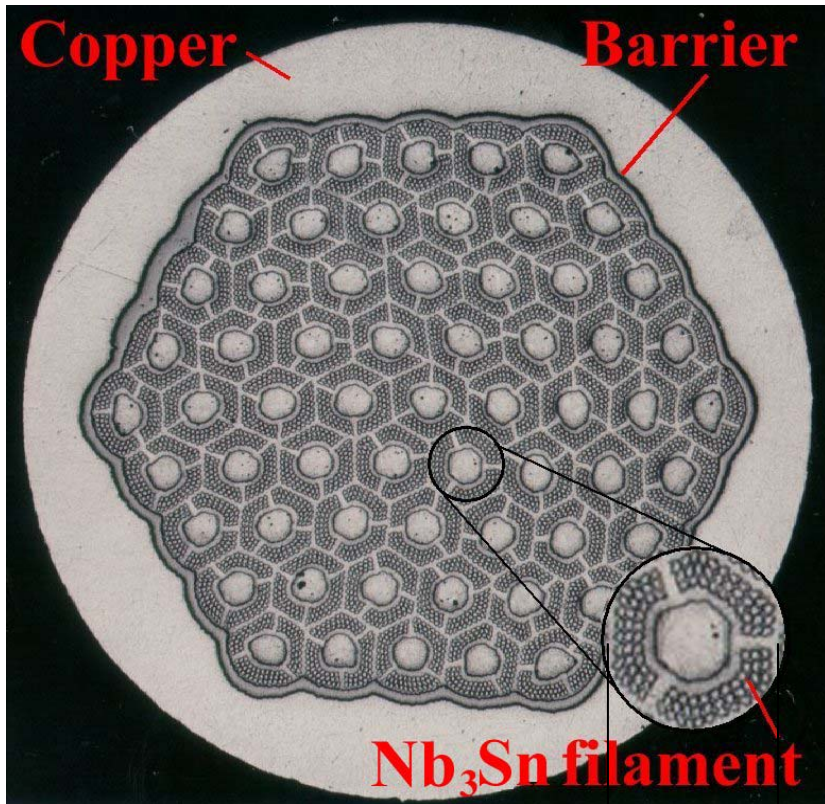
Persistent currents are induced in a type II superconductor when the field is changed. These bipolar currents are the source of severe field distortions at low excitation. They generate all multipoles allowed by the coil symmetry.





Nb₃Sn

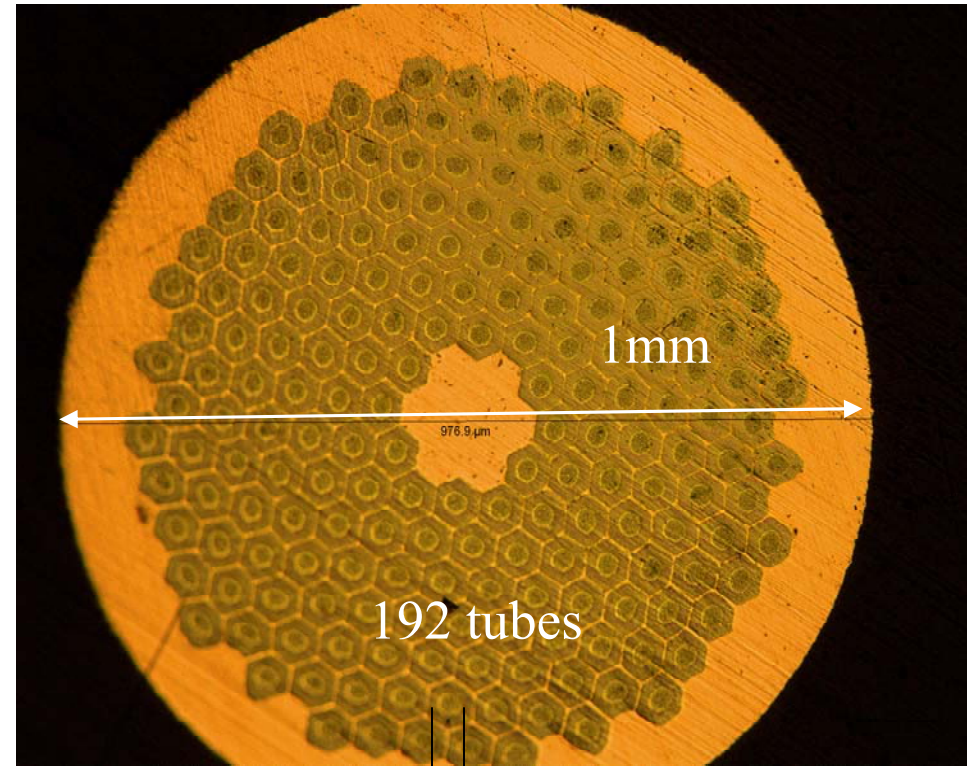
Internal Tin



61 subelements

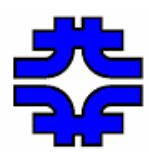
100 μm

Powder-in-Tube (PIT)



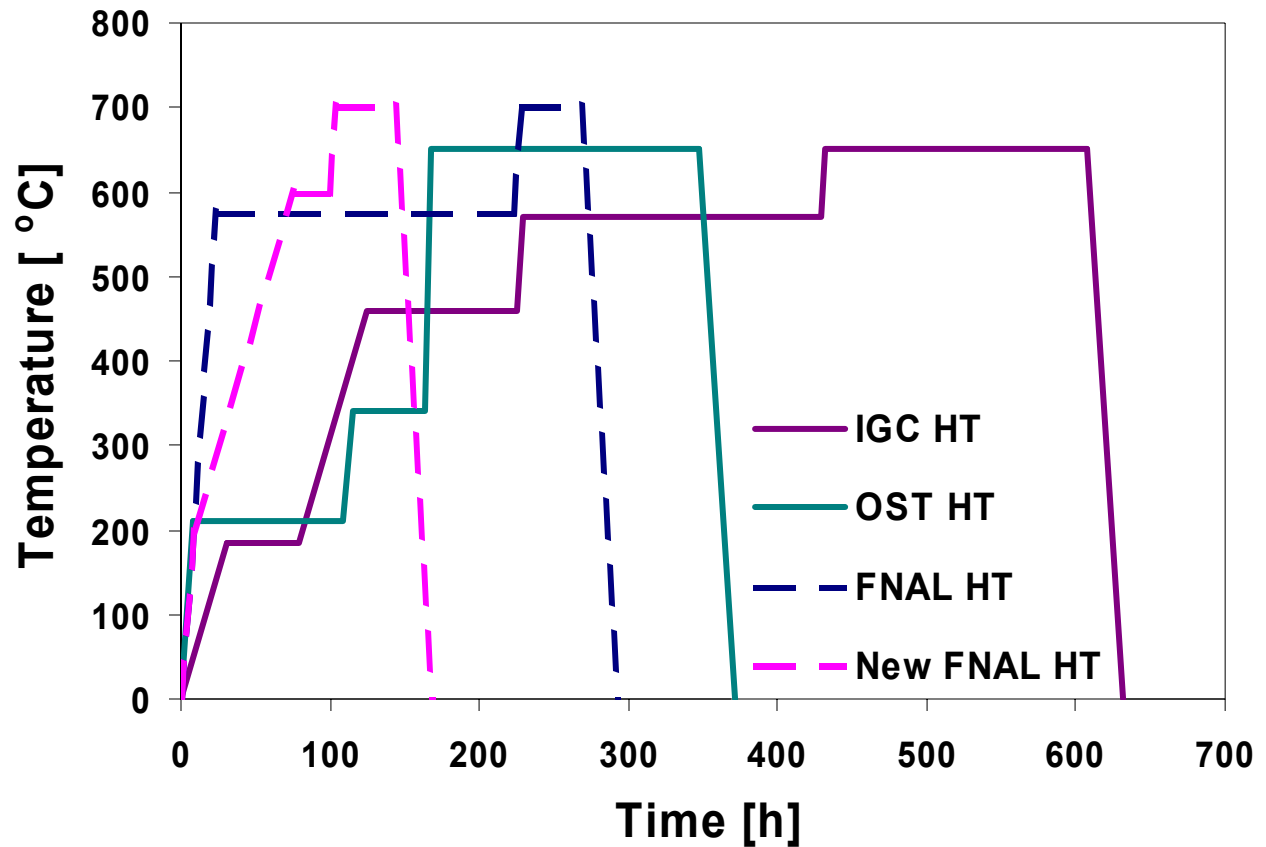
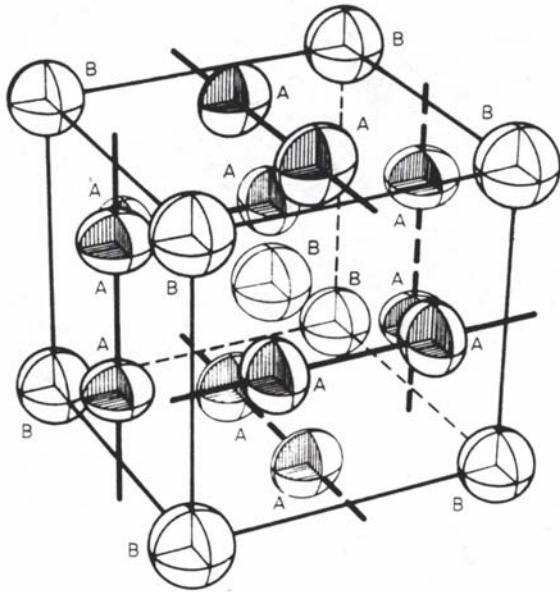
192 tubes

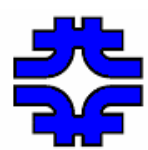
50 μm



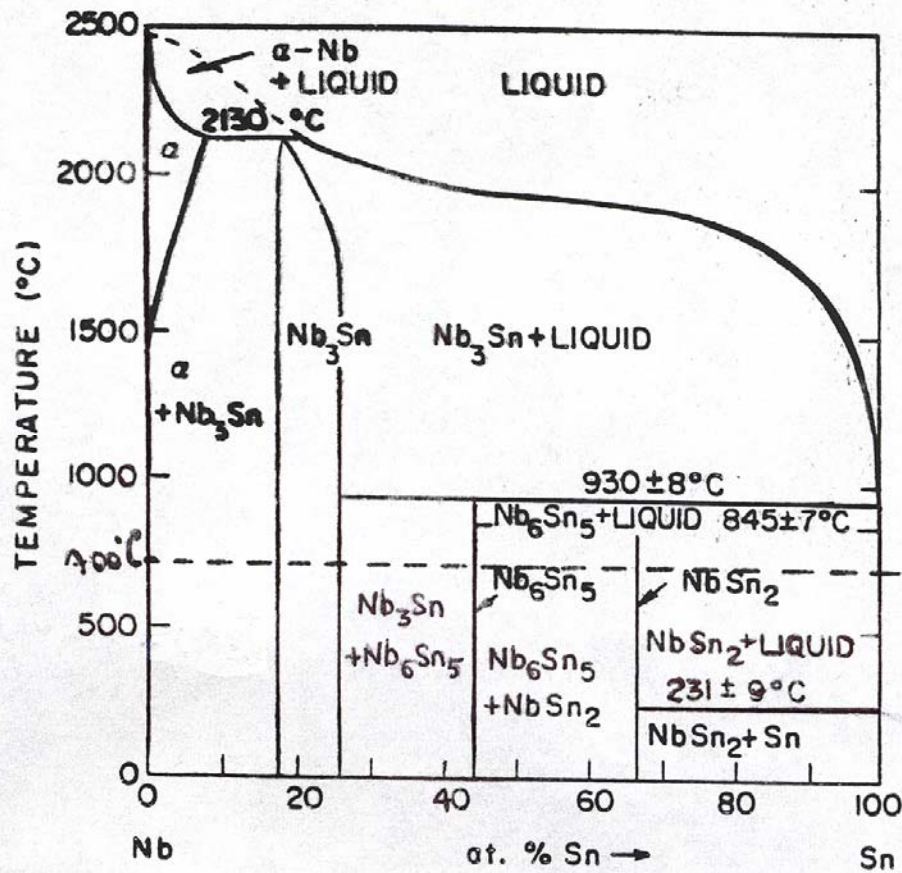
Heat Treatments

Nb₃Sn A15 crystal structure

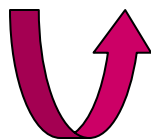




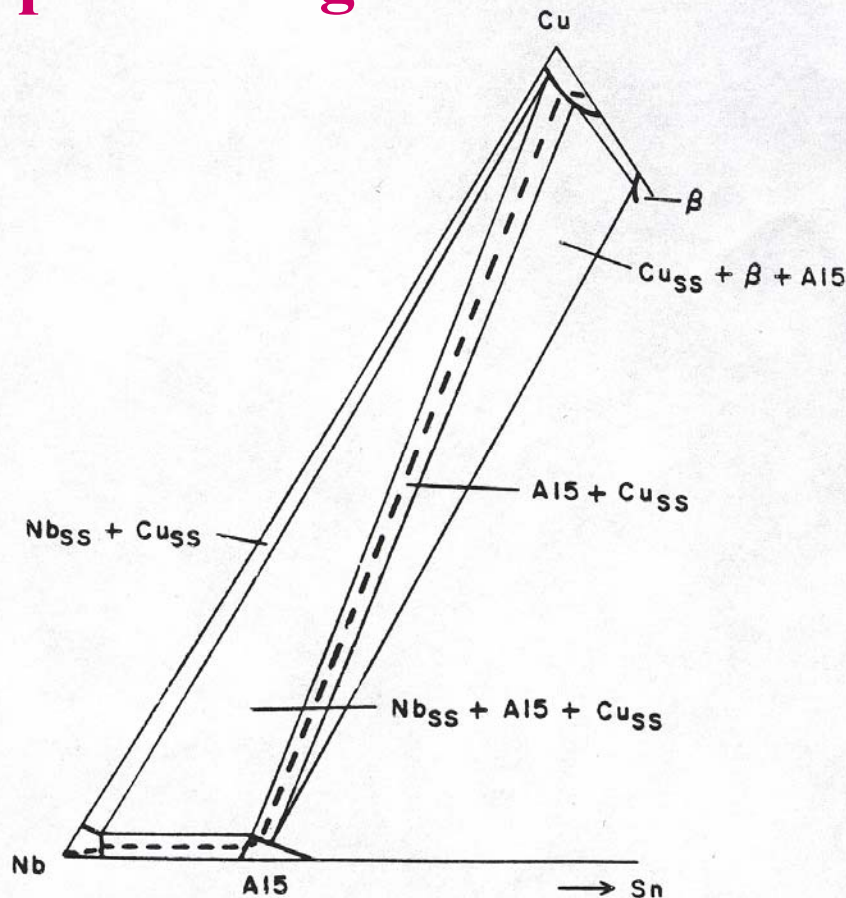
Nb₃Sn Phase Diagram



Nb-Sn binary phase diagram



Nb-Cu-Sn ternary phase diagram

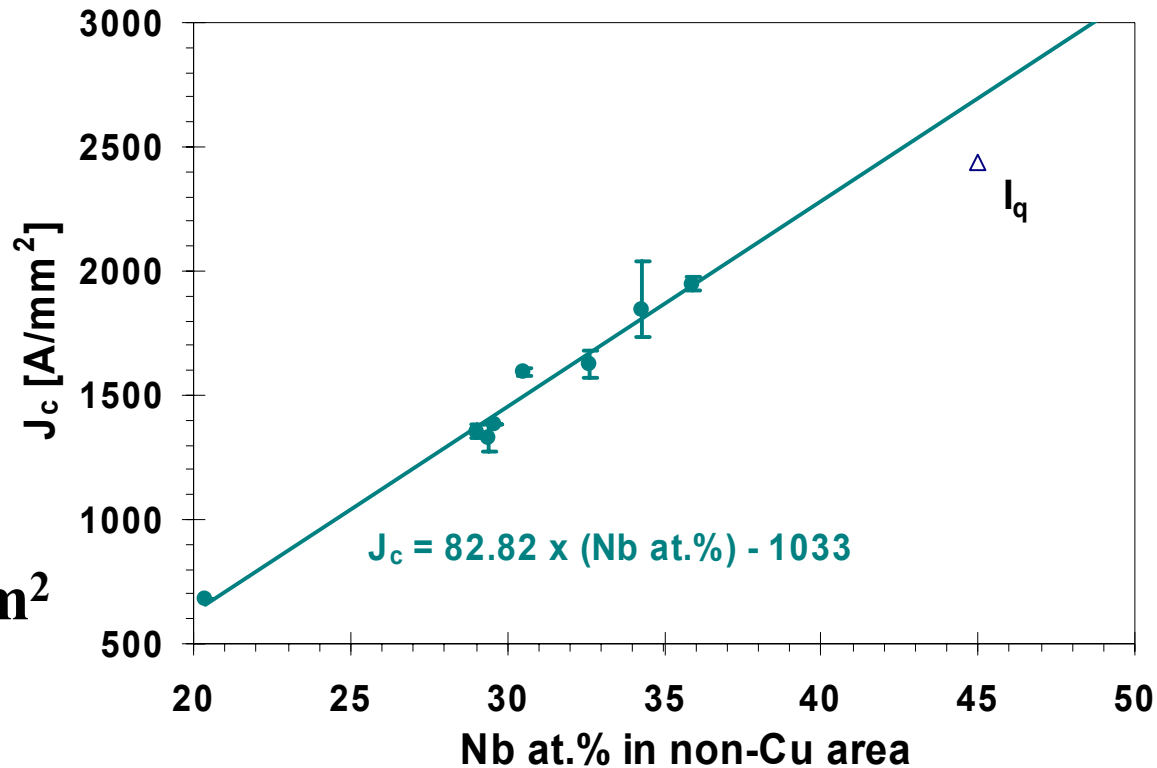


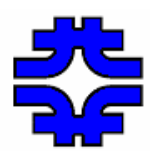


Parameters that control J_c in Nb_3Sn

Atomic percentage of Nb in the non-Cu section

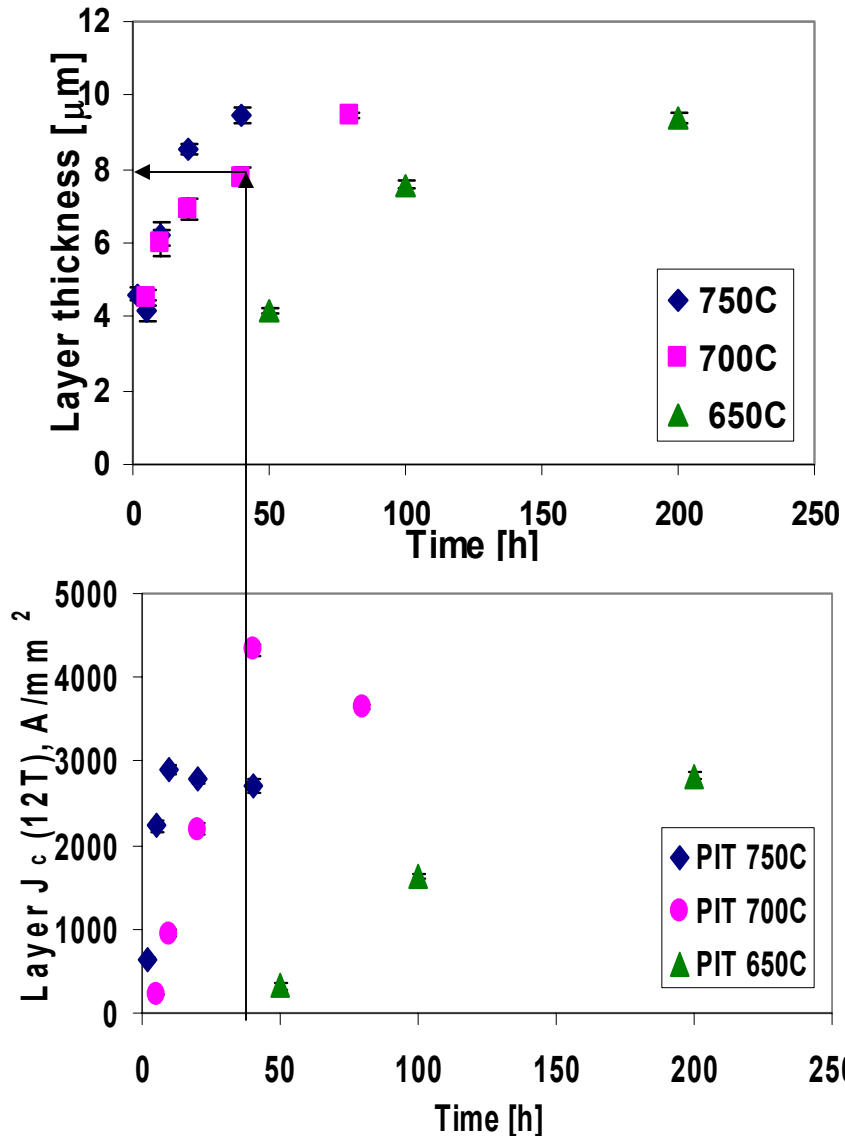
- For 3000 A/mm², one needs 50 at. % Nb
- For the present technology, one can estimate a maximum intrinsic J_c of 5000 A/mm² by extrapolation to 75 at.% Nb



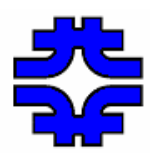


Strand Design Optimization – Filament Size

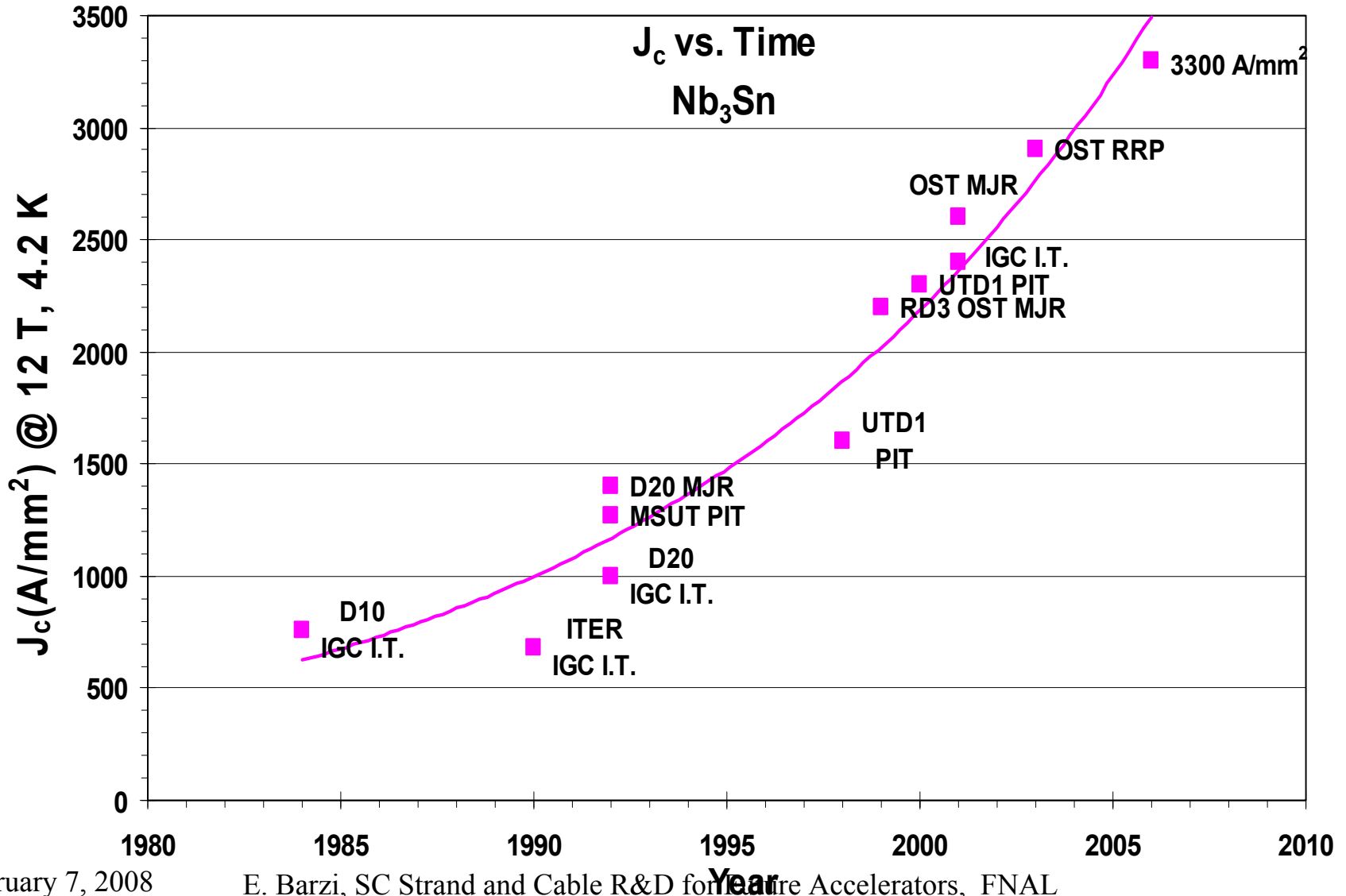
PIT

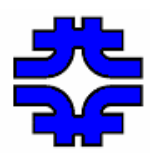


For a given technology, through measurement of the SC layer thickness and associated layer J_c with time and temperature, a filament size optimized for max J_c can be found.

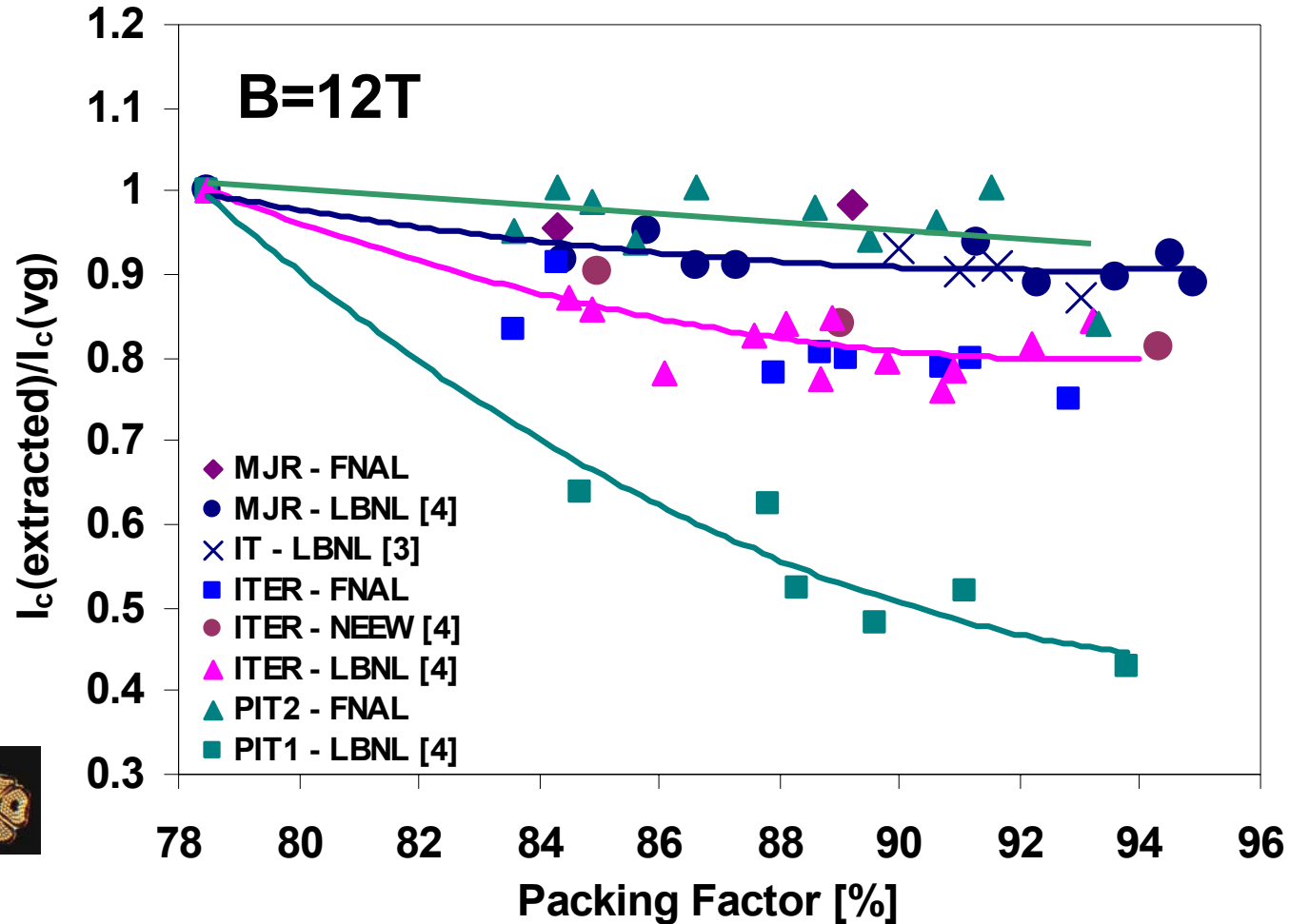
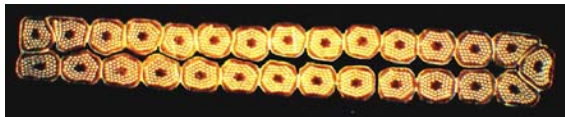
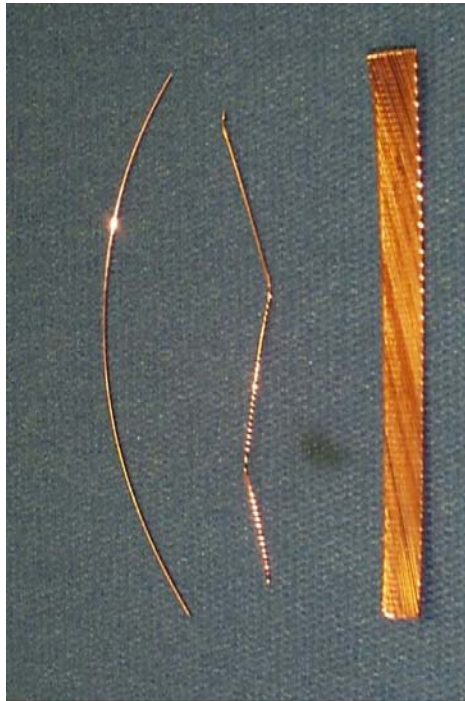


Progress in time of $J_c(12\text{ T}, 4.2\text{ K})$

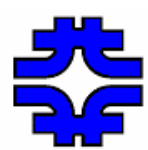




Results of Cabling Degradation

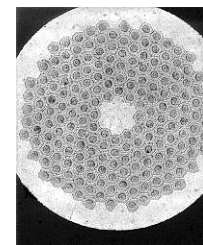
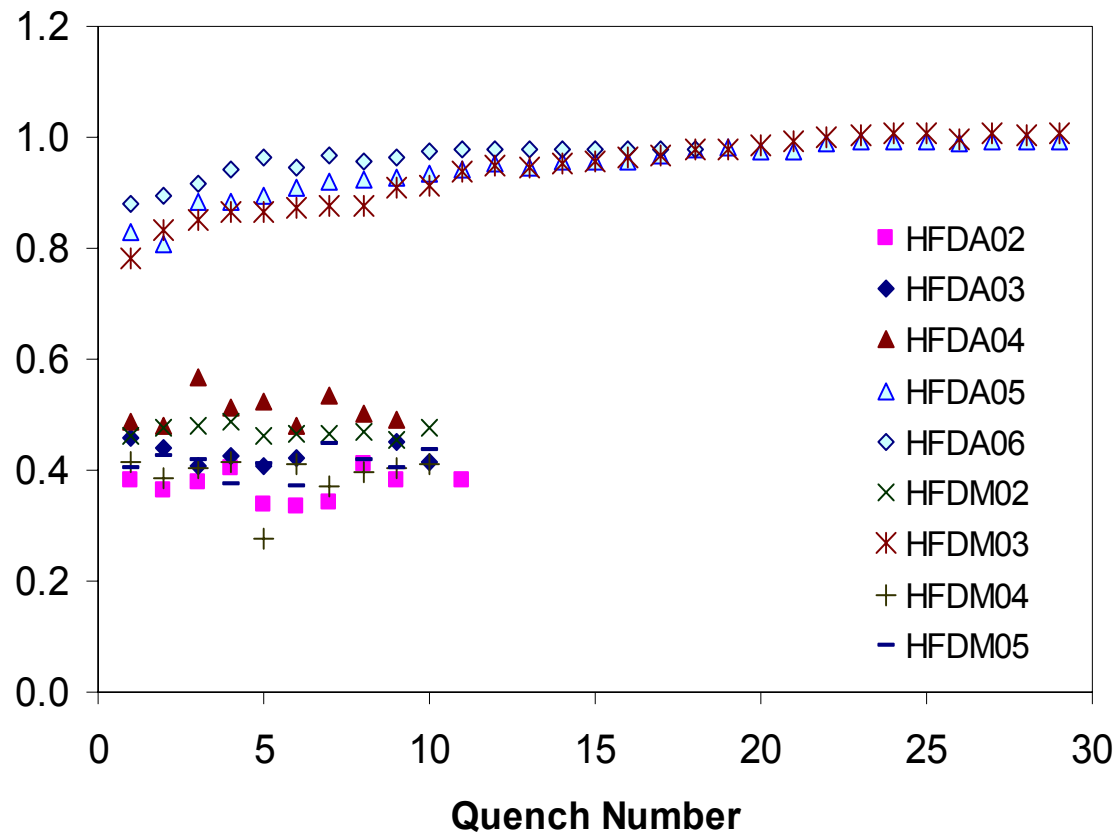


The level of degradation depends on the strand ability to withstand plastic deformation, and on cable packing factor.

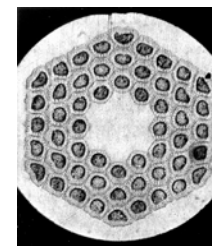


Magnet Test Results

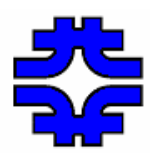
- **There were two families of magnets.**
- **They differed in the SC material.**
- **The cables had the same keystone geometry (~88% PF), with ceramic insulation or S2-glass plus ceramic binder.**



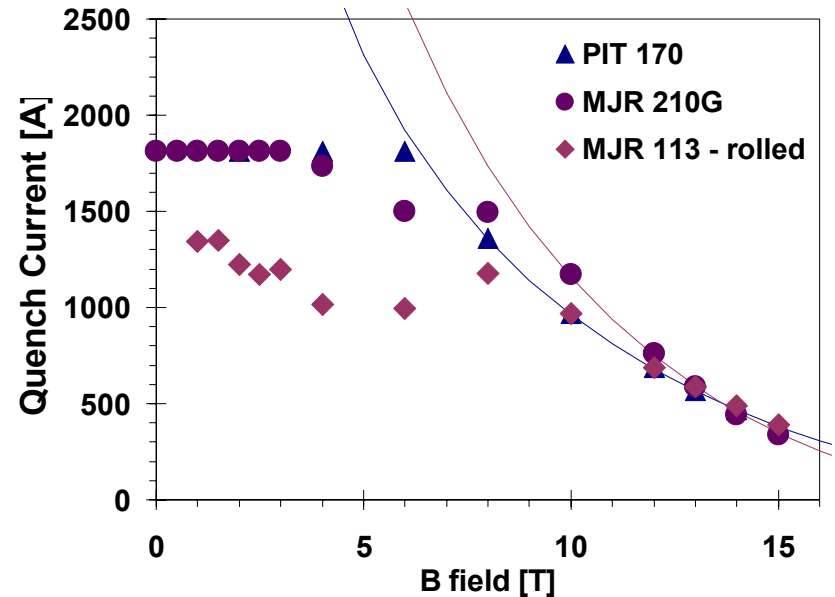
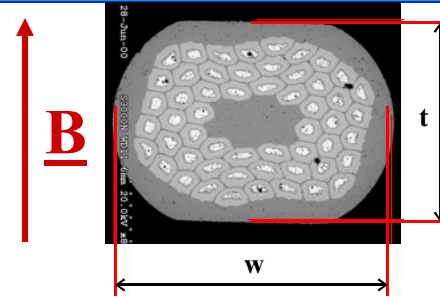
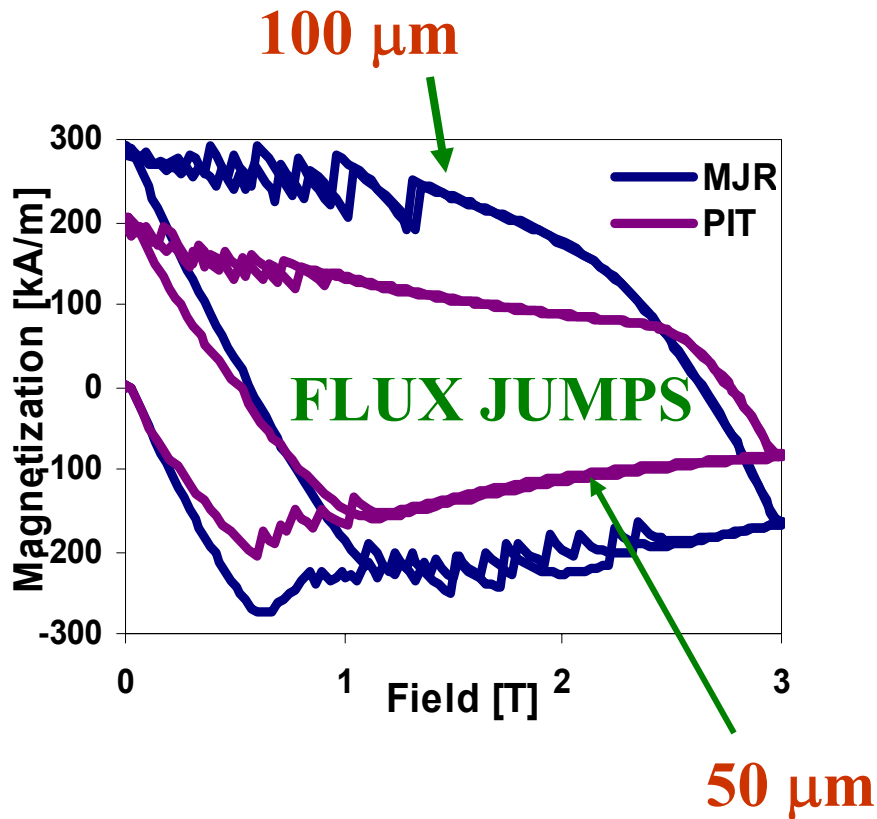
$D_{\text{eff}}: 50 \mu\text{m}$



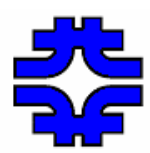
$D_{\text{eff}}: 80 - 110 \mu\text{m}$



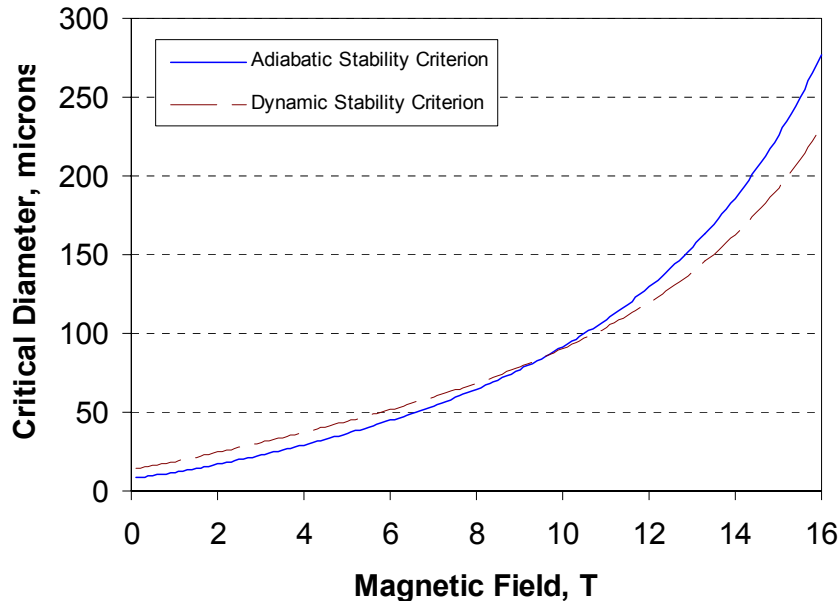
Effects of Subelement Size



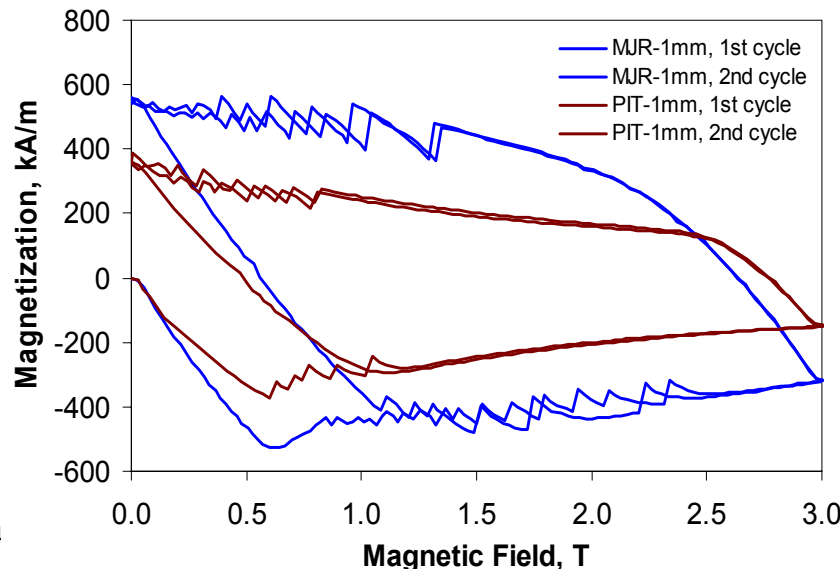
It had always been known that excessive filament sizes could lead to instabilities, but the practical effect on Nb_3Sn magnets had not been acknowledged before us.



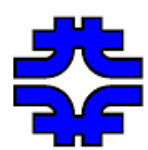
Adiabatic and Dynamic Stability Criteria



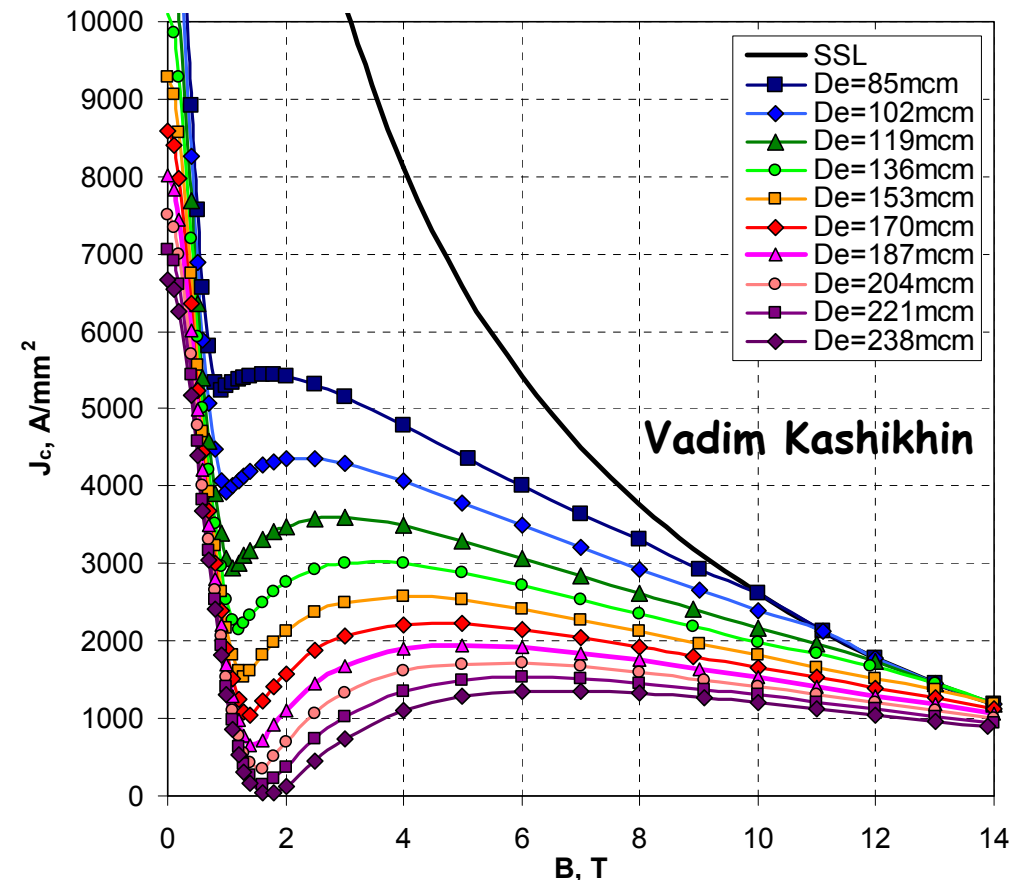
- Key parameters are J_c , T_c and D_{eff} as well as γC (adiabatic criterion) or k (dynamic criterion).
- These are very conservative criteria, as they predict zero transport current for Nb_3Sn strands with $J_c \sim 2 \text{ kA/mm}^2$, at $B < 13 \text{ T}$ for $D_{eff} \sim 150 \text{ }\mu\text{m}$ and $B < 6 \text{ T}$ for $D_{eff} \sim 50 \text{ }\mu\text{m}$.



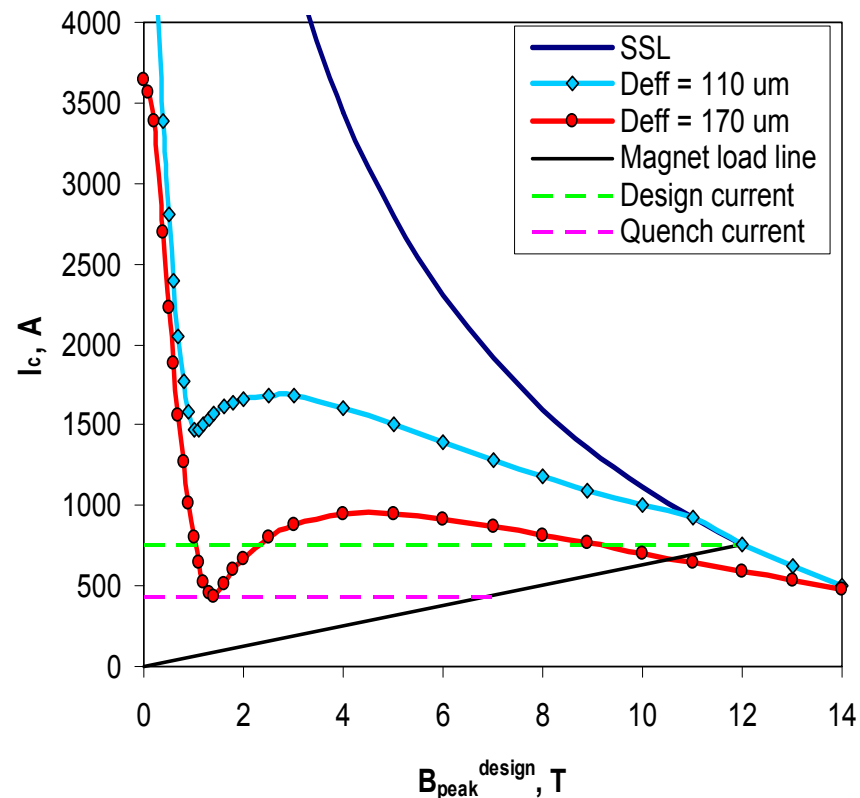
Wilson, Brechna, ...



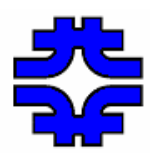
Enthalpy Stabilization Analysis



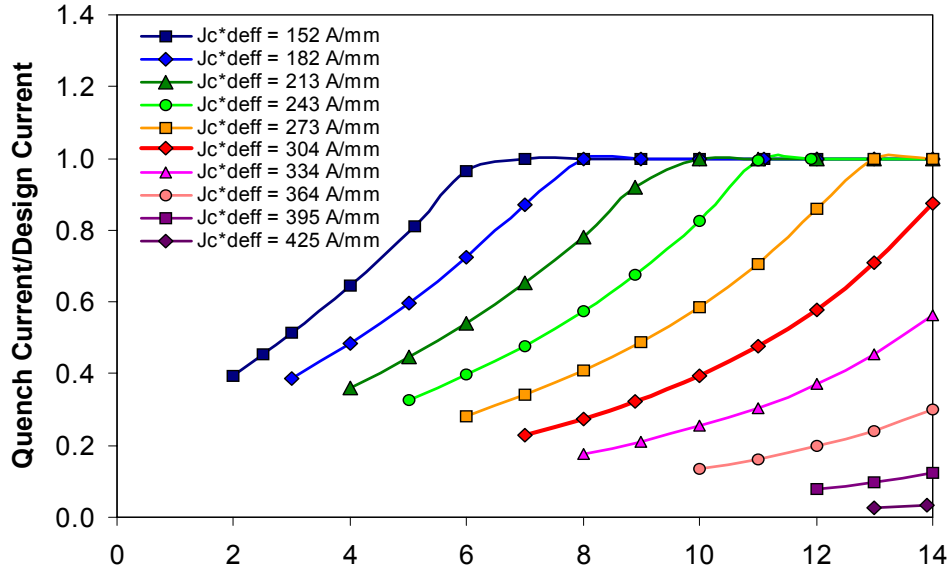
Transport current density of strands with various D_{eff} for $J_c(12T, 4.2K)=1800$ A/mm²



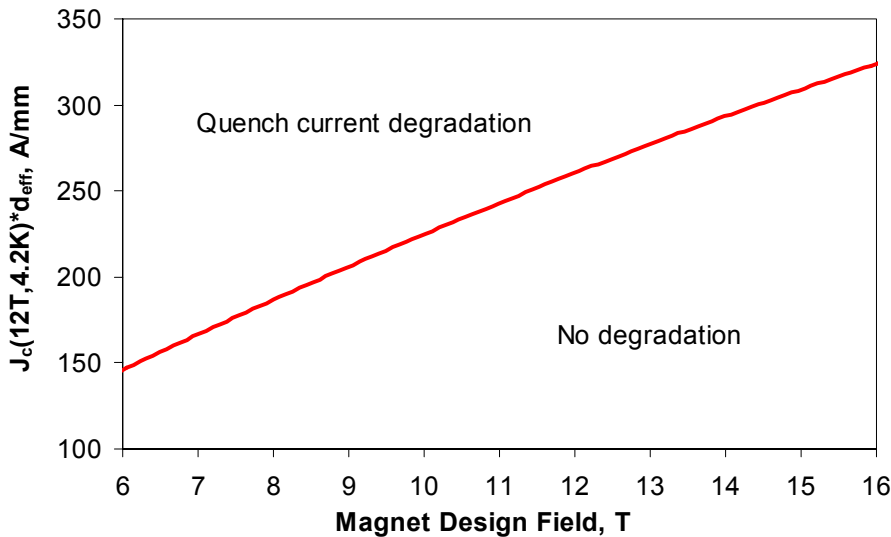
For strands with large D_{eff} and high J_c the maximum transport current at low B is smaller than at high B



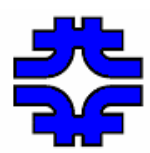
Magnet Stability Predictions



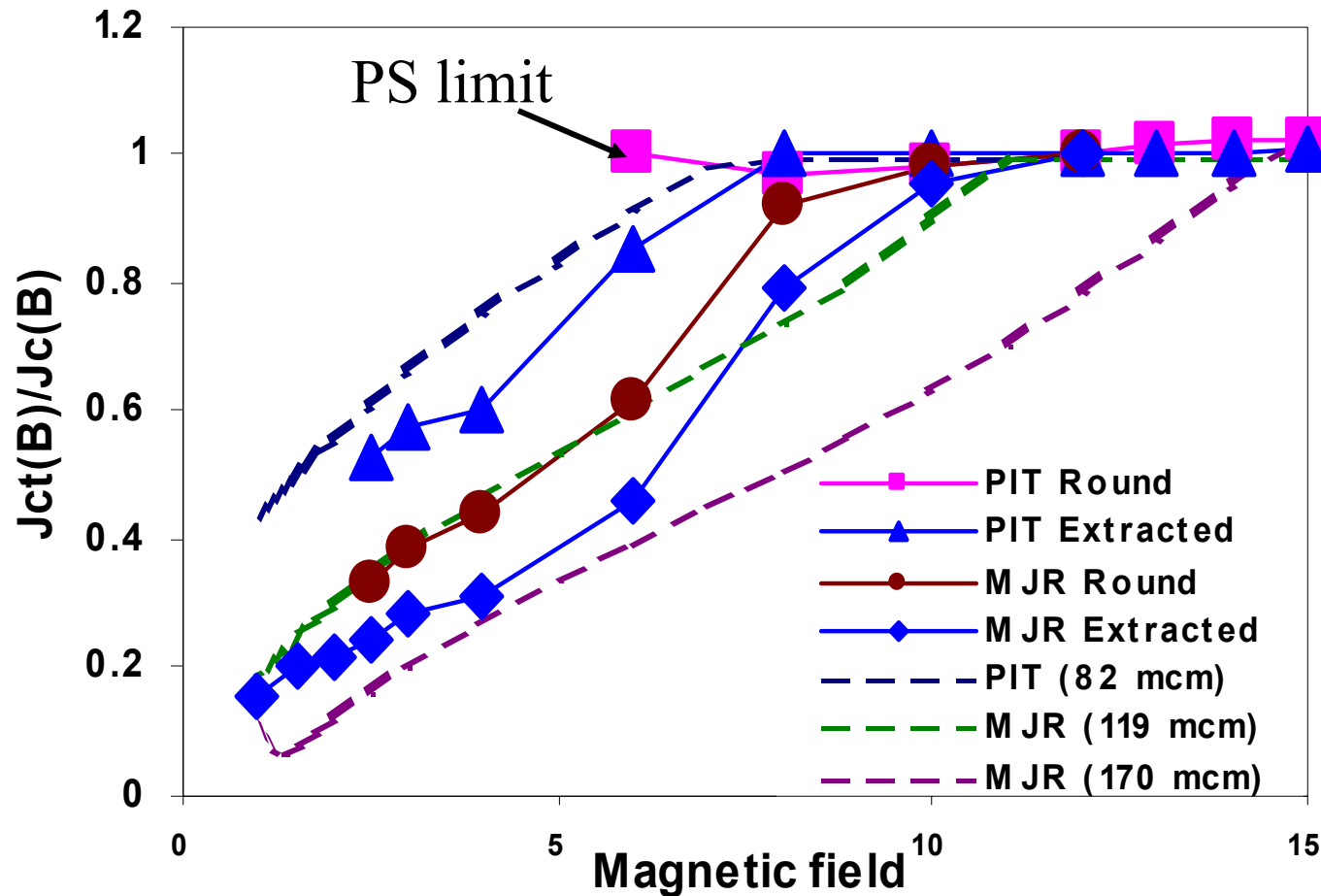
- Top plot shows the fraction of short sample current a magnet can carry as a function of peak design field for various $J_c \cdot D_{eff}$.



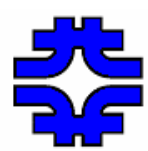
- Bottom plot shows the maximum $J_c \cdot D_{eff}$ allowed as a function of magnet peak design field.



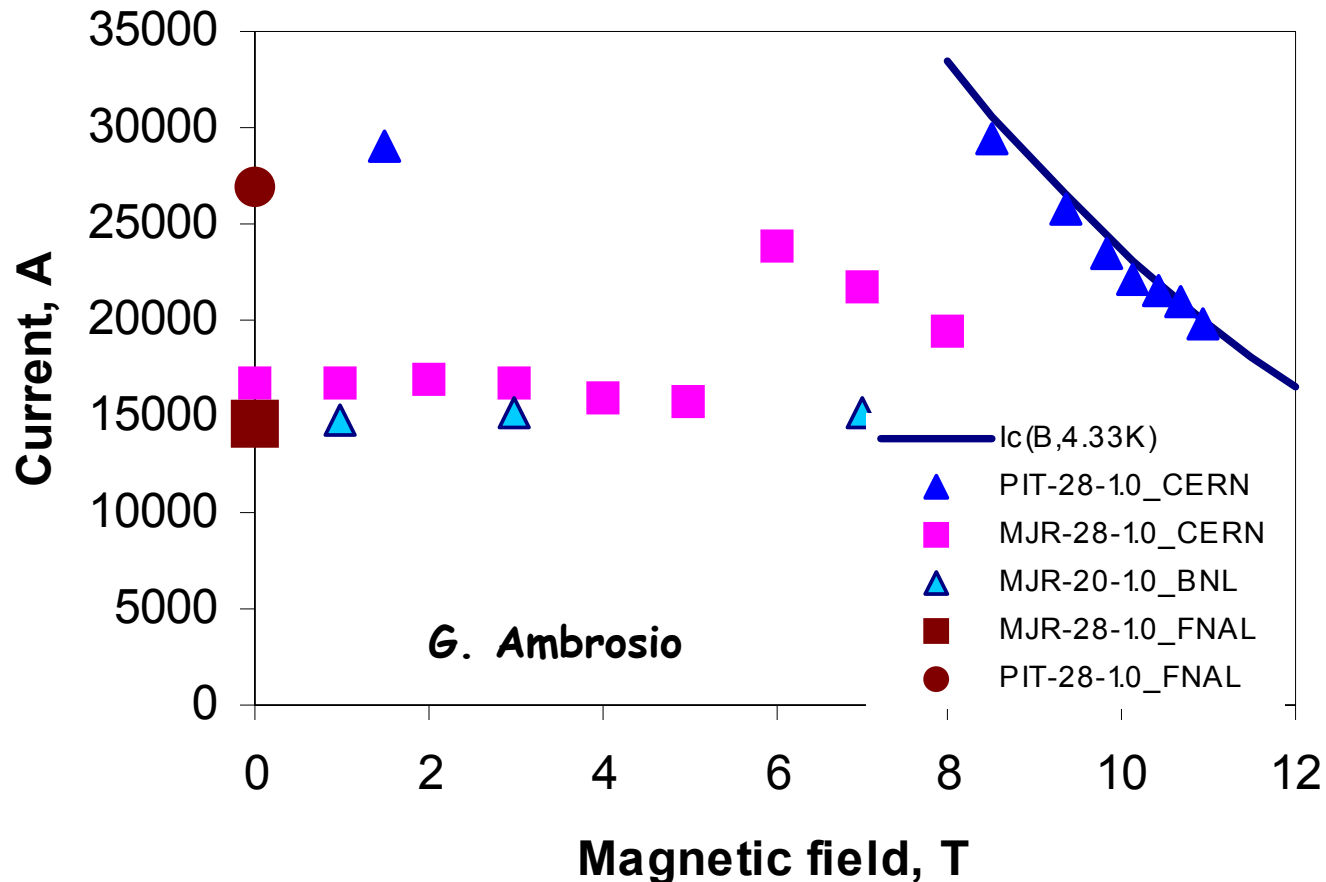
Effect of D_{eff} on Normalized I



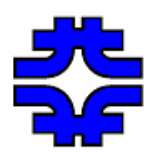
At a given field, current degradation increases with increasing D_{eff} .



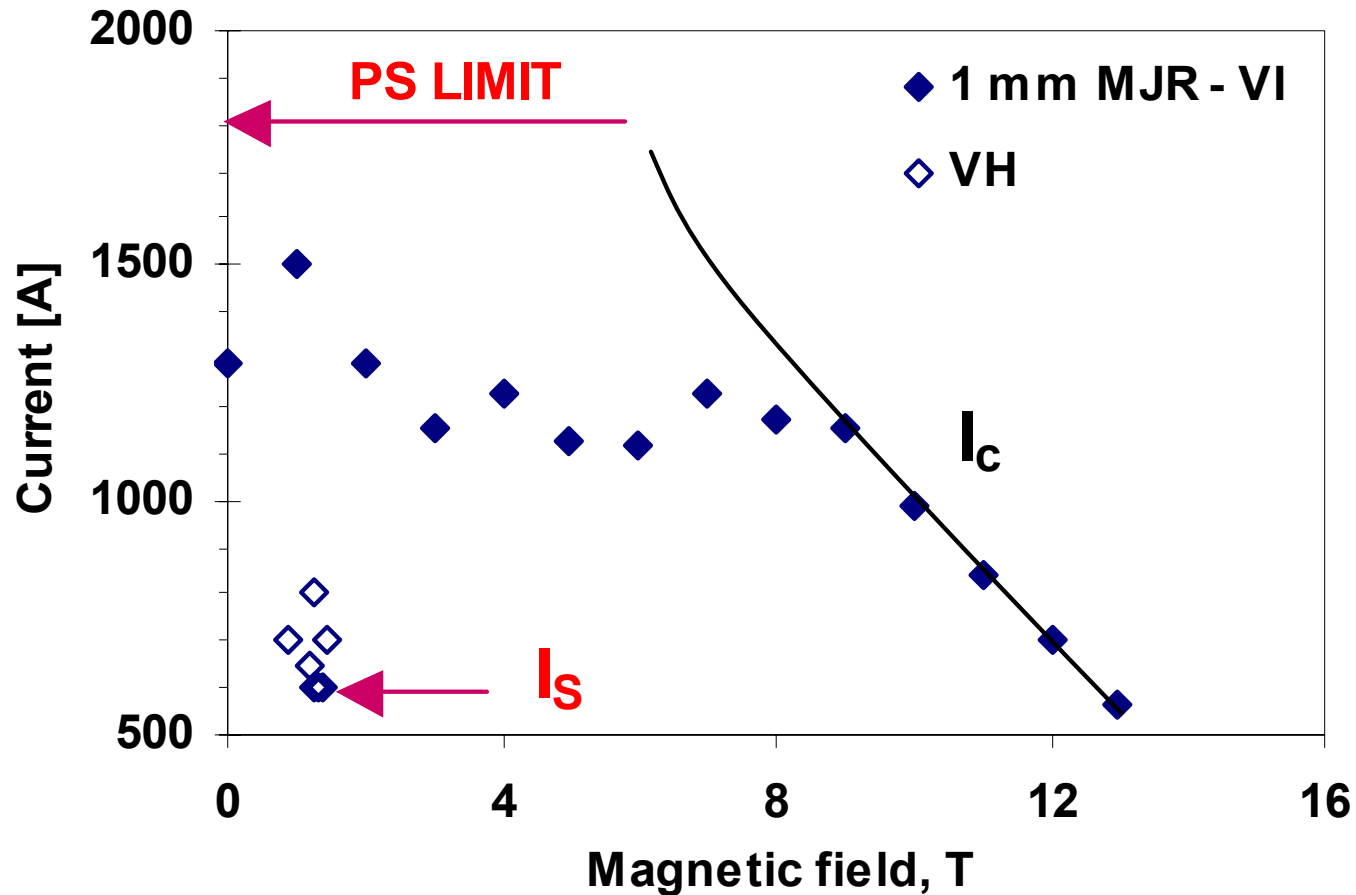
Cable Tests



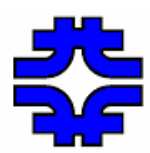
Cable samples tested at BNL ($B < 7$ T, 4.3 K), CERN ($B < 10$ T, 1.8-4.2 K) and Fermilab ($B < 2$ T, 2.8-4.5 K) confirmed unstable behavior of conductors with large D_{eff} .



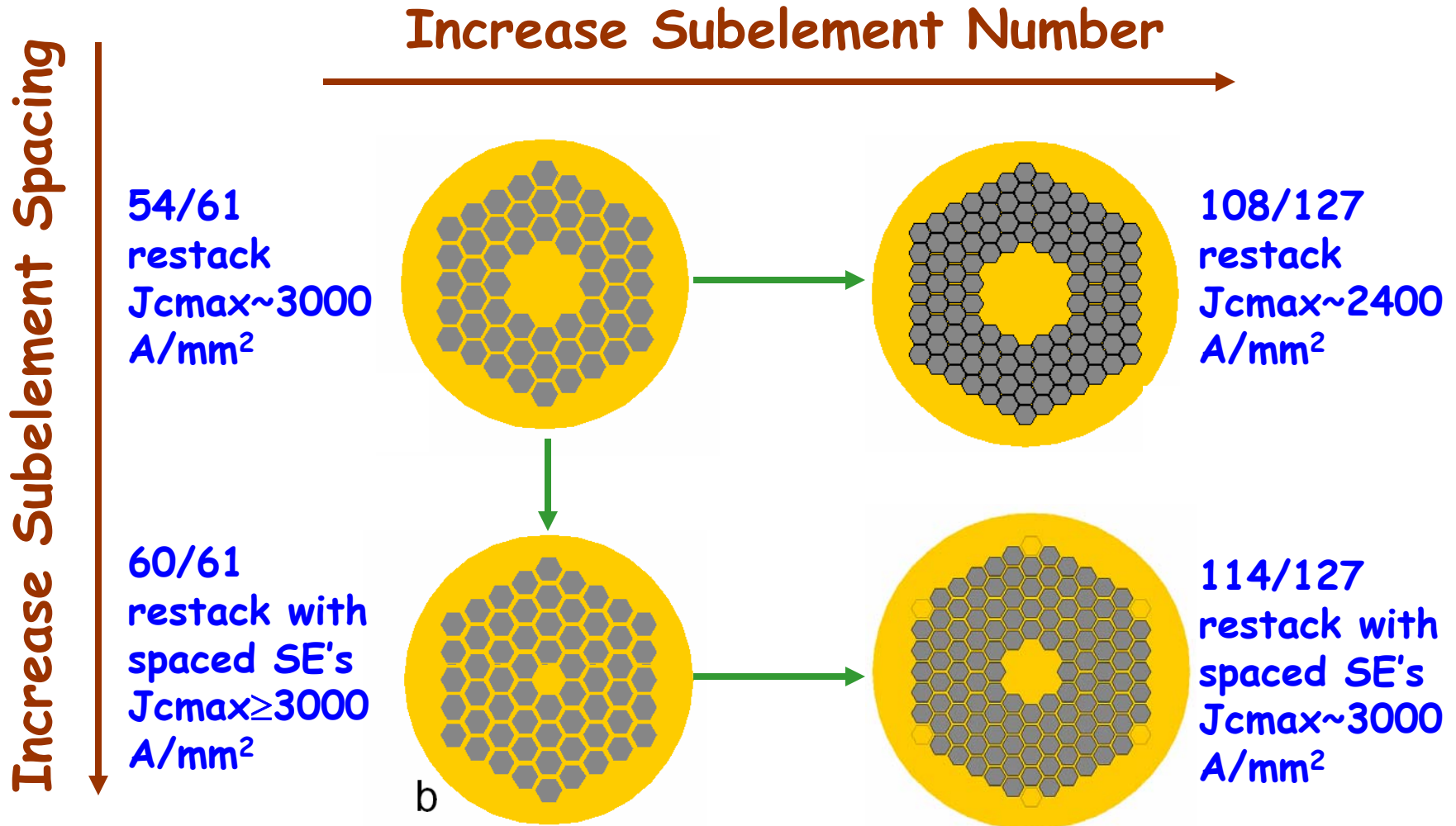
VI and VH Measurements

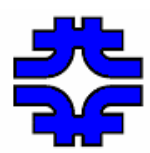


Based on our model's predictions, FNAL and other LABS introduced a VH test to pinpoint the minimum quench current predicted.

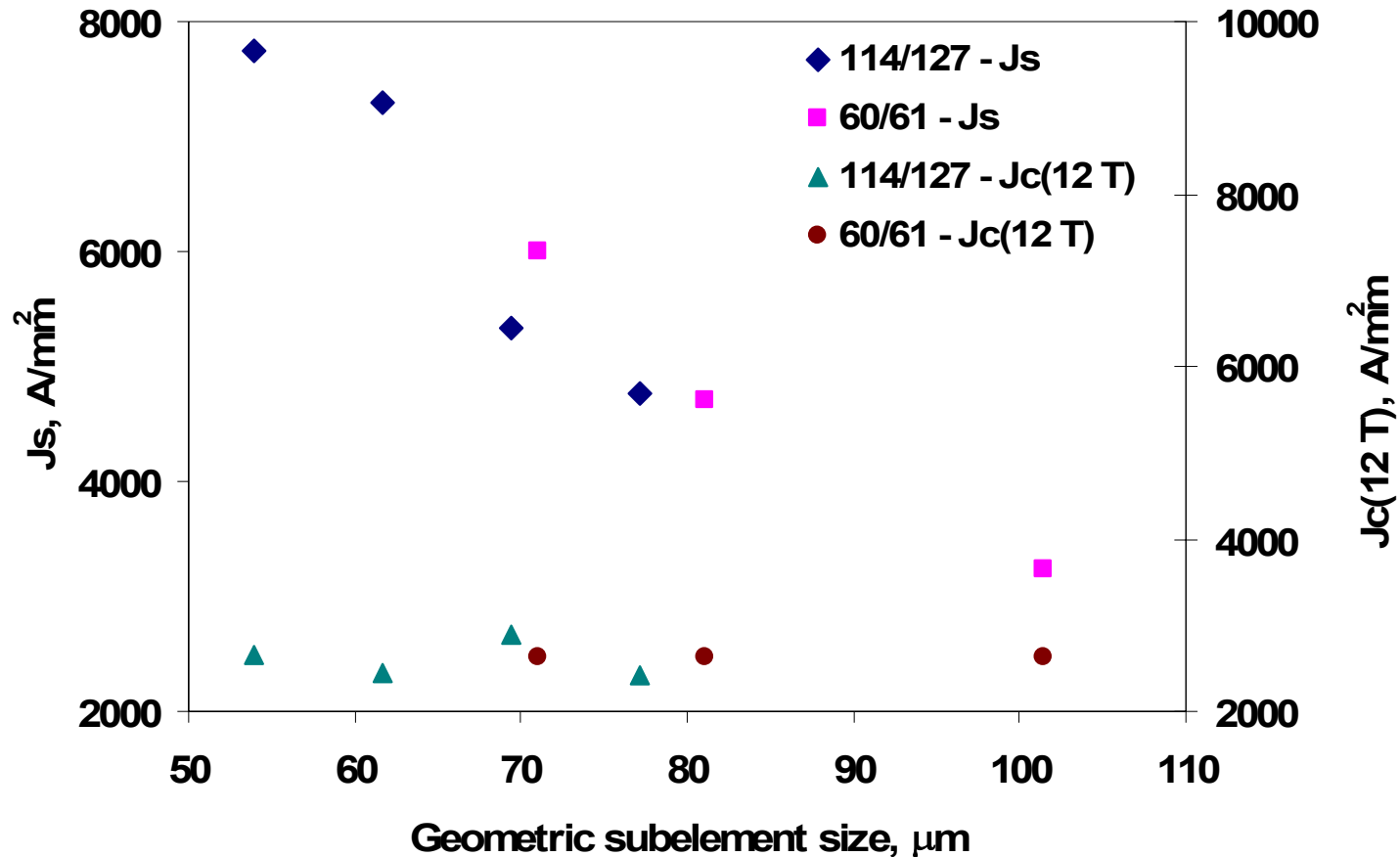


RRP Strand Development with OST

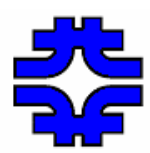




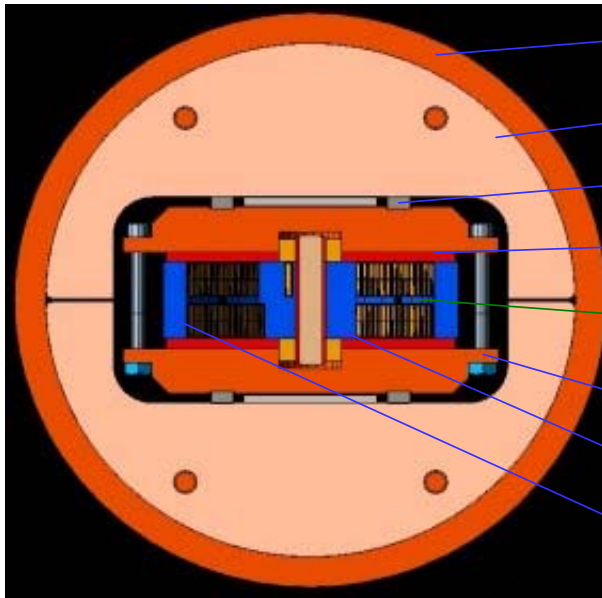
Effect of Subelement Size



Clear dependence of J_s with subelement size for round strands with similar J_c 's and RRR's.



Small Racetrack (SR)



Cylinder – Al 6061 – T6

Yoke – 1010 Steel

Load key – 1018 Steel

Skin – 1010 Steel

Interlayer spacer – G10

Pressure Pad – 1018 Steel

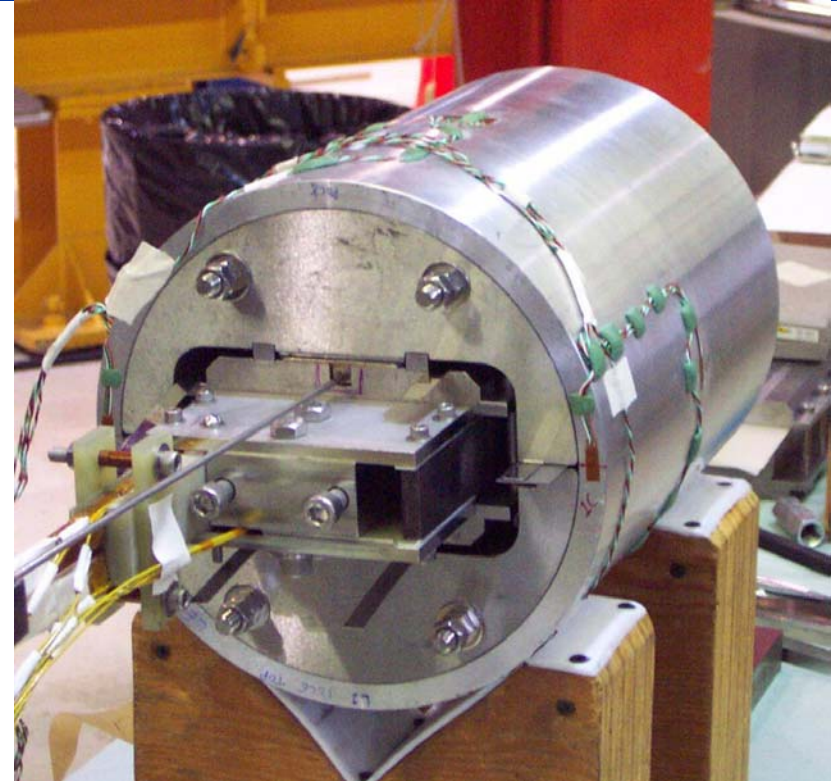
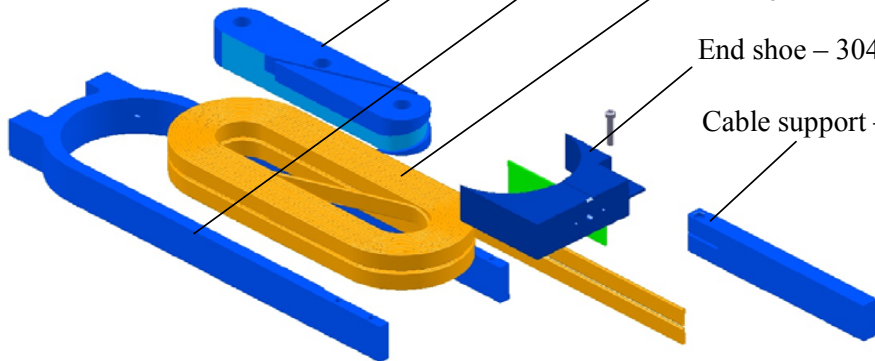
Pole piece – 1010 Steel

Horseshoe – 304 steel

Two layer coil –
Nb₃Sn cable

End shoe – 304 steel

Cable support – G10



- **LBNL design**
- **Simple to fabricate**
- **Used as cable test before fabricating dipoles**



SR02 and SR03

1 mm MJR (54 el.) 1 mm RRP (108 el.)

$d_{\text{eff}} = 110 \mu\text{m}$



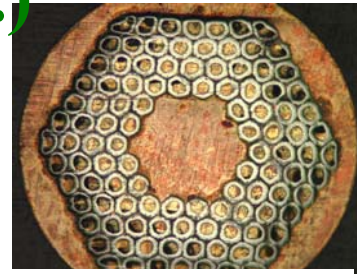
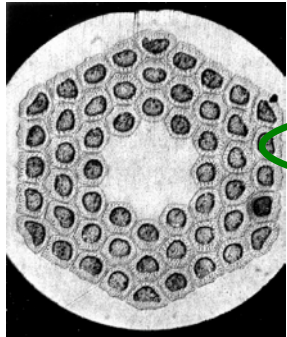
$d_{\text{eff}} = 80 \mu\text{m}$

$J_c = 2100 \text{ A/mm}^2$

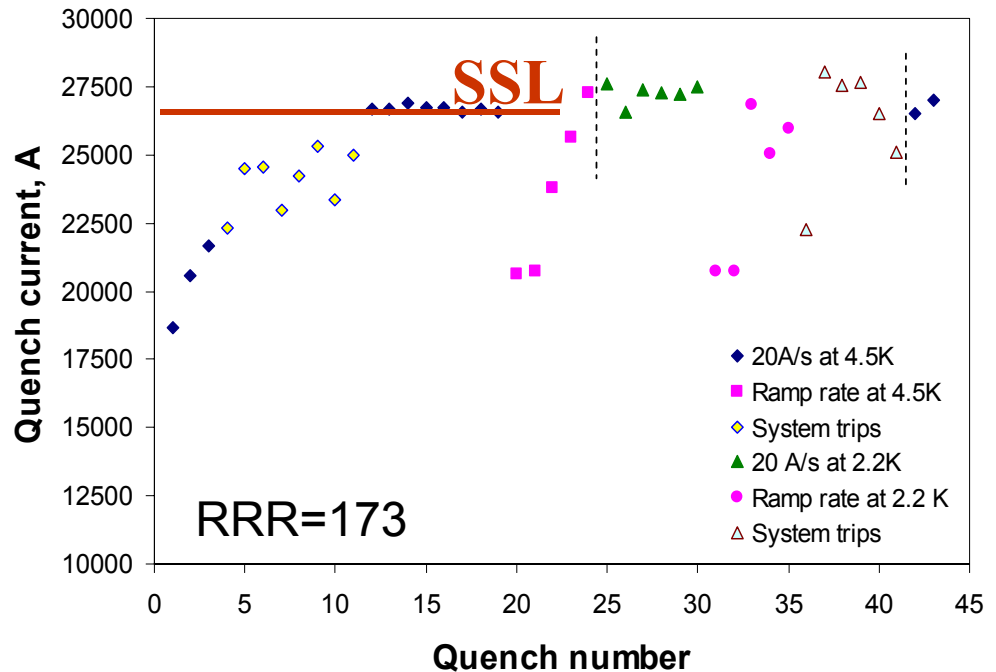
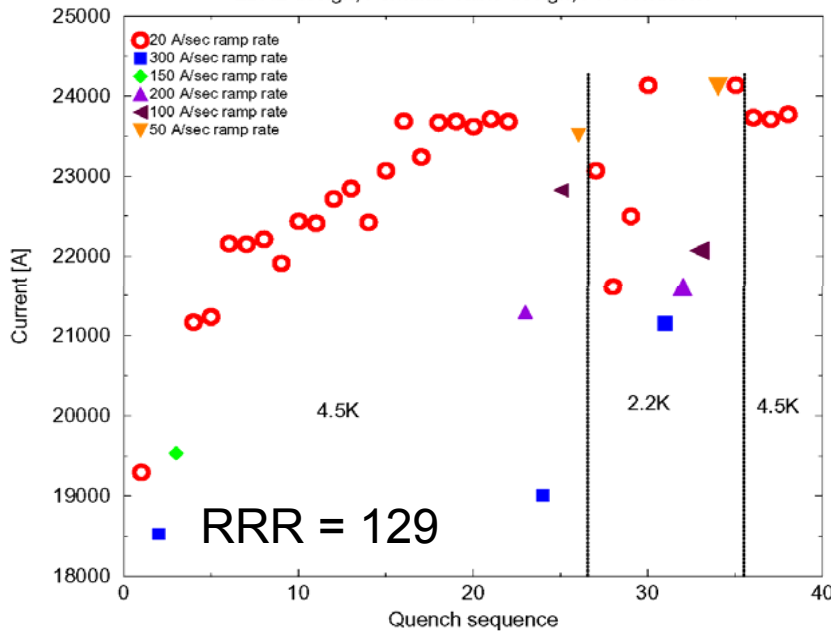
$J_c = 2300 \text{ A/mm}^2$

SR01 Quench History

SSL

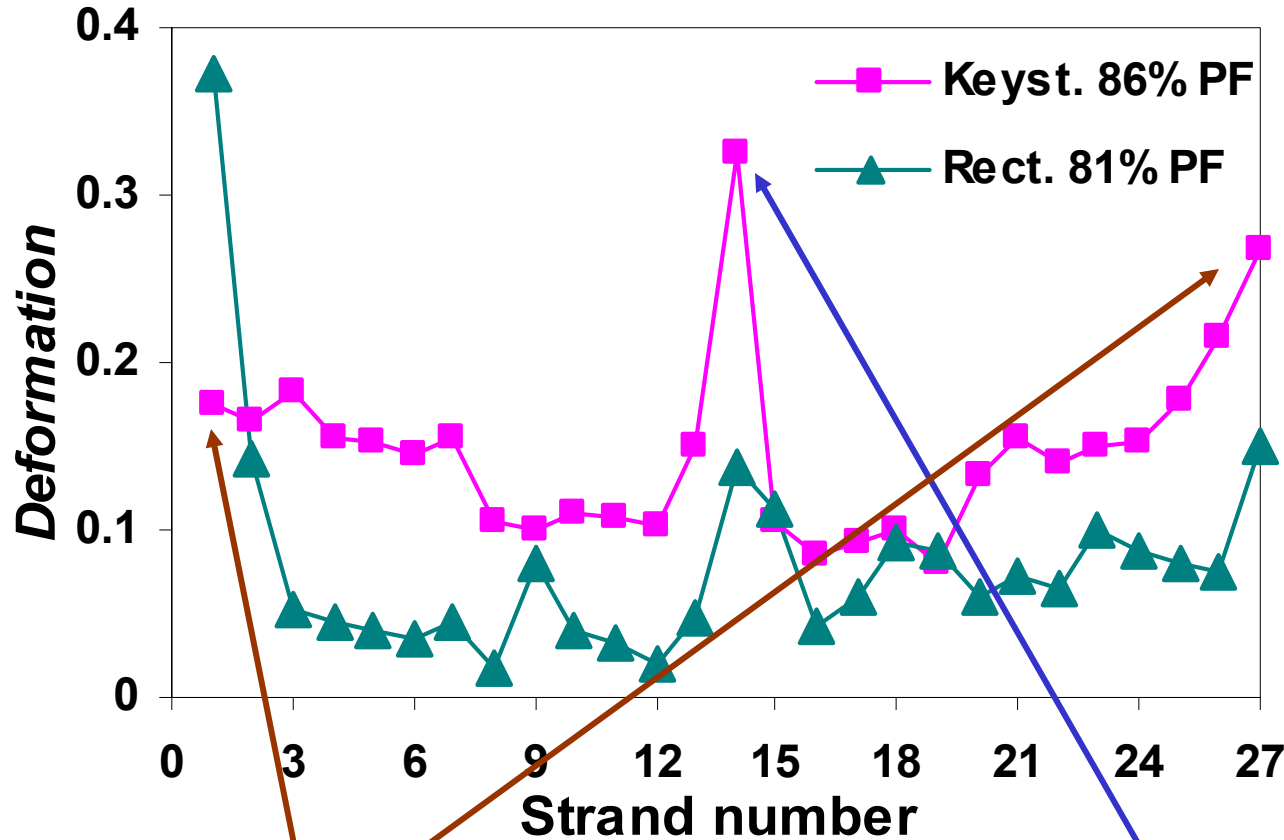


LBNL design, Fermilab cable design, PIT conductor

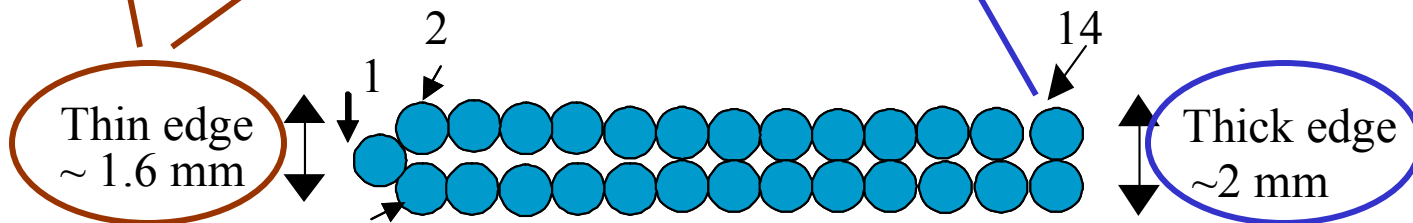




Deformation of Strands in Cables



$$Deformation = \frac{d_{max} - d_{min}}{d_0}$$





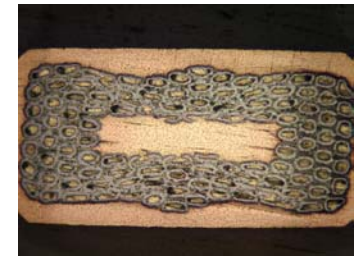
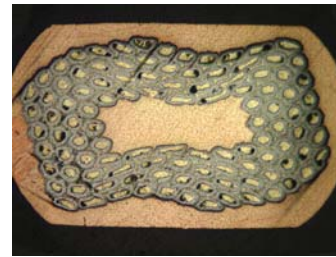
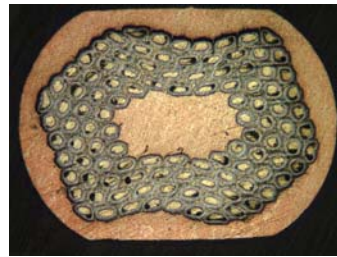
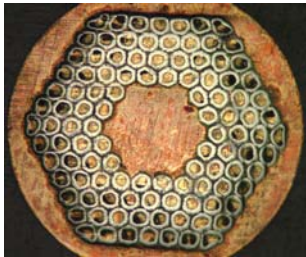
Effects of Cabling on Subelement Size

- **At least two phenomena during Rutherford cabling can increase the effective filament size:**
 - * **deformation, which changes the filament size distributions, with the average filament size typically increasing.**
 - * **filaments sometimes merging into each other creating larger non-Cu areas with somewhat continuous barriers. If filaments are fused together, the strand sees a larger d_{eff} and its instability can dramatically increase locally.**

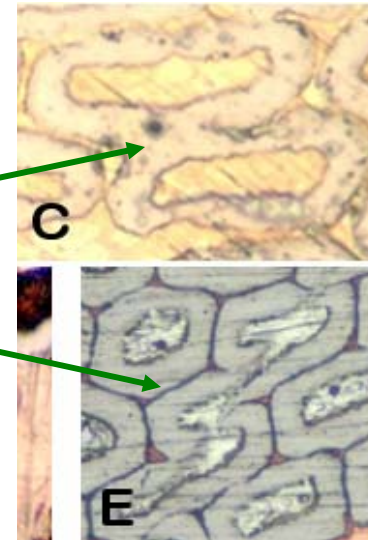


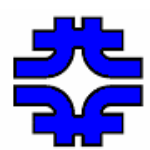
Simulating Deformation

This can be better seen by simulating cabling deformation using homogeneously rolling to decreasing thicknesses.

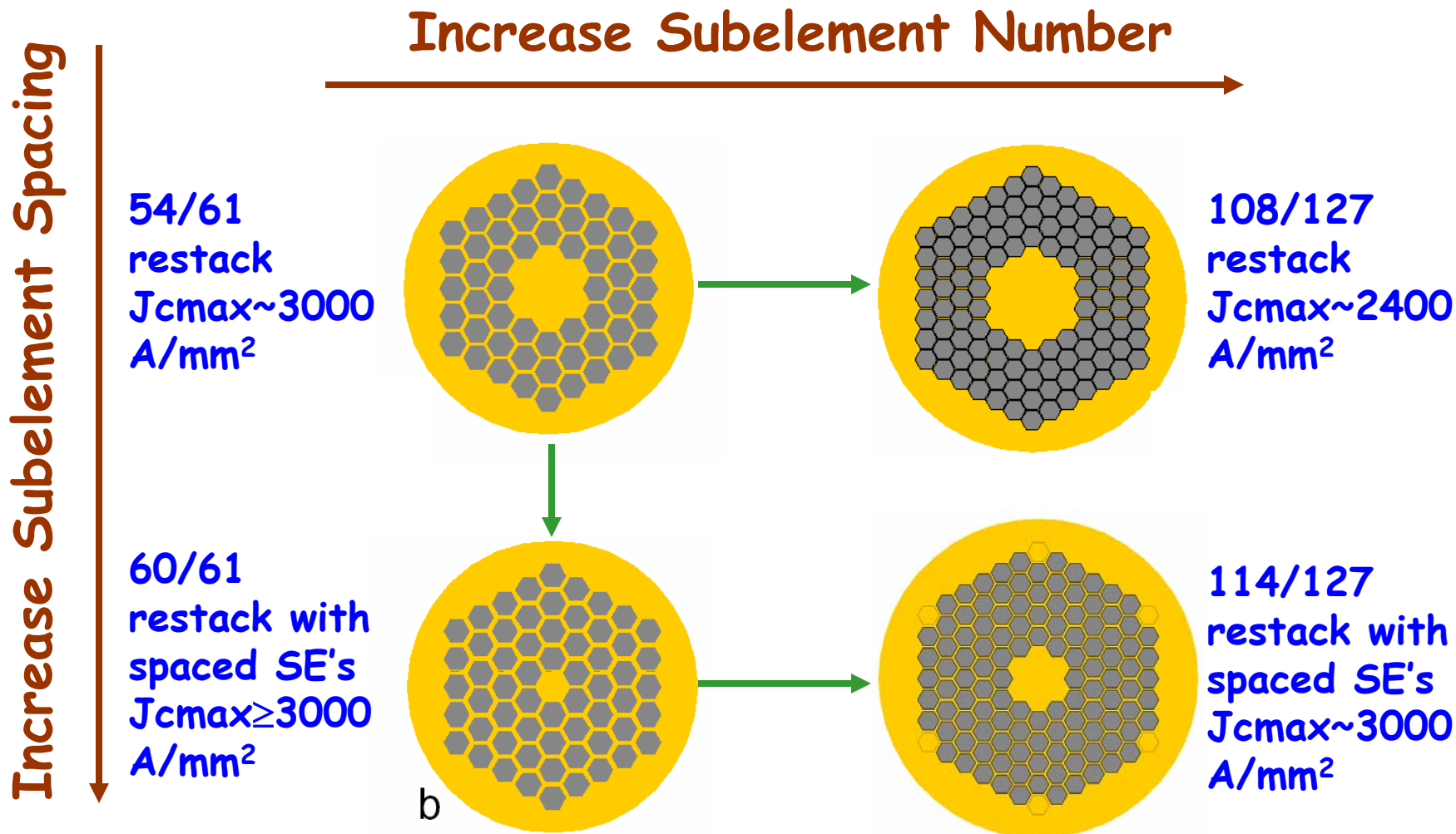


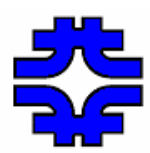
**MERGING OF
SUBELEMENTS**



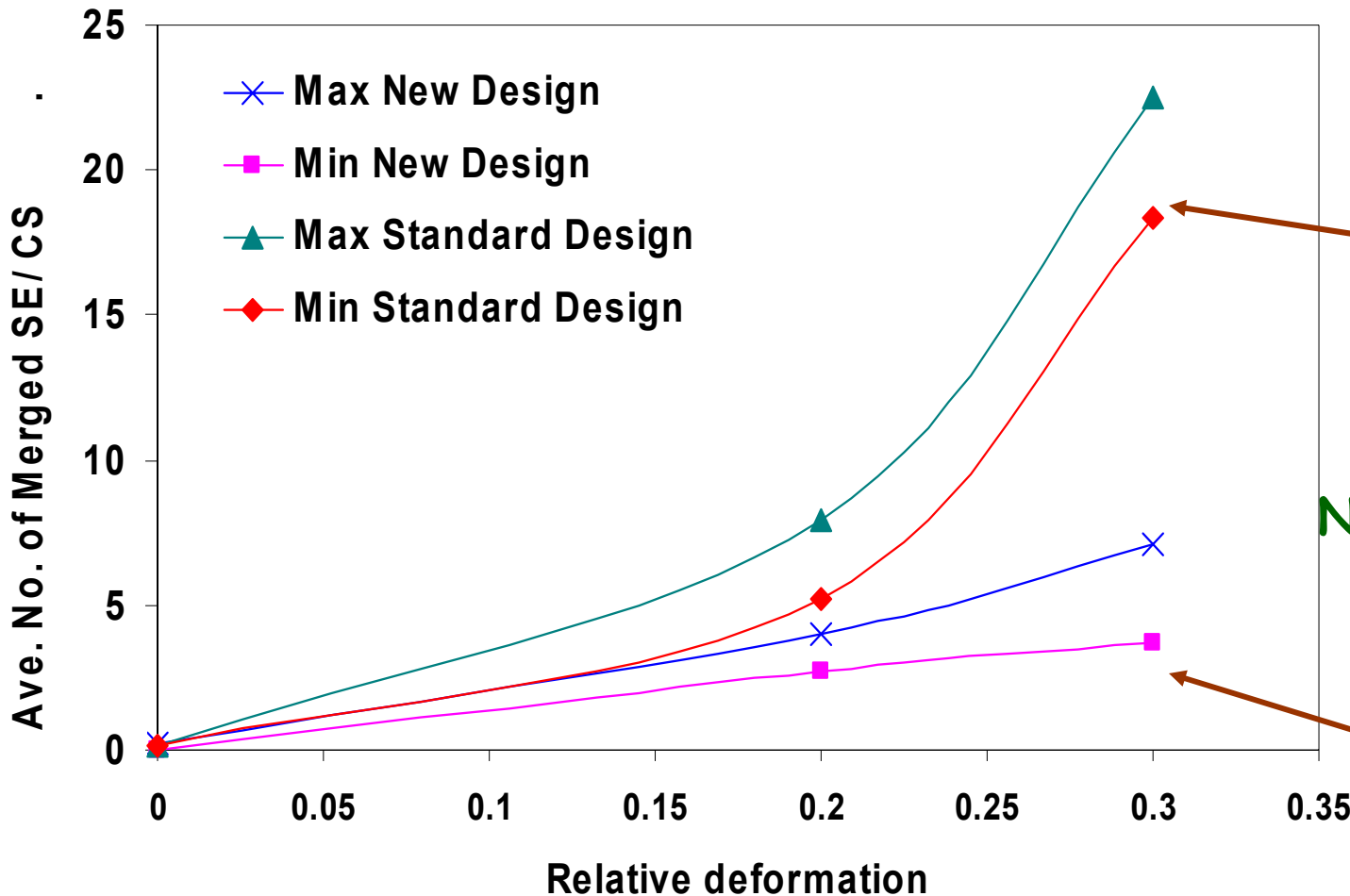


RRP Strand Development with OST

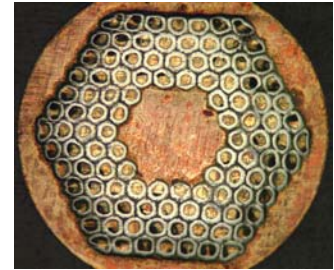




Merging Analysis

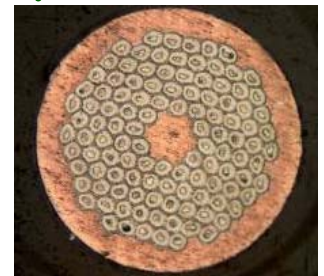


Standard design



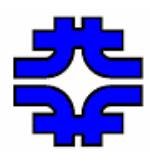
108 el.

New design with spaced SE's

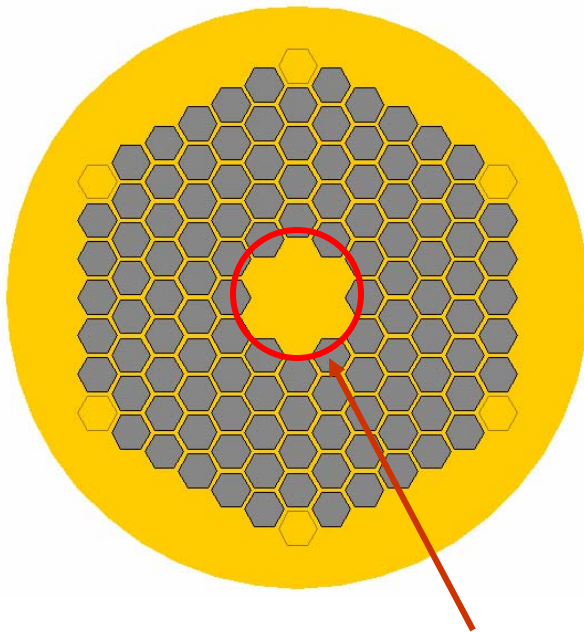


114 el.

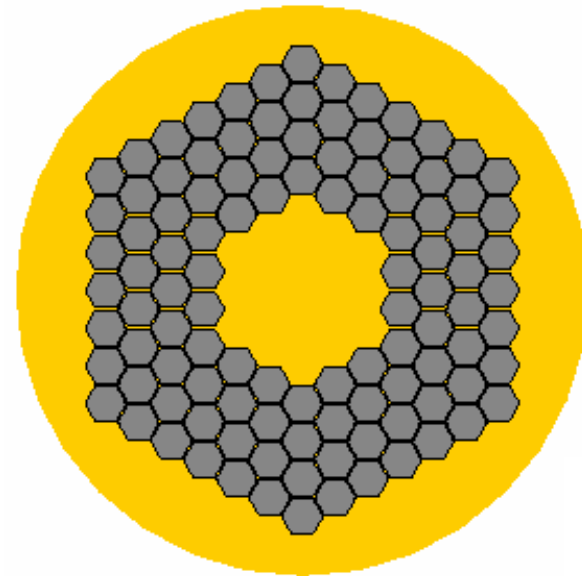
The merging in the new design was lower.



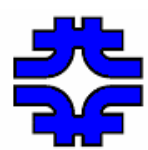
Refinement of the Design with OST



Remove inner row

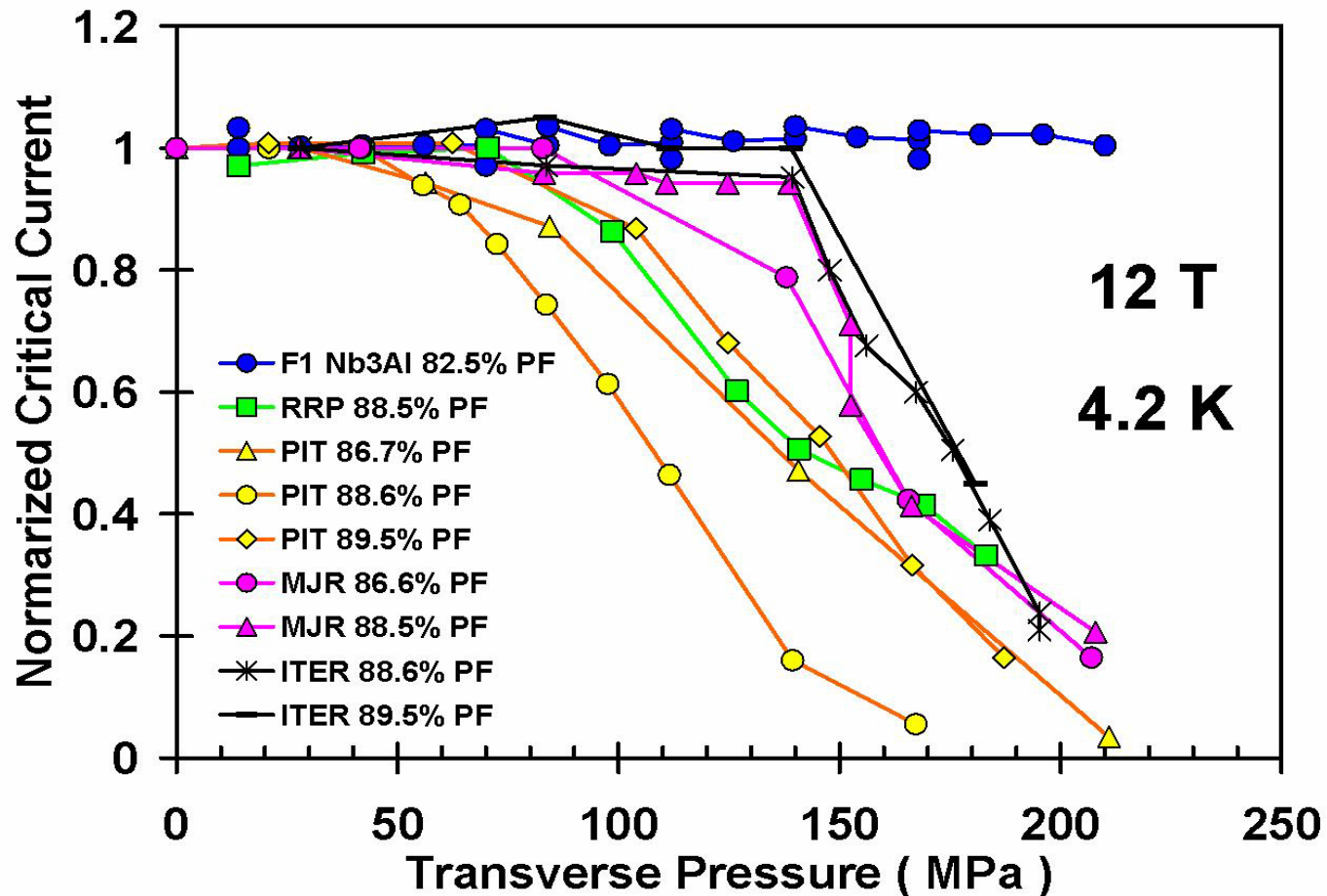


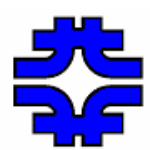
**Remove inner row and add
back corners**



Nb₃Al Comeback

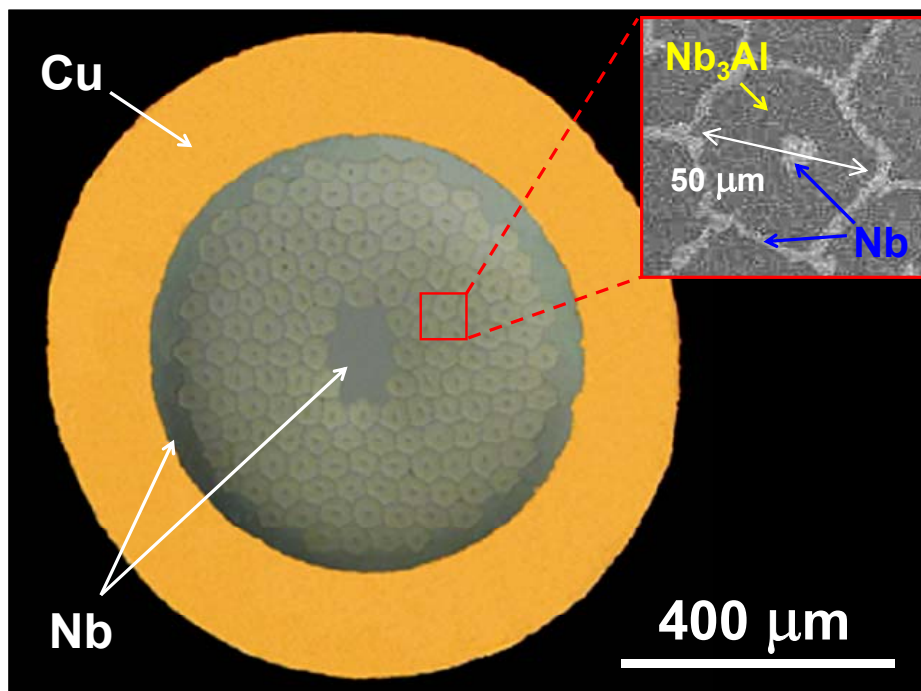
In collaboration with Akihiro Kikuchi, from the National Institute of Material Science (NIMS), Tsukuba, Japan, since 2005



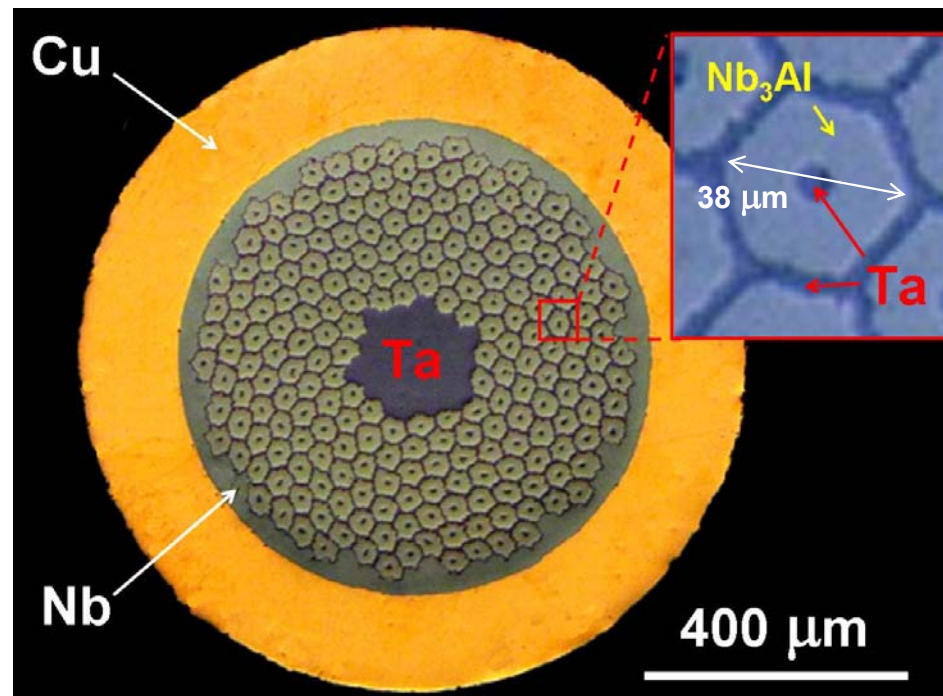


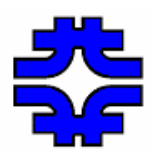
Nb₃Al Strand Designs

(a) F1-Nb₃Al strand (2006)



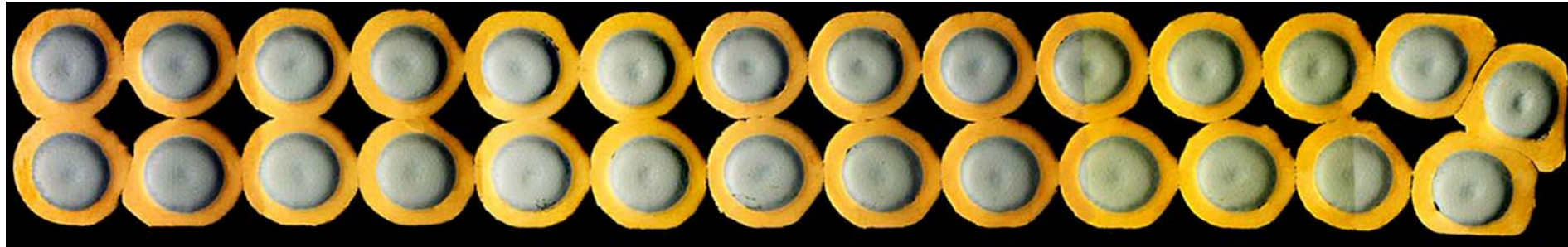
(b) F3-Nb₃Al strand (2007)





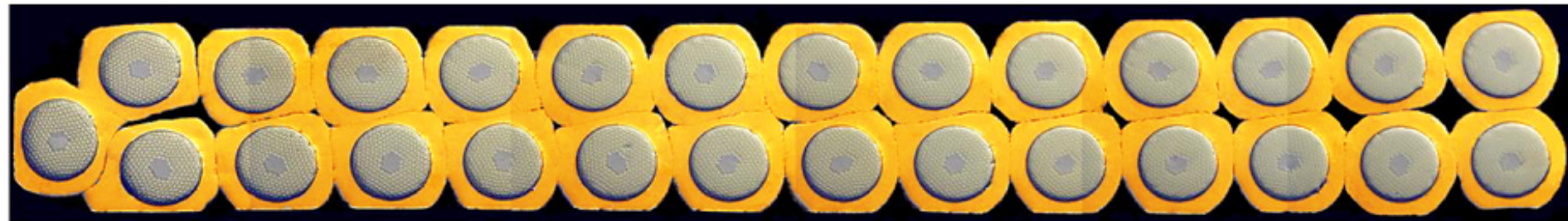
Nb₃Al Rutherford Cable R&D

(a) Low Compaction F1-Nb₃Al Cable (2006)

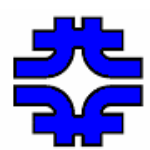


Width: 14.17 mm, Thickness: 1.99 mm, Rectangular, PF: 82.5 %

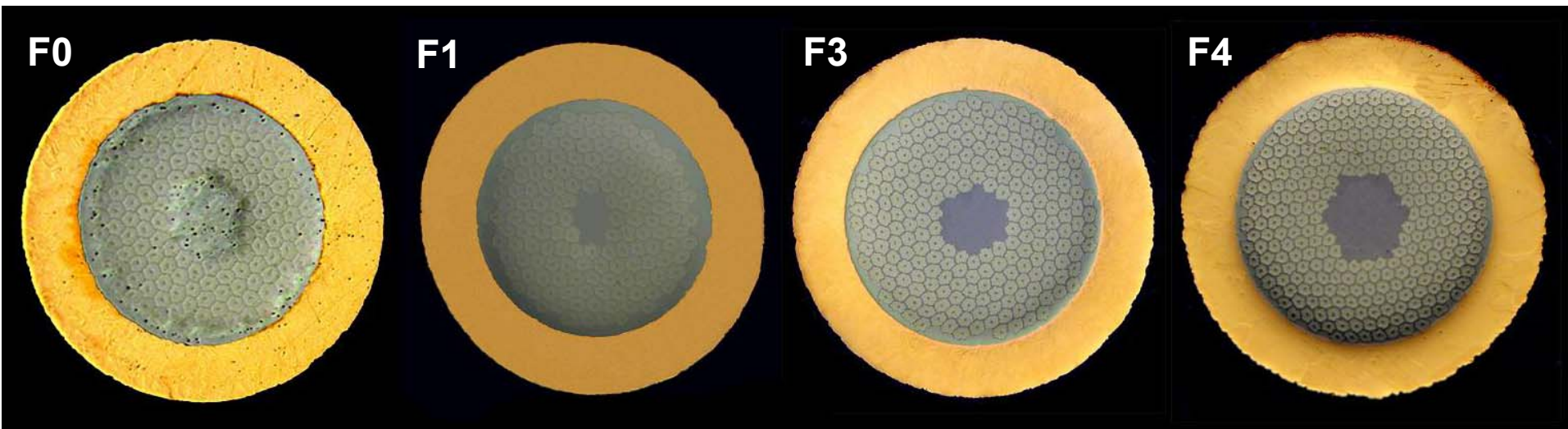
(b) Highly Compacted F3-Nb₃Al Cable (2007)



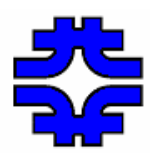
Width: 14.18 mm, Thickness: 1.78 mm, Keystoned, PF: 87.0 %



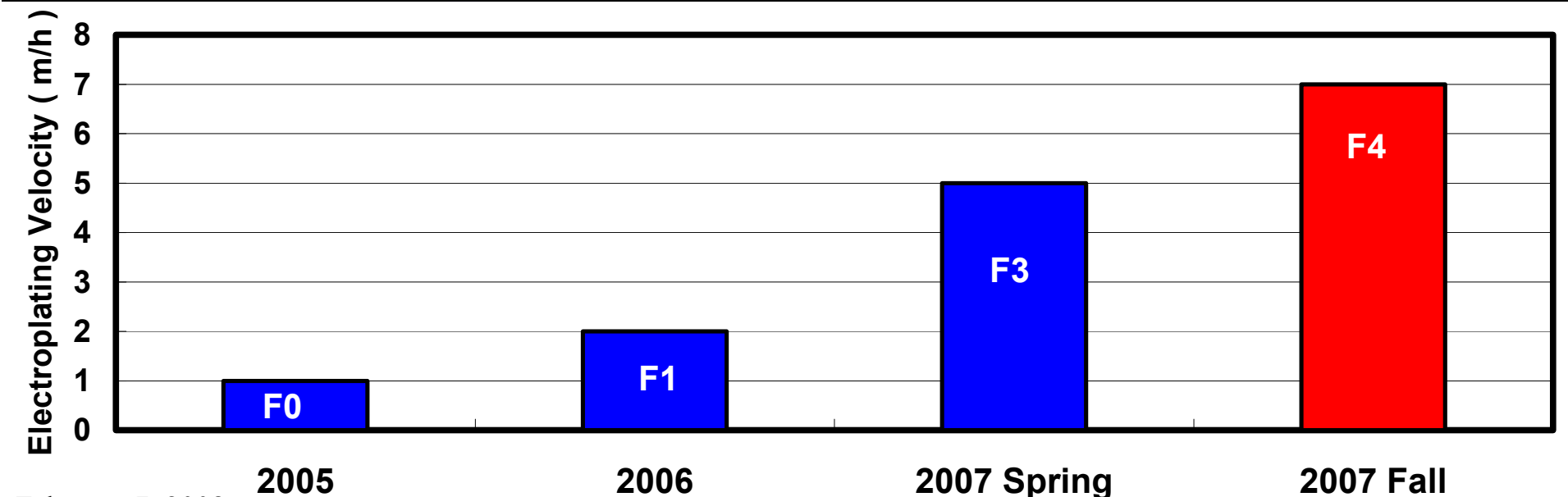
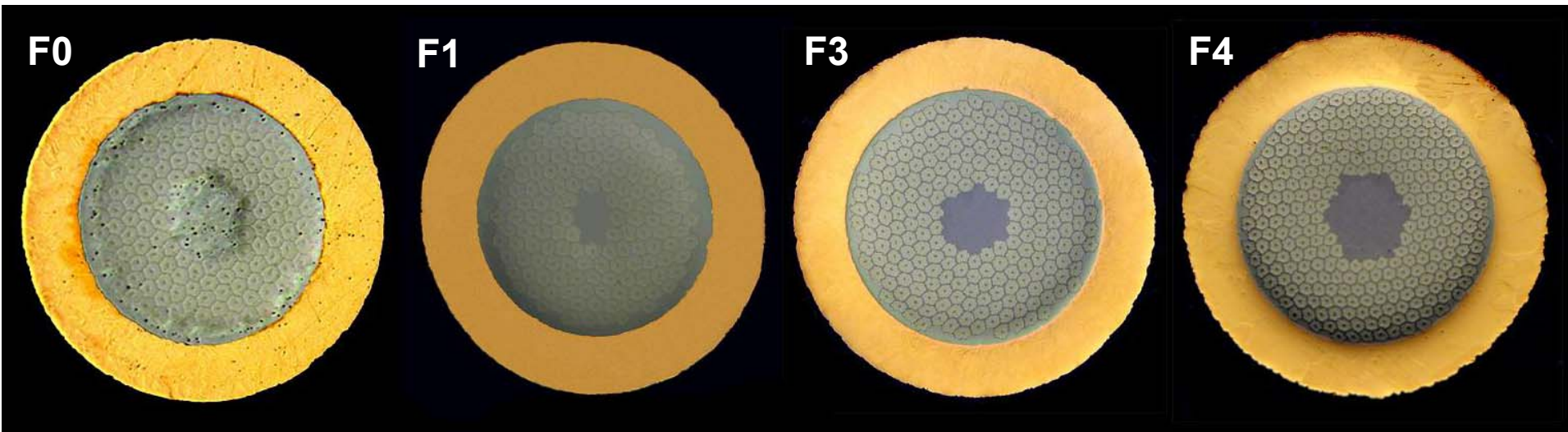
Nb₃Al strand specification

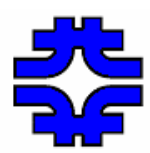


	F0	F1	F3	F4
Strand dia. (mm)	1.03	1.03	1	1.04
Filament dia. (mm)	50	50	38	38
Filament number	132	144	222	276
twist pitch (mm)	362	362	none	45
Cu ratio	1 (50%)	1 (50%)	1 (50%)	0.87 (46.6%)

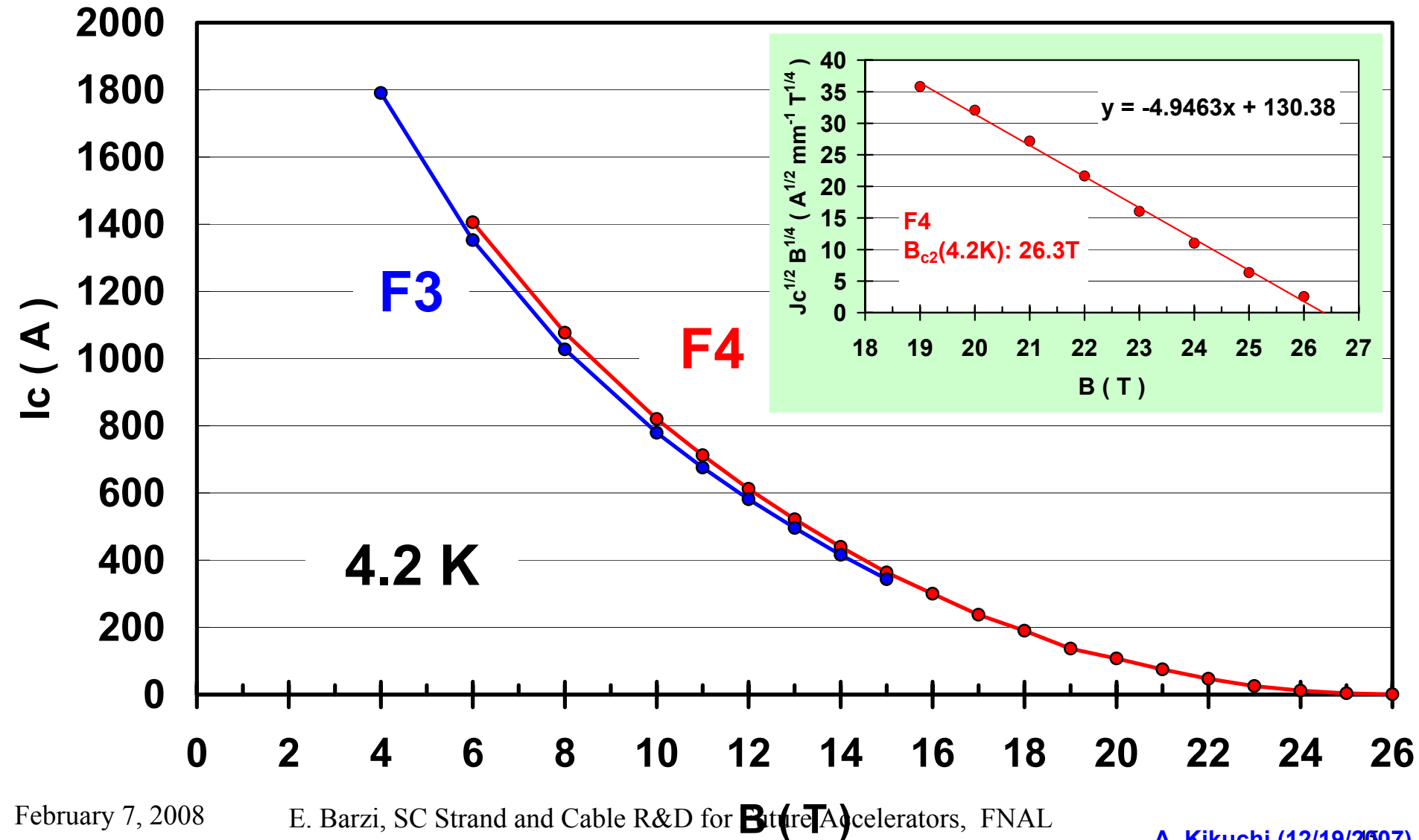


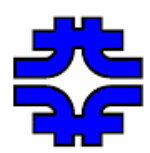
Electroplating Velocity





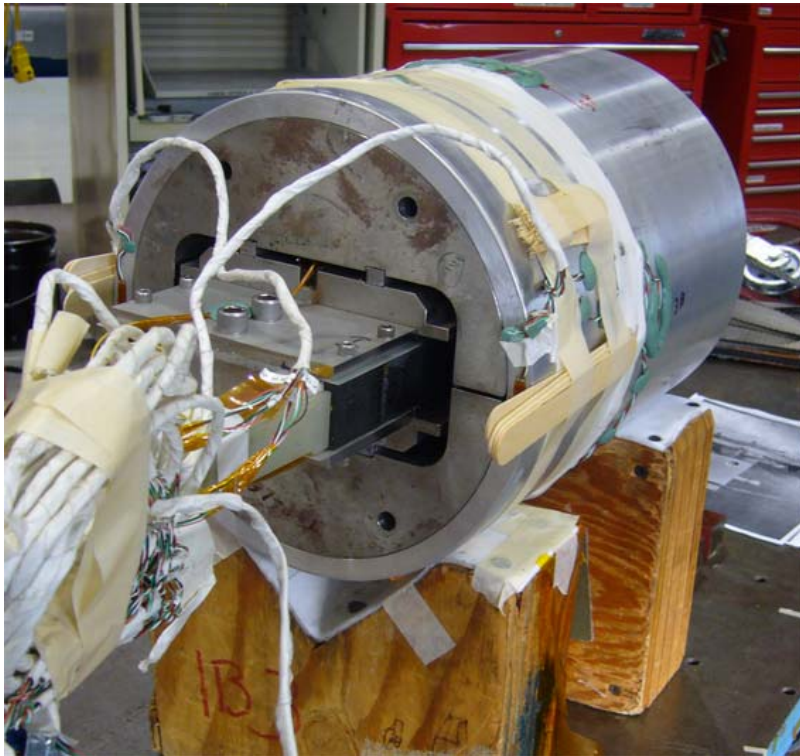
Ic and Bc2 of F4



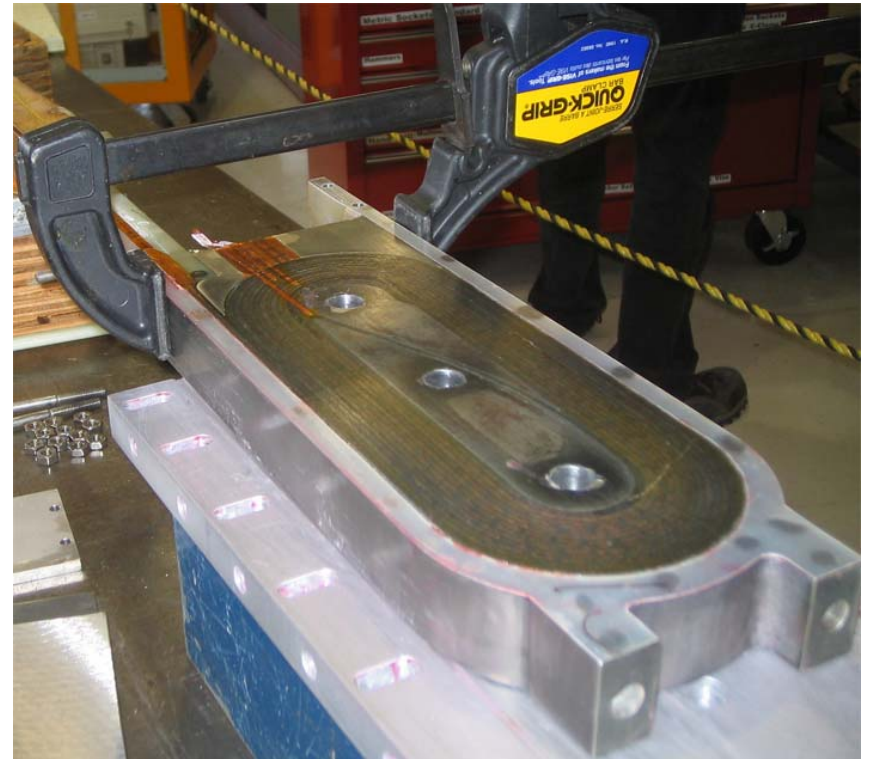


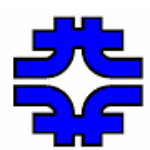
Nb₃Al Small Racetrack Magnets

(a) SR-04 (2006) - TESTED



**(b) SR-05 (2007)
TO BE TESTED**



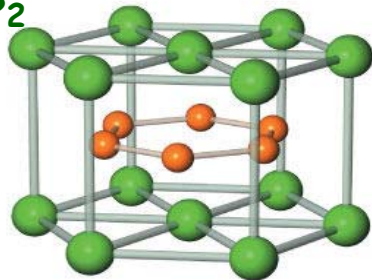


HTS Crystal Structure

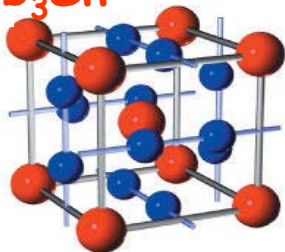
NbTi



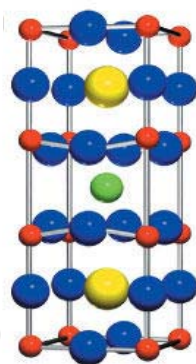
MgB₂



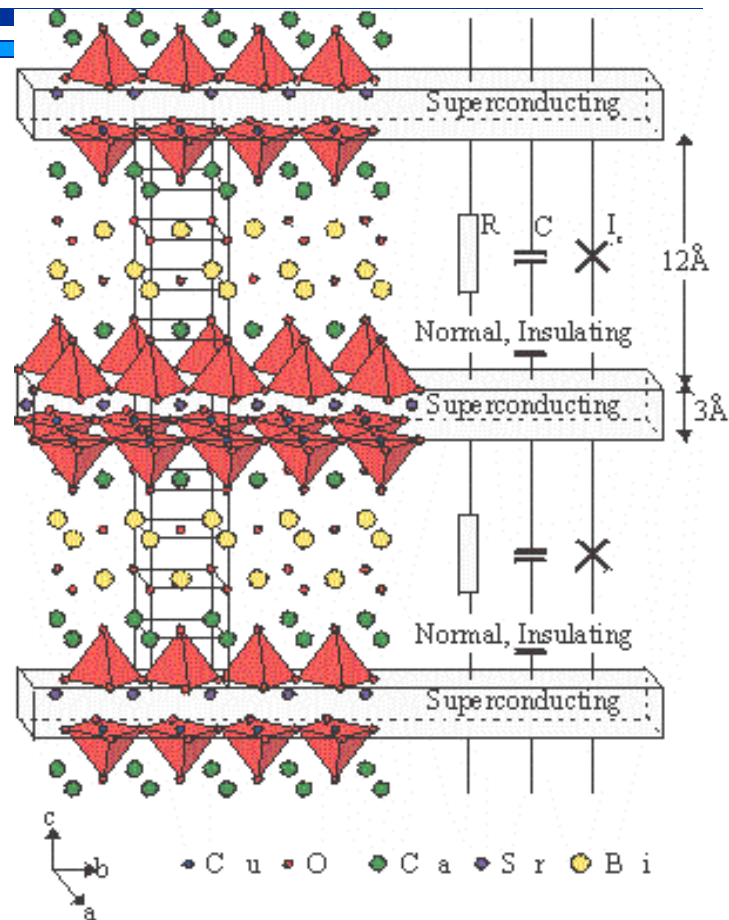
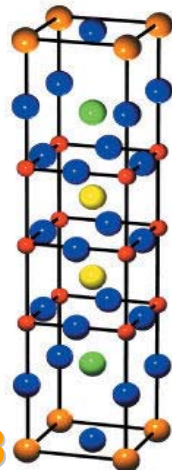
Nb₃Sn



YBCO



BSCCO-2223



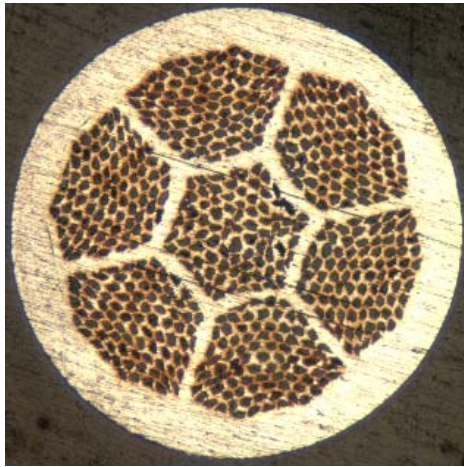
Anisotropic layered structure



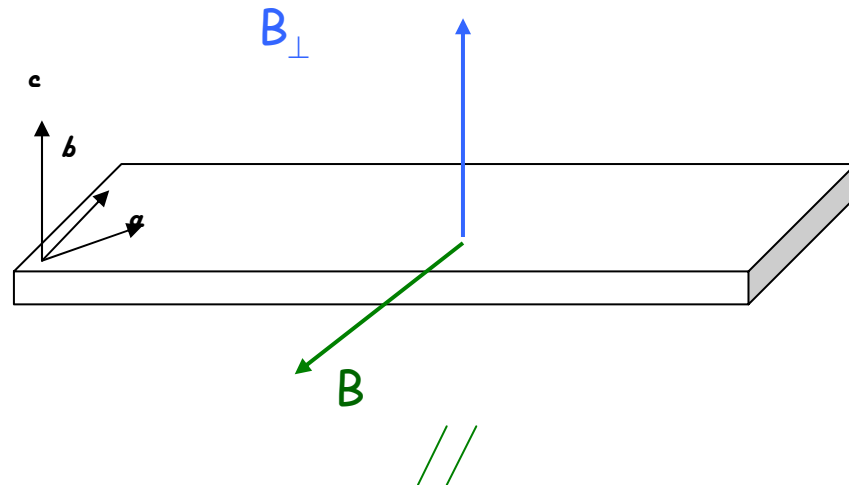
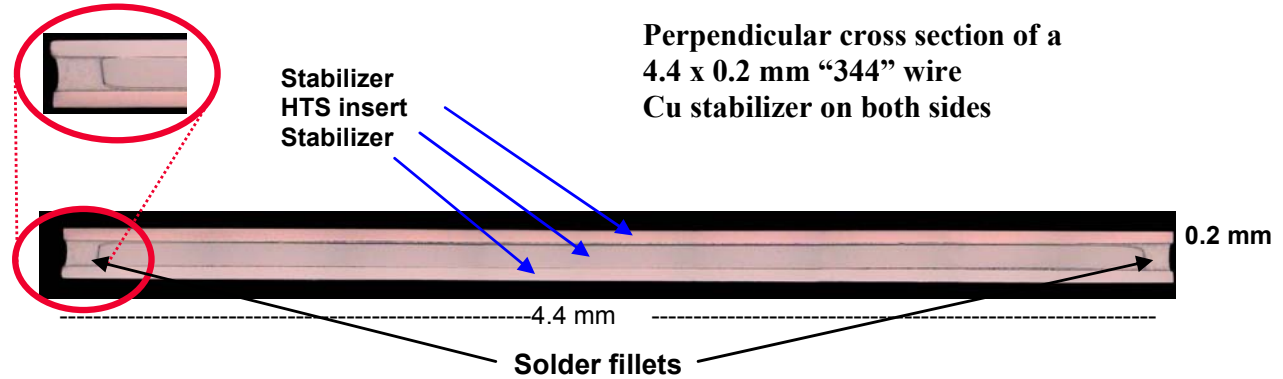
- o Suppression of H^* compared to H_{c2} :
- o Anisotropy of J_c and H_{c2} parall. (ab plane) and perp. (c direction) to the superconducting layers

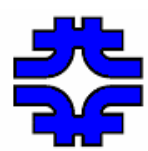
Round Wires and Anisotropic Tapes

2nd Generation Coated YBCO



BSCCO 2212



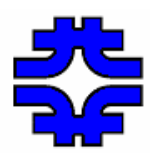


R&D for HTS

MISSION

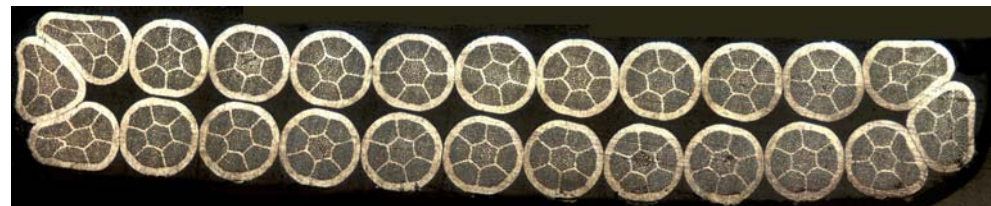
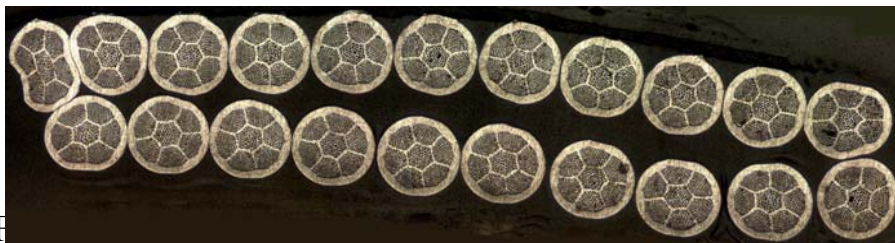
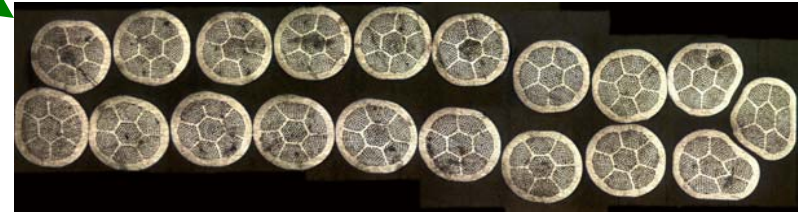
The experiment at FNAL to confirm that ionization cooling is an efficient way to shrink the size of a muon beam would pave the way for Muon Collider machines, which require in their last stages of cooling and of acceleration very high field (> 25 T) solenoids.

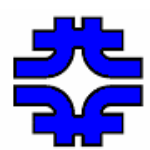
- Monitor state-of-the-art HTS's and keep all options open
- Solve the powder leak problem in Bi-2212
- Understand field and temperature dependence of anisotropy



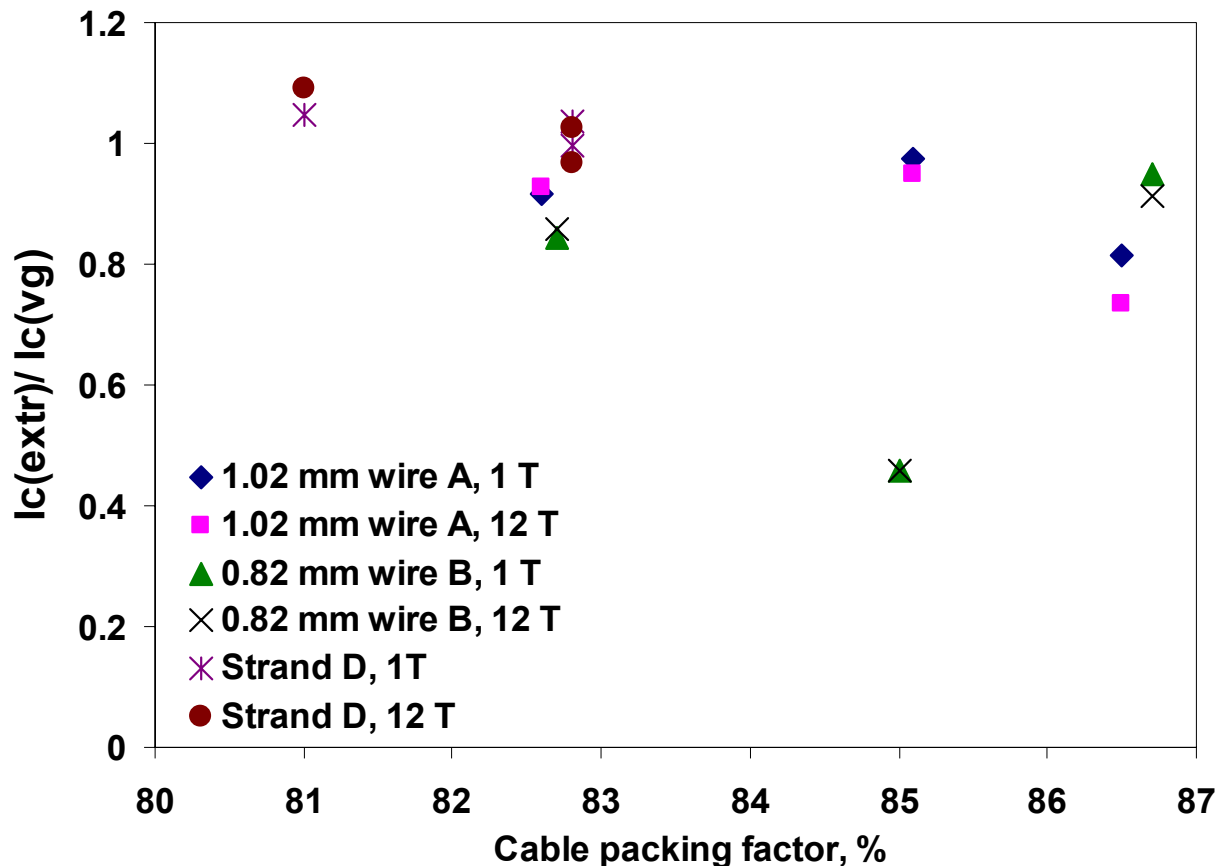
Cable Samples

Cable ID	No. strands	Strand size, mm	Strands used	Ave. thickness, mm	Average width, mm	PF, %	Tested
1	19	1.02	A	1.938 ± 0.003	9.992 ± 0.050	82.6	Y
2	“	“	“	1.883 ± 0.007	9.987 ± 0.031	85.1	N
3	“	“	“	1.848 ± 0.009	10.008 ± 0.022	86.5	Y
4	24	0.81	B	1.554 ± 0.008	9.921 ± 0.072	82.7	Y
5	“	“	“	1.51 ± 0.010	9.928 ± 0.035	85.0	N
6	“	“	“	1.485 ± 0.014	9.896 ± 0.051	86.7	Y
7	27	0.692	D (24), copper (3)	1.309 ± 0.011	9.876 ± 0.059	81.0	N
8	24	0.81	D (20), B (4)	1.551 ± 0.022	9.921 ± 0.056	82.8	Y
9	21	0.911	D	1.711 ± 0.007	9.959 ± 0.082	82.8	Y

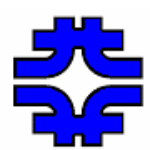




I_c of the Extracted Strand

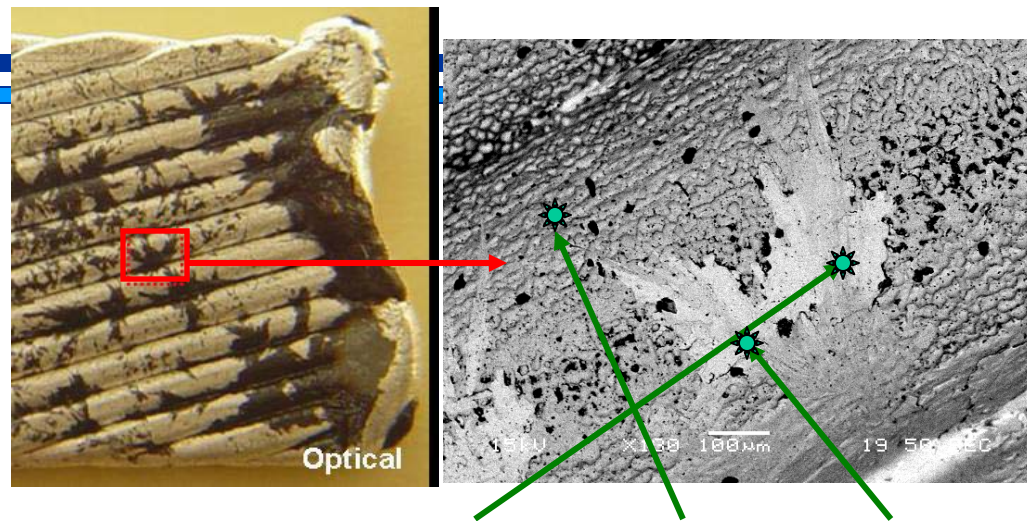


There is no noticeable dependence on B. Besides for a reproducible single case, the I_c degradation of the extracted strands was less than 20% at least up to 85% of packing factor. Strands of different designs behave differently to cabling. For instance the I_c degradation is larger for strand B, which is an older design that had not been optimized for cabling.



SEM/EDS Cable Surface Analysis

The surface of all the cables after reaction showed black spots embedded in the silver coating.



For all the cables, tested at self-fields of 0.1 to 0.3 T, an I_c degradation of about 50% was measured. This was much larger than the reduction found on the extracted strands.

Spectrum No.	1	2	3
Element	At. %	At. %	At. %
Ag (L)	0	100	0
Bi (M)	14.91	0	3.59
Sr (L)	9.04	0	2.21
Ca (K)	5.53	0	0.78
Cu (L)	11.49	0	5.80
Mg (K)	0	0	29.33
O (K)	59.03	0	58.28
Totals	100.00	100.00	100.00

A. Kikuchi

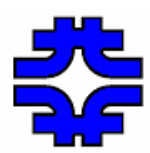
Bi-2212? **Bi-2212+MgO?**
Caused by filament powder leaks



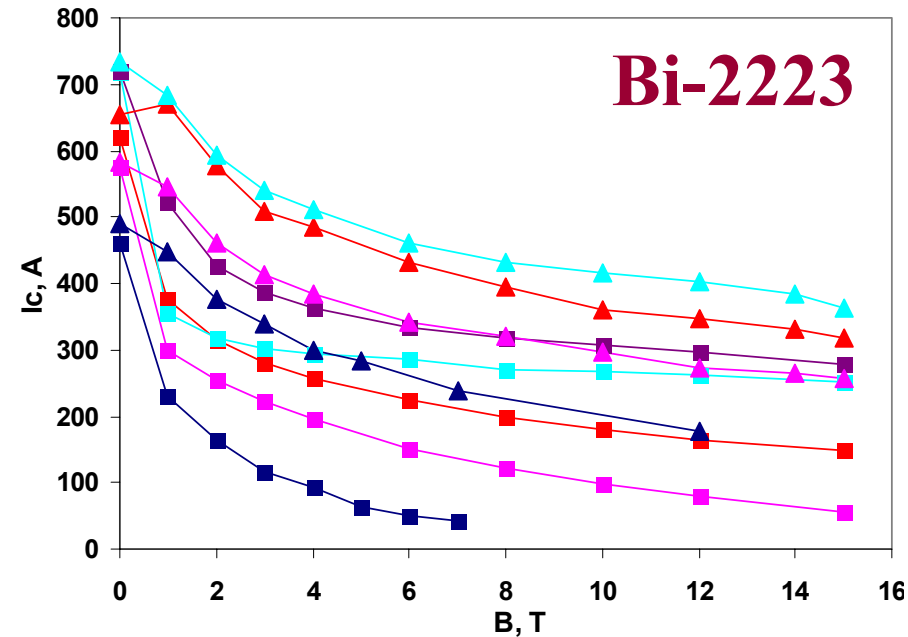
Conclusions from I_c Tests and SEM/EDS

Further analysis would be desirable, but it is already clear that the performance of these cables has been drastically degraded because of changes in the microstructure and chemical composition due to powder leaks during heat treatment.

However, because no leaks were observed on the extracted strands, which performed well, this problem may not be as much related to the strand ability to withstand deformation as to the Ag0.2%Mg alloying of the sheath AND/ OR the heat treatment of the cables itself, i.e. oxygen distribution on hidden surfaces, temperature inhomogeneities, and such.



Critical Currents

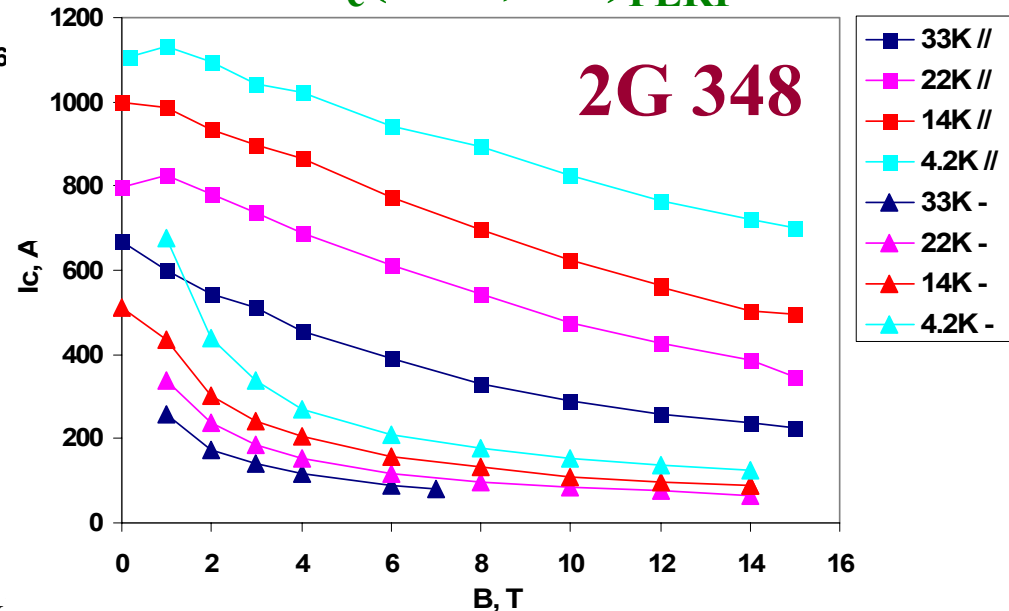


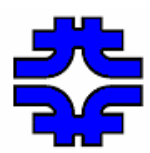
$$I_c(77K, 0T) = 121 \pm 1 \text{ A}$$

$$I_c(77K, 0T)_{\text{PAR}} = 127 \pm 1 \text{ A}$$

$$I_c(77K, 0T)_{\text{PERP}} = 153 \pm 1 \text{ A}$$

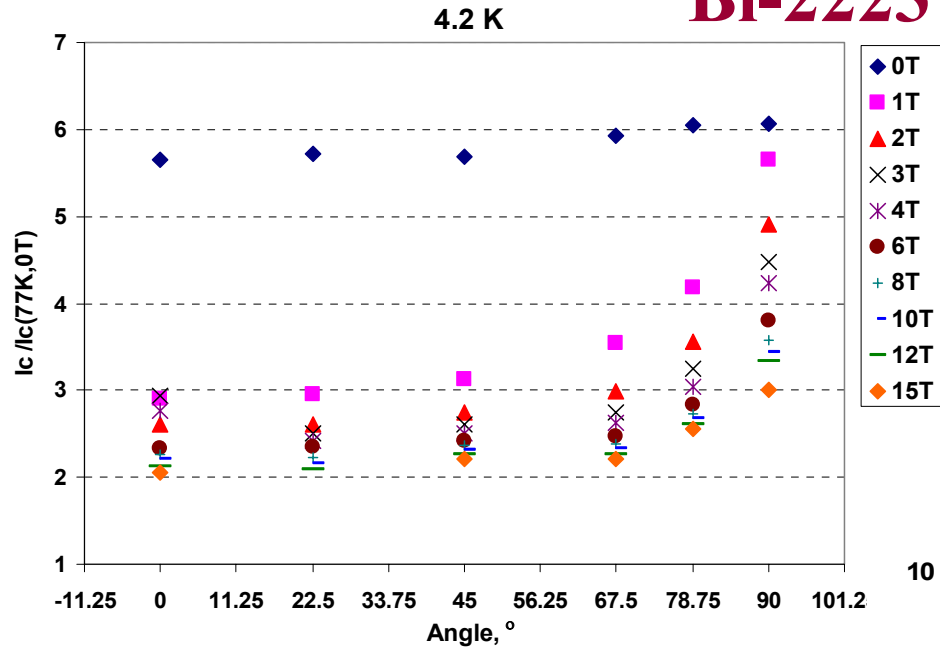
Effective pinning is maintained for the parallel direction over the entire field range





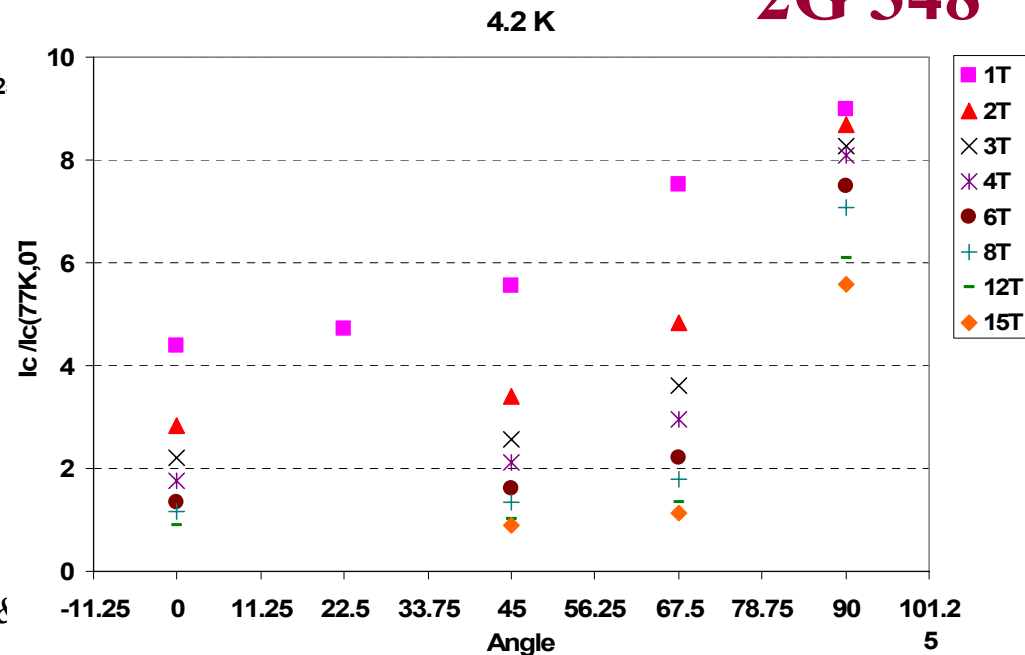
Angular Dependence at 4.2 K

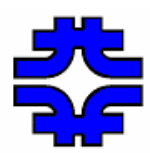
Bi-2223



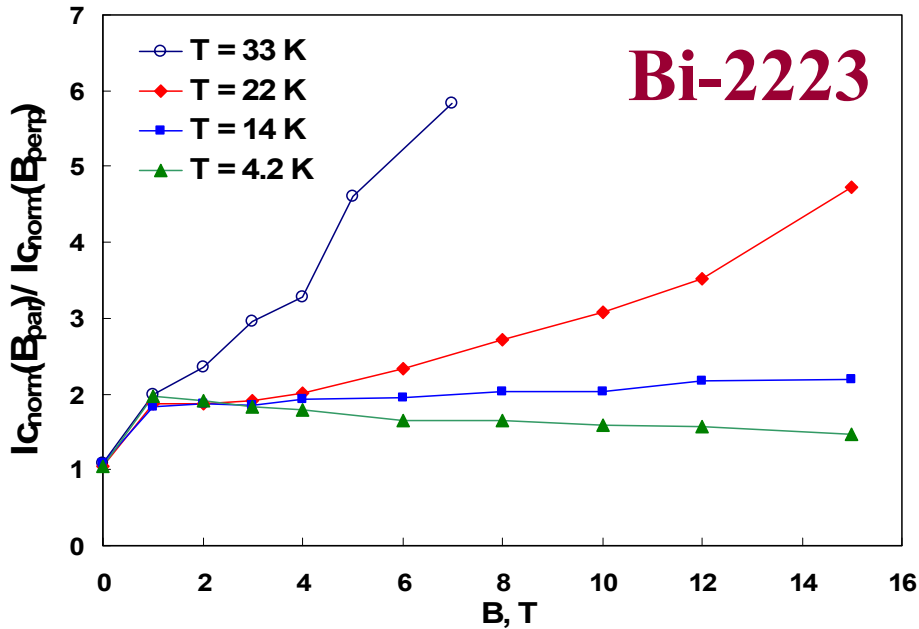
Most of the I_c reduction occurs between 90 and 45 degree.

2G 348





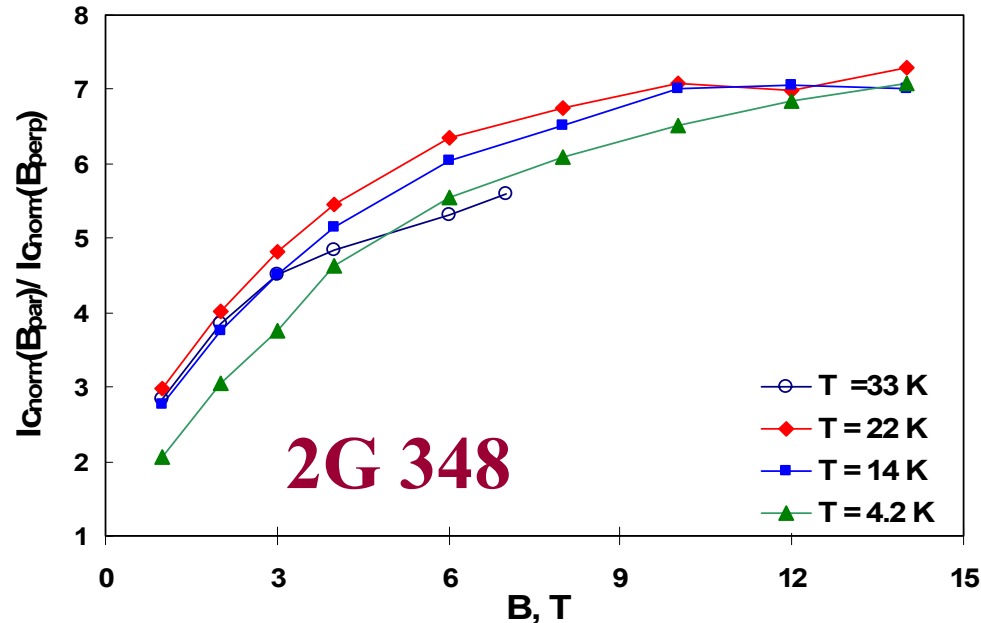
B and T Dependence of Anisotropy

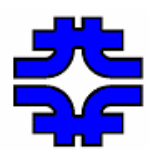


← The B dependence has a linear trend, where the slope value increases with T.

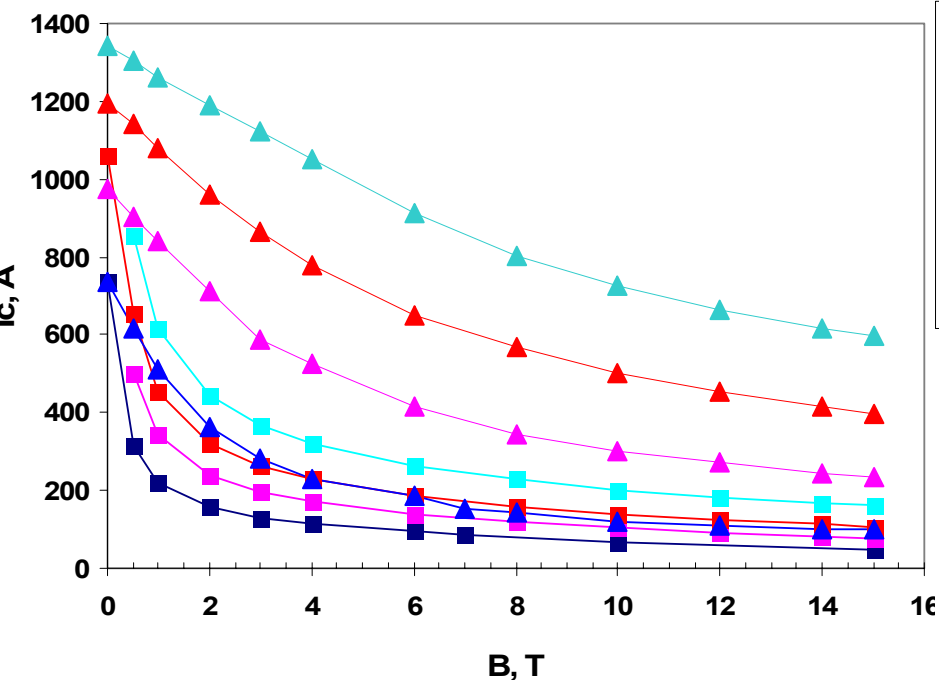
No observable T dependence. The ratio saturates at ~7.

$$\frac{I_c(B_{PAR}) / I_c(77K, 0T)_{PAR}}{I_c(B_{PERP}) / I_c(77K, 0T)_{PERP}}$$



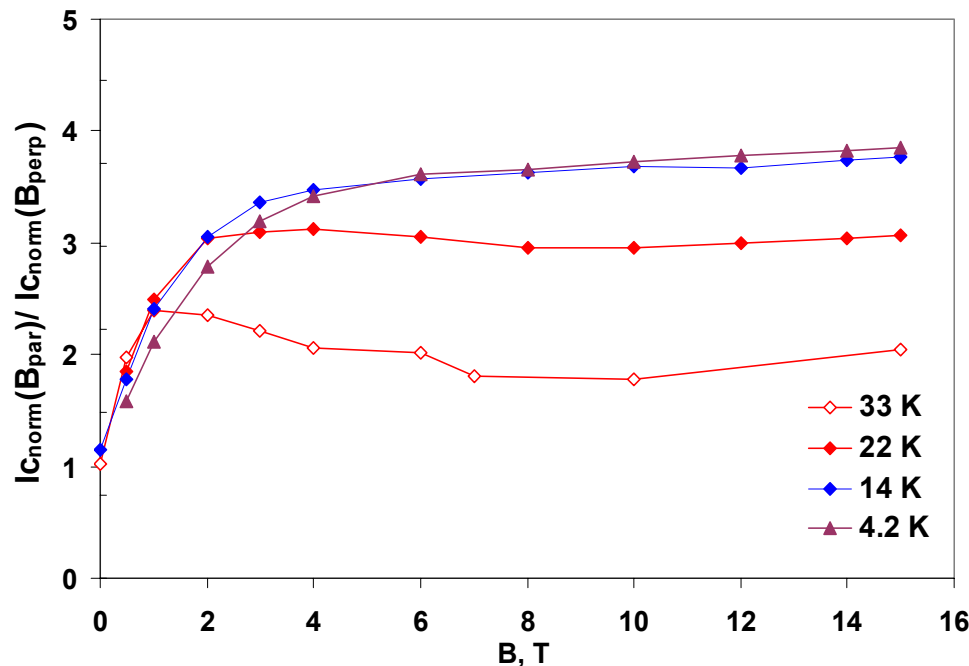


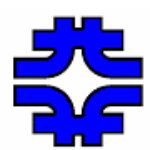
Comparison with Super Power 2G



$I_c(77\text{K}, 0\text{T}) = 106 \pm 1 \text{ A}$

Ratio saturates, but
decreases with temperature





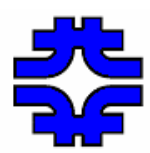
30T Hybrid Magnet at NIMS



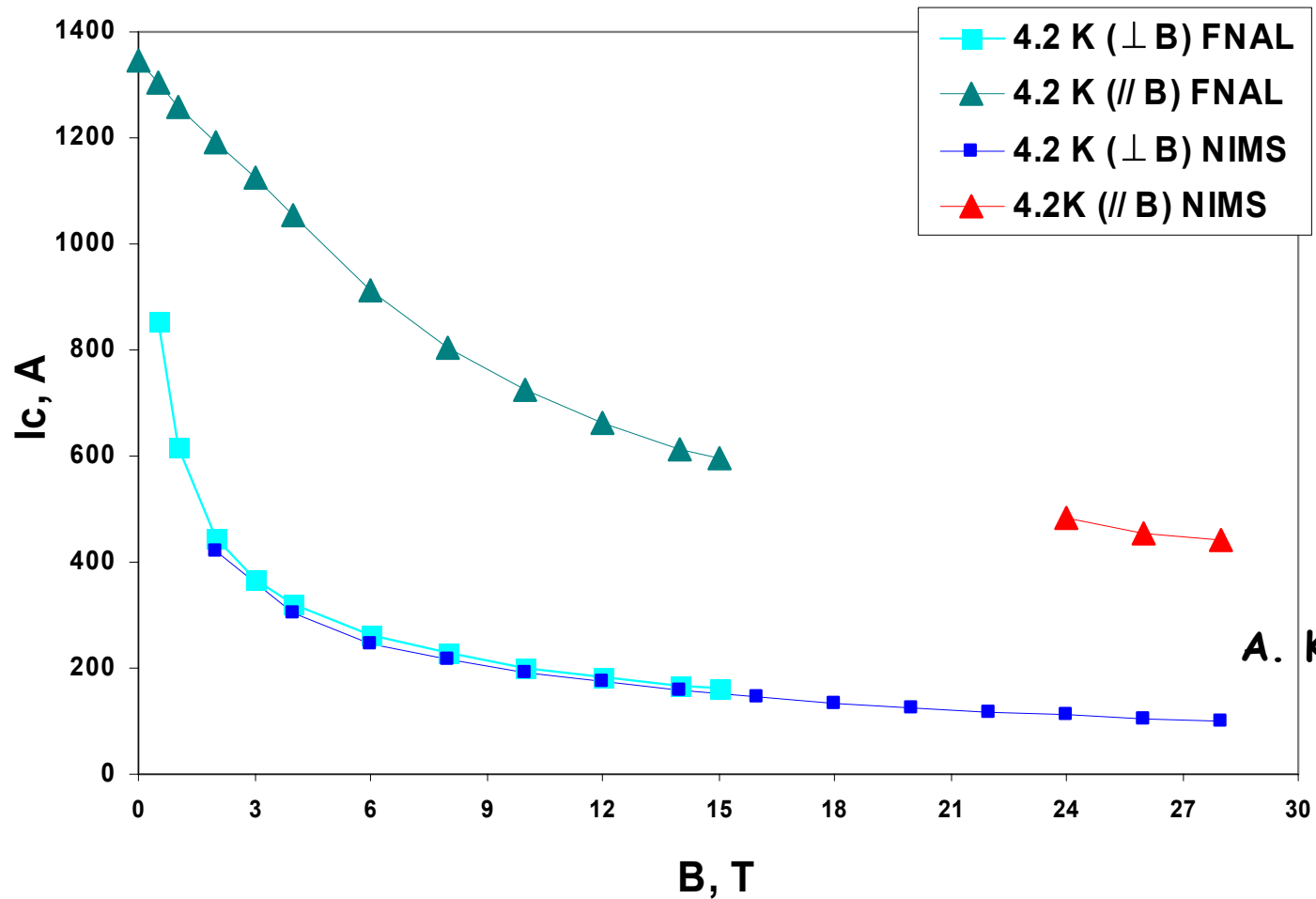
52 mm bore (room temperature)

February 7, 2008

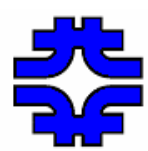
E. Barzi, SC Strand and Cable R&D for Future Accelerators, FNAL



Super Power 2G YBCO up to 28 T

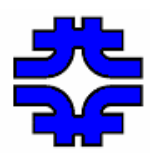


A. Kikuchi



Conclusions

- **A major effort of the superconductor development program goes into supporting magnet programs for future accelerators**
- **For LTS, after contributing to the J_c improvements the focus is now on:**
 - * **Studying the degradation of SC properties due to cabling in order to help Industry improve their strand design**
 - * **Measuring the acceptable stresses for various Nb_3Sn and Nb_3Al technologies to assess their applicability at various fields**
 - * **Using magnet data to set up an evaluation and prediction procedure**
- **For HTS, the focus is on:**
 - * **Monitor state-of-the-art HTS's and help solve the major challenges to push J_c .**



Some of the People





Superconductor R&D Group

SCIENTISTS/ENGINEERS:

- Emanuela Barzi (Univ. of Pisa)
- Daniele Turrioni (Univ. of Pisa)
- Vito Lombardo, Bardeen Fellow (Sant'Anna School, Pisa)

OPERATION ADMINISTRATOR:

- Allen Rusy

TECHNICAL SPECIALISTS AND TECHS:

- Tom Van Raes, Marianne Bossert



Graduate Students

- **Cristian Boffo – '99, Univ. of Udine:** *“Magnetization measurements at 4.2K of multifilamentary superconducting strands.”*
- **Michela Fratini – '01, Univ. of Pisa:** *“A device to test critical current sensitivity of Nb₃Sn cables to transverse pressure.”*
- **Sara Mattafirri – '02, Univ. of Pisa:** *“Kinetics of phase growth during the Cu-Sn diffusion process and the Nb₃Sn formation. Optimization of superconducting properties.”*
- **Licia Del Frate – '03, Univ. of Pisa:** *“Design of a low resistance sample holder for instability studies of superconducting wires.”*
- **Vito Lombardo – '07, Sant'Anna School, Pisa:** *“Automation of Short Sample Facility for critical current and low field instability measurements of superconducting strands at cryogenic temperatures.”*
- **Marco Danuso – in progress, Sant'Anna School, Pisa:** *“Parametric analysis of forces and stresses in superconducting magnets windings.”*



Equipment

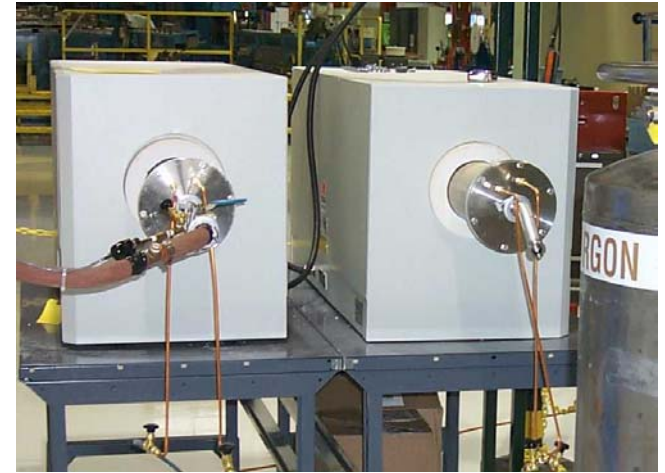
15/17T Teslatron -'98



14/16T Teslatron -'05

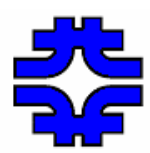


Two 1100°C tube furnaces-'98



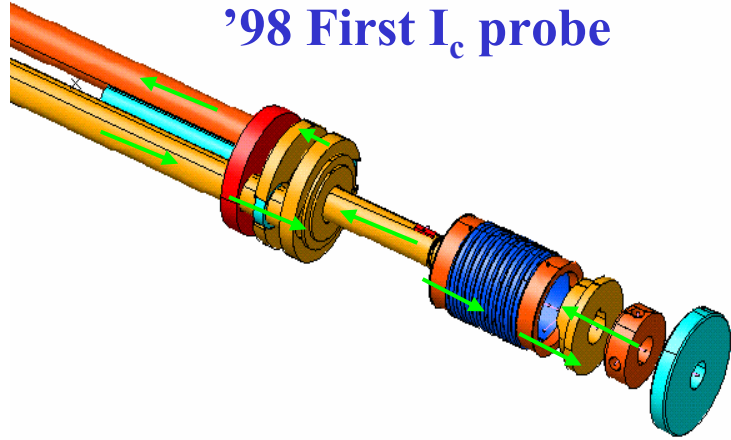
SEM and Optical microscopes-'00



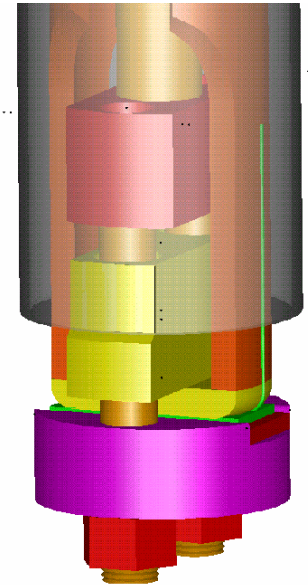


Probes for Strand Tests

'98 First I_c probe



'99 Magnetization
C. Boffo Laurea Thesis



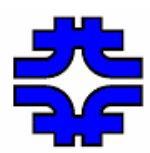
'01 Transverse pressure
M. Fratini Laurea Thesis



'05 HTS probe



'03 Low resistance probe
L. Del Frate Laurea Thesis



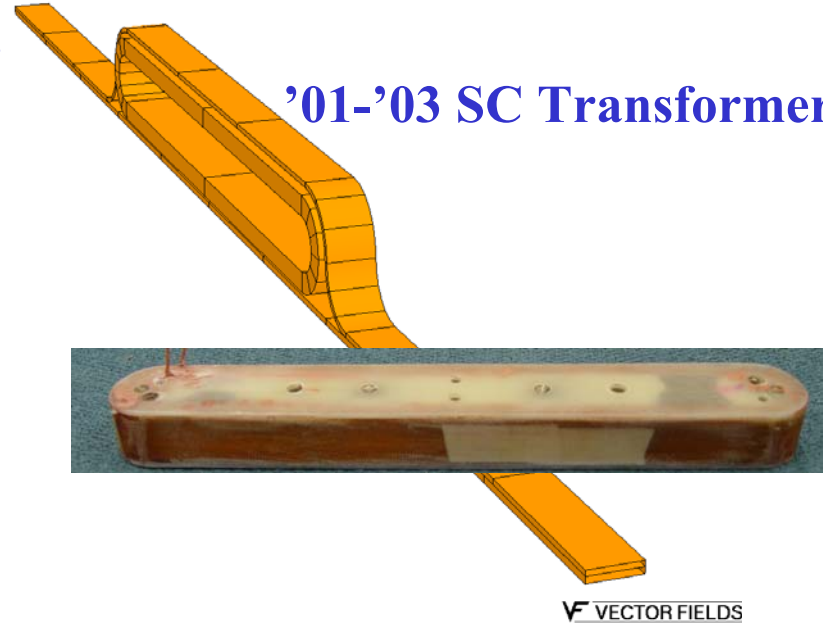
Fixtures for Cable Tests

'00-'01 Cable sample holder for NHMFL tests

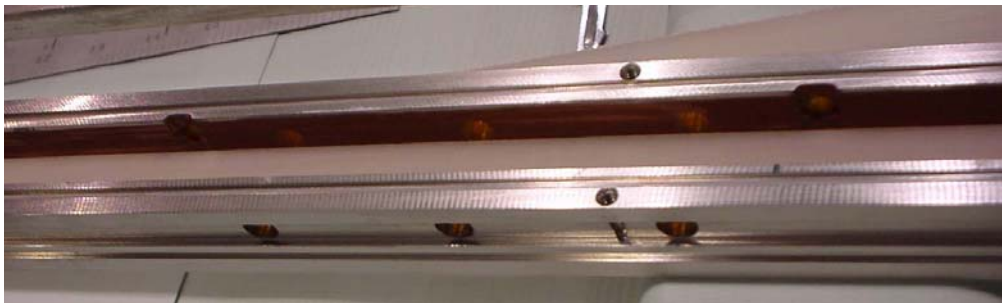


21/Apr/2004 13:33:03

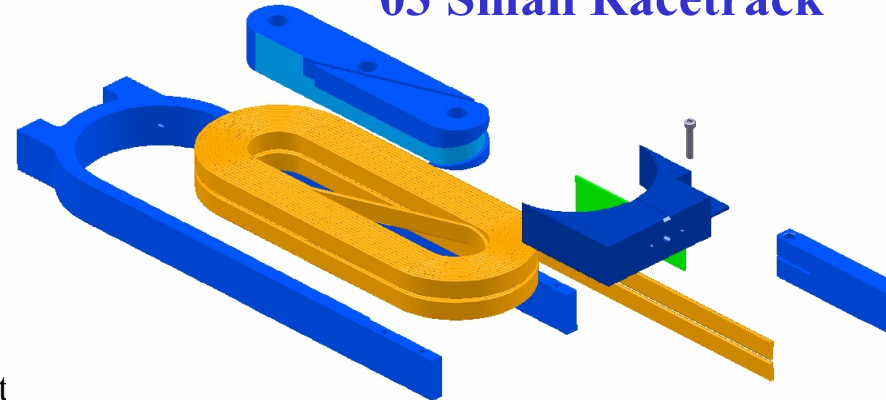
'01-'03 SC Transformer



'04 Cable sample holder for Cern tests



'03 Small Racetrack

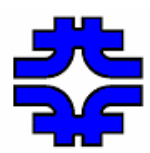




Cable Machine



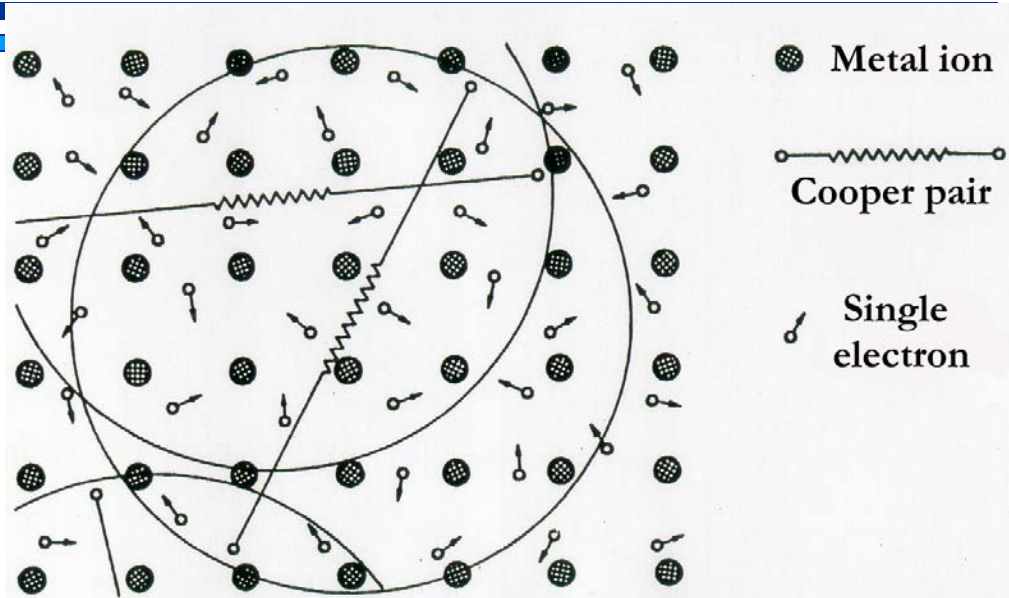
- **Strand number: up to 42**
- **Strand diameter: 0.3-1.5 mm**
- **Cable transposition angle: 8-16 degree**



Theories on Superconductivity...

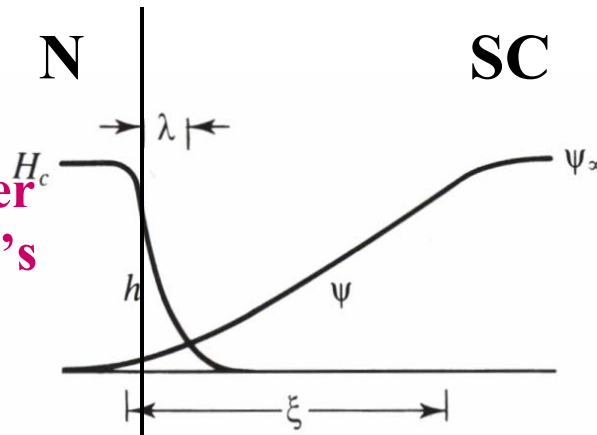
BCS

Microscopic theory.
Predicts the existence of an energy gap $\Delta \propto kT_c$ between the ground state and the quasi-particle excitations of the system.

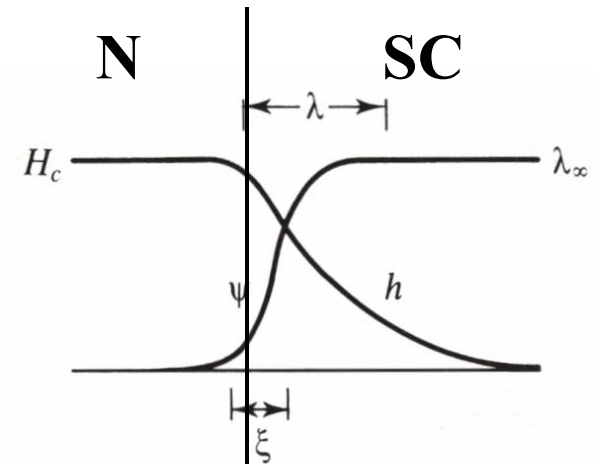


Ginzburg-Landau

Introduces a complex wavefunction ψ as an order parameter within Landau's theory of second-order phase transitions.



$\kappa \ll 1$ **Type I**

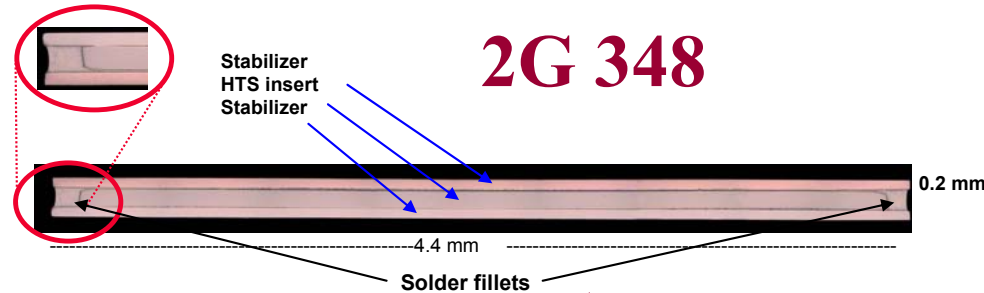
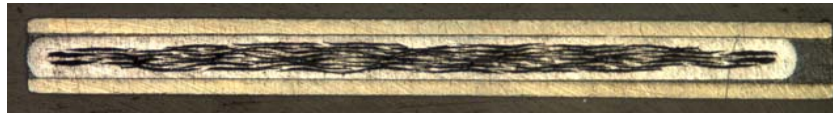


$\kappa \gg 1$ **Type II**

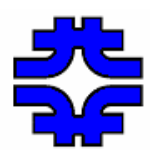


Samples under Comparison

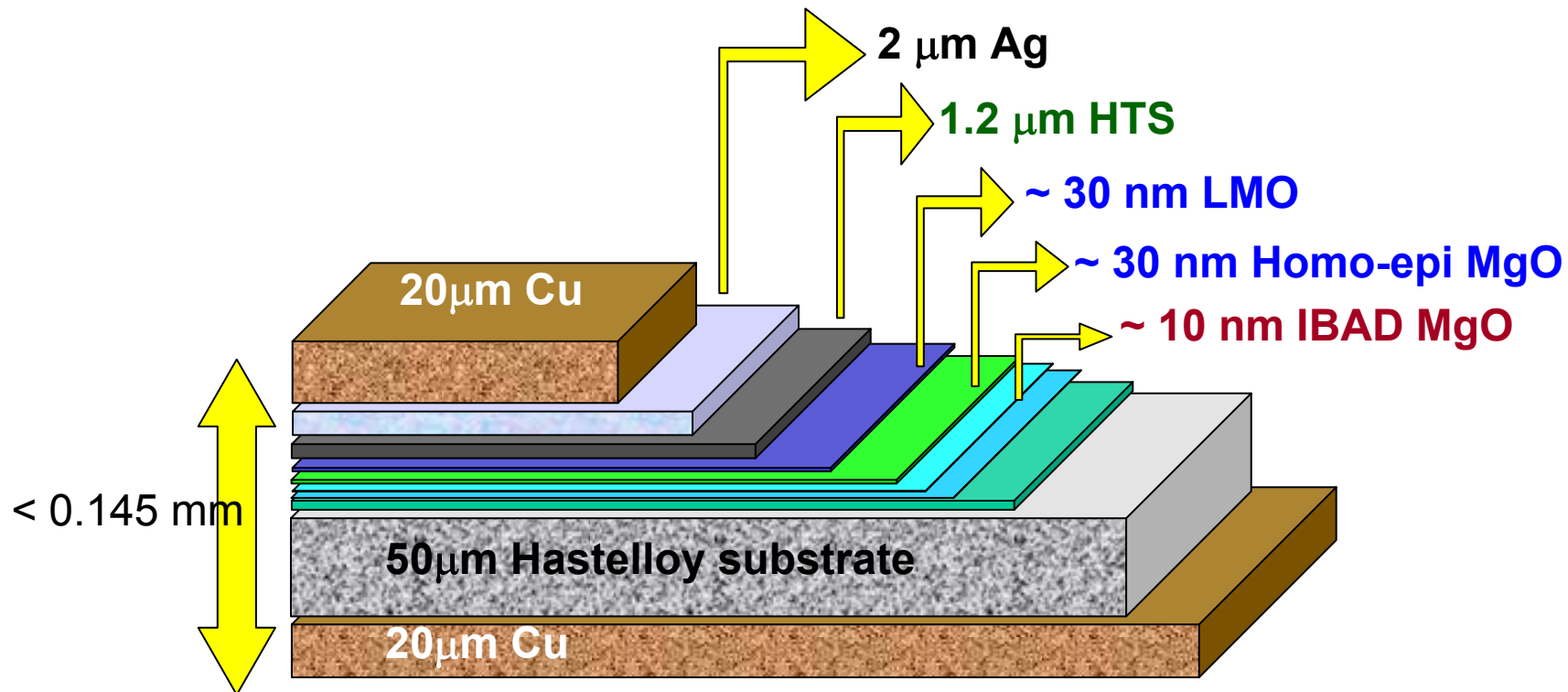
Bi-2223

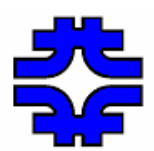


	Hermetic BSCCO-2223 tape	348 Superconductor
Min I_c (77 K, self-field, 1 $\mu\text{V}/\text{cm}$)	115 A	110 A
Average thickness t_T	0.31 mm	0.2 mm
Average width w_T	4.8 mm	4.8 mm
Laminate	stainless	copper
Laminate thickness	2 x 0.037 mm	2 x 0.050 mm
YBCO layer thickness		1.4 μm
Min. critical bend diameter	50 mm	50 mm
Max. rated tensile strain (95% I_c retention)	0.3 %	0.3 %

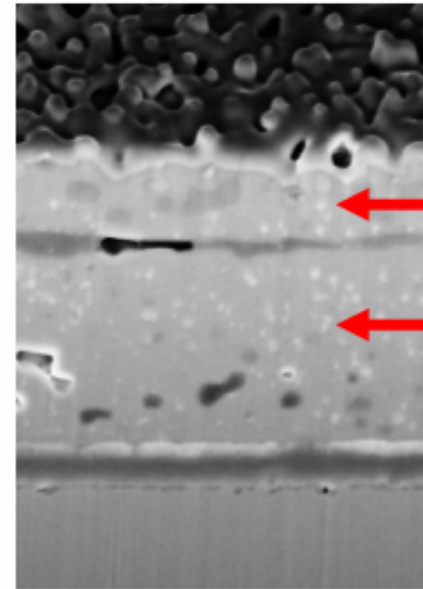
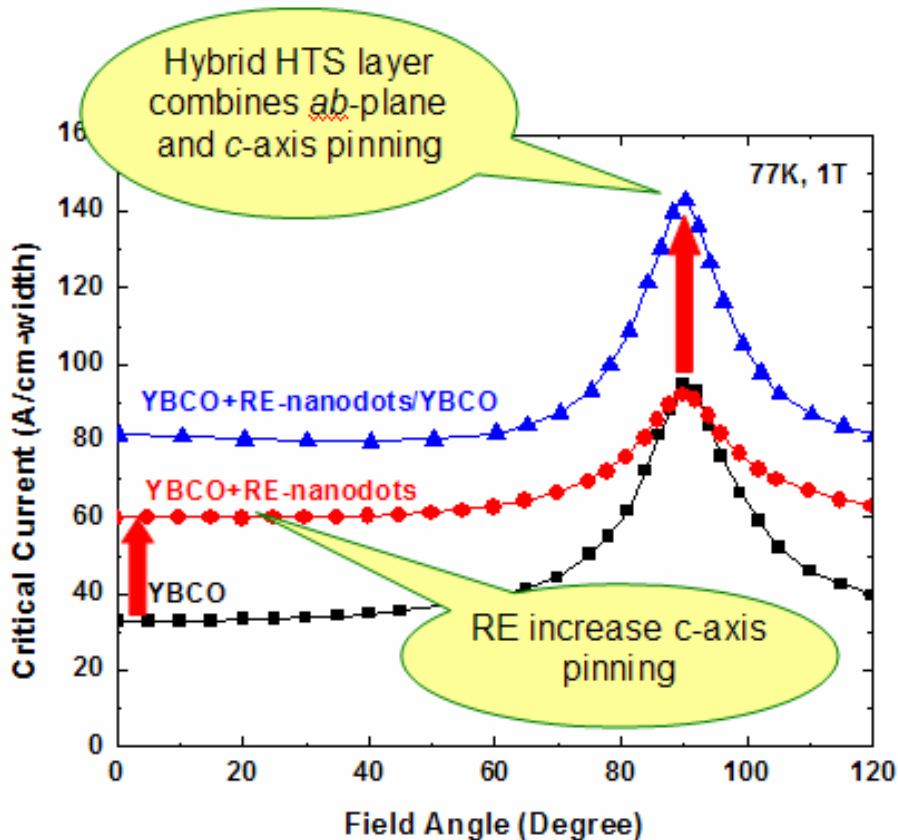


SuperPower 2G HTS Wire™



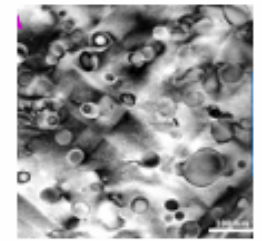
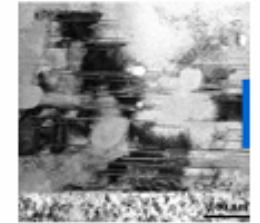


Flux Pinning Enhancement in 2G Coated Conductors by AMSC

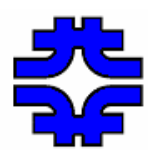


High density 124 intergrowths in top

High density Dy nanodots in bottom



- The 1.4 μm thick superconducting layer is a hybrid:**
- * Top layer is undoped YBCO with planar defects
 - * Bottom layer is doped with RE oxide for *c*-axis pinning



Labs side by side

FOR STRAND TESTS:

FNAL: 15/17 T, 1800 A

14/16 T, 1000 A

LBNL: 14 T, 2000 A

BNL: 11.5 T, 1200-1500 A

Test Capabilities

	BNL	LBNL	FNAL
I_c at 4.2 K	Y	Y	Y
I_c at 1.9 K	Y	N	Y
Low field magnetization	Y	N	Y
High field magnetization	N	N	Y
I_c under transverse pressure	N	N	Y
Cable test at self-field	Y	N	Y
Cable test at field	Y	N	N

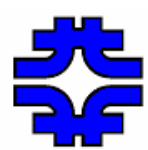
FOR CABLE TESTS:

**FNAL: 28,000 A SC transformer for tests at self-field (<2 T)
(Small racetrack coils for tests at field)**

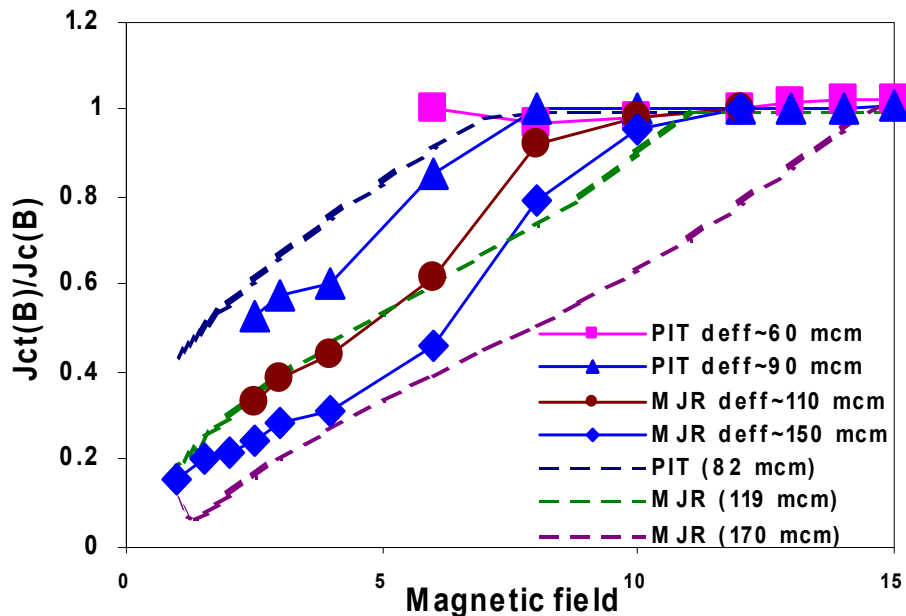
BNL: Cable test facility, 7 T max, 25,000 A max

LBNL: (Sub-scale racetrack coils for tests at field)

CERN: Fresca facility, 10 T max, 32,000 A (40,000 w/transformer)

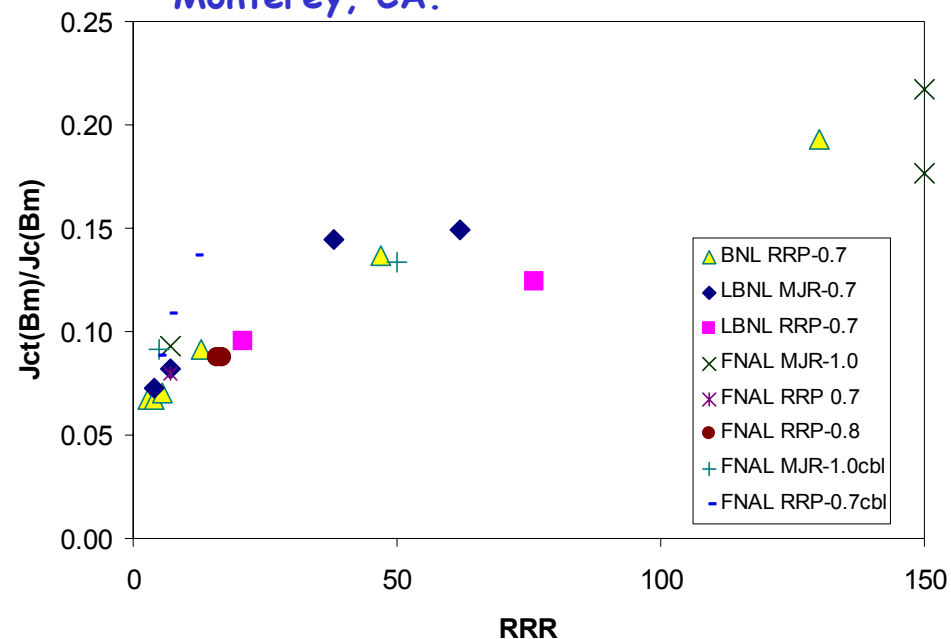


Effect of D_{eff} and RRR



At a given field, current degradation increases with increasing D_{eff} .

Summary of measurements on strands and cables at the various Labs, LSW 2004, Monterey, CA.



High RRR improves strand stability, although the absolute effect is small.